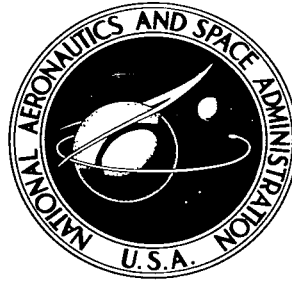


**NASA TECHNICAL NOTE**



**NASA TN D-4138**

*c.1*

**NASA TN D-4138**

LOAN COPY: TECHNICAL  
AERONAUTICS  
KIRTLAND AFB, TX

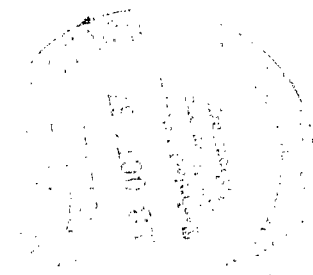
0130752



# DESIGN AND FABRICATION CONSIDERATIONS FOR A 1/10-SCALE REPLICA MODEL OF THE APOLLO/SATURN V

*by Sumner A. Leadbetter, H. Wayne Leonard,  
and E. John Brock, Jr.*

*Langley Research Center  
Langley Station, Hampton, Va.*





DESIGN AND FABRICATION CONSIDERATIONS

FOR A 1/10-SCALE REPLICA MODEL

OF THE APOLLO/SATURN V

By Sumner A. Leadbetter, H. Wayne Leonard,  
and E. John Brock, Jr.

Langley Research Center  
Langley Station, Hampton, Va.

NATIONAL AERONAUTICS AND SPACE ADMINISTRATION

DESIGN AND FABRICATION CONSIDERATIONS  
FOR A 1/10-SCALE REPLICA MODEL  
OF THE APOLLO/SATURN V

By Sumner A. Leadbetter, H. Wayne Leonard,  
and E. John Brock, Jr.  
Langley Research Center

SUMMARY

A 1/10-scale replica model of the Apollo/Saturn V launch vehicle was constructed for studies of vehicle dynamics at the Langley Research Center. This model was designed to duplicate, in miniature, as many of the full-scale structural elements as was economically and technically feasible. The project represents advancements in the state of the art of dynamic modeling and exemplifies the current limit of practical accomplishment in construction of dynamic models.

This paper outlines the design philosophy, describes the model as it relates to the prototype, and documents solutions to some design and fabrication problems which were encountered. It is believed that the experience gained in the design and construction of the model will provide designers of future models with an insight to the pitfalls and compromises which may dictate deviations from true miniature reproduction of certain hardware items. Subsystems, such as plumbing, pressurization systems, and suspension systems, are discussed along with simulated components, such as propellant and oxidizer liquid masses.

INTRODUCTION

The structural dynamic characteristics of a space vehicle must be known accurately to insure control system stability, structural integrity, and proper protection against the vibration environment in which the payload or crew will be required to function. The response of the vehicle to unsteady or transient loads, such as ground winds, launch noise, guidance and control pulses, unsteady engine burning, or winds aloft, must be predictable from the time the vehicle is assembled at the launch site until it has traversed the complete flight trajectory. Analytical studies are not always complete or reliable for complex structural configurations because of the extreme difficulty in adequately representing the structural elements mathematically and the lack of proper definition of component boundary restraints and interactions. The use of properly scaled dynamic models to

obtain experimental data can permit an evaluation of proposed analytical assumptions and techniques and can provide vehicle designers with valuable information on proposed designs early in their development cycle. Such models can also be extremely useful in evaluating structural modifications and payload changes without expensive and time-consuming full-scale construction and testing.

The degree of geometric similarity which is maintained between the dynamic model and its prototype will influence the applicability, amount, and type of information which may be obtained from model tests. Valuable data indicative of overall vehicle response may be obtained from models bearing little physical resemblance to the prototype, but having the correct mass and stiffness characteristics. However, in order to determine local vibratory responses, coupling effects, and component resonant effects, it is important that the model components be fabricated from materials comparable to the prototype and that they incorporate as many of the structural details of the prototype components as possible. The philosophy of replica geometric scaling offers an economically competitive and technically superior approach to the design of such detailed models if they can be designed and constructed to reasonable scale. The choice of scale factor is dependent upon the degree of similitude desired, economics, and the state of the art in material forming and fabrication.

The Langley Research Center has, for many years, utilized dynamic models in the investigation of aeroelastic stability phenomena. (See, for example, refs. 1 to 3.) The concept of utilizing dynamically scaled models for launch-vehicle structural dynamics studies was extended to the Saturn I vehicle as reported in references 4 to 9. This work verified the premise that the dynamic characteristics of large complex vehicles can be accurately determined through model tests. The degree of confidence in dynamic model data was further advanced by the correlation obtained between data obtained from a scaled model of an operational Air Force booster and data from the full-scale vehicle in flight as reported in references 10 and 11.

The Saturn V launch vehicle, presently conceived as the prime lunar and planetary exploration booster, is an extremely large and complex structure. This vehicle will serve as the transporter for the Apollo lunar landing spacecraft. The Langley Research Center has undertaken an experimental and analytical program designed to study the dynamic behavior of the Apollo/Saturn V through the use of two dynamic models. One is a replica model, for which a scale factor of 1:10 was selected after careful study to provide the smallest practical model with true geometric scaling of all primary and many secondary structural members. The other, a much simpler model, is a 1/40-scale dynamic model with only the general mass and stiffness distributions of the prototype scaled. The purposes of this report are to discuss the 1/10-scale structural replica model as related to the full-scale vehicle design, to document solutions to some typical and often difficult design and fabrication problems encountered, and to provide designers

of future models with some insight as to the compromises which can dictate deviations from true replica reproduction in certain areas.

## DESCRIPTION OF PROTOTYPE SPACE VEHICLE

### Saturn V Launch Vehicle

The Saturn V launch vehicle is basically an aluminum structure of semi-monocoque construction with internally pressurized and unpressurized areas separated by internal bulkheads. Three powered stages (S-IC, S-II, and S-IVB), an instrument unit and the Apollo spacecraft are shown in the sketch in figure 1. The lift-off weight of the vehicle is approximately 6 million pounds (26.69 mega newtons).

S-IC stage.- The first stage of the Saturn V launch vehicle, shown in figure 2 on its ground transporter, has a nominal diameter of 396 inches (10.06 m). It has a LOX/RP-1 propulsion system and is powered by five F-1 engines with a total thrust of 7.5 million pounds (33.36 mega newtons). The fuel and oxidizer are in separate pressurized tanks, the LOX tank being forward. The tanks are joined by an unpressurized intertank structure. Internal construction, material, and fabrication of the two tanks are similar. The cylindrical portion of each tank is made up of four quarter-sections joined by longitudinal welds. Integrally milled, tee-section stringers, located on the interior surface, provide additional structural rigidity. All bulkheads are elliptical in shape and are constructed from gores welded together. The bulkheads are joined to the cylindrical tank and skirt sections through a Y-section ring welded to the equator of each bulkhead. The domed-truss structure shown in figure 2 at the forward end of the S-IC stage is a handling fixture and is not a part of the flight hardware.

Ring-type slosh baffles are fusion welded to the internal stringers in each tank and cruciform-type baffles are located in each lower bulkhead. Five insulated tunnels lead through the fuel tank to permit passage of suction ducts which supply LOX to the engines.

The four outboard engines are attached to thrust posts located on the periphery of the aft skirt section. A cruciform beam supports the center engine. Four holddown posts provide anchor points for mounting the vehicle to the launcher. Aerodynamic fairings and stabilizing fins are provided at each outboard engine location. With the exception of the intertank structure, which is of corrugated-skin—ring-frame construction, all unpressurized skirts and fairings have extruded hat-section stringers riveted to the external surface.

S-II stage.- The second stage of the Saturn V vehicle, shown in figure 3, has the same nominal diameter of 396 inches (10.06 m) as the first stage. The two stages are joined by a series of skin-stringer type shells with hat-shaped stringers riveted to the external surface. In this stage, the propulsion system consists of five J-2 engines

burning liquid hydrogen with LOX as the oxidizer and having a total thrust of about 1 million pounds (4.448 mega newtons). The fuel tank is forward and the oxidizer tank is aft. An insulated common bulkhead separates the two pressure vessels.

The cylindrical portion of the fuel tank has integral circumferential and longitudinal stiffeners machine milled on the inside surface to form a rectangular grid pattern. Five longitudinal and four circumferential fusion welds are utilized to assemble the cylinder. The upper fuel tank bulkhead and lower LOX tank bulkhead are fabricated of gores fusion welded together to form elliptical diaphragms. The common bulkhead is a sandwich structure consisting of gores, fusion welded to an elliptical shape and bonded to a fiber-glass honeycomb core.

The thrust structure, visible in figure 3, consists of a truncated cone with hat-shaped stringers riveted along the external structure. Thrust longerons, at the four out-board engine locations, transmit the engine force. The center engine is mounted at the center of a cruciform beam. All unpressurized shell structures are skin-stringer types with extruded hat-shaped stringers riveted to the skin.

S-IVB stage.- The third stage (S-IVB) of the Saturn V vehicle has a liquid-hydrogen—liquid-oxygen propulsion system utilizing a single J-2 engine, located on the stage center line, with 200,000-pound (889,600 N) thrust capability. This stage, shown in figure 4, has a nominal diameter of 260 inches (6.60 m). The oxidizer tank is located aft of the fuel tank. An insulated common bulkhead separates the two tanks. A square waffle pattern having a 45° orientation to the vehicle longitudinal axis is machine-milled on the inner surface of the fuel-tank cylindrical section. Longitudinal fusion welds are used to join the six sheets forming this cylinder. Construction of the hemispherical bulkheads follows the pattern described for the S-II stage. The unpressurized structure fore and aft of the tankage, including the conical interstage, is of skin-stringer construction with extruded hat-shaped stringers riveted to the outside of the skin.

Instrument unit.- The instrument unit (IU), which is not illustrated, is a short cylindrical structure having a nominal diameter of 260 inches (6.60 m). Structurally, the instrument unit is a sandwich shell consisting of aluminum face sheets bonded to an aluminum honeycomb core. Instrument packages are mounted to the inner walls of the structure.

## Apollo Spacecraft

The Apollo spacecraft is composed of four substructures: lunar module (LM), service module (SM), command module (CM), and launch escape system (LES). The spacecraft without the LM and LM adapter is shown in figure 5.

Lunar module.- The lunar module (LM) is a two-stage, soft-landing spacecraft which will carry two astronauts to the lunar surface from lunar orbit and subsequently

return these two men to a rendezvous with the orbiting command module. In the launch configuration the LM is attached at four points inside the LM adapter cone. This adapter structure is a conical frustum of aluminum face and honeycomb core sandwich material with diameters of 154 and 260 inches (3.91 and 6.60 m) at the fore and aft ends, respectively. The adapter also serves as an interstage-type structure between the Saturn V instrument unit and the service module.

Service module.- The service module (SM) is an aluminum honeycomb shell with radial beams and has a nominal diameter of 154 inches (3.91 m). Equipment on this part of the spacecraft supplies the power for midcourse correction, retro-braking into lunar orbit, return flight propulsion, and reentry braking.

Command module.- The command module (CM) is a conical frustum fabricated of steel face-and-core honeycomb with interior accommodations and instrumentation for three astronauts. From this section of the spacecraft, the crew will perform monitoring and control functions through launch, translunar flight, lunar orbit, return flight, and reentry.

Launch escape system.- The launch escape system (LES) consists of a titanium open truss tower supporting a launch escape motor. The motor is a solid-propellant device with a steel case and having a nominal diameter of 26 inches. The tower attaches to the top of the command module cone and is jettisoned just after second-stage ignition.

## MODEL DESIGN APPROACH

### Concept

The reduced-scale Apollo/Saturn V model was conceived as a tool for studying the local and general vibration response characteristics of the prototype vehicle to unsteady ground and flight loads. Data obtained from the model could then be utilized to define potential vibration-induced problems which may adversely affect the prototype and could suggest remedial approaches to these problems even before fabrication of the prototype. At the same time these data would prove very useful in validating procedures and techniques developed for analytical investigation of the structural dynamic characteristics of the prototype and subsequent modifications to the prototype.

In order to meet these goals, the model would ideally be a perfect subscale replica of the prototype. However, practical fabrication limitations as well as economic considerations dictate some departures from the direct-scaling concept. The success of any dynamic-model program will depend upon the degree of success achieved in simulating or representing the structural dynamics properties of the full-scale vehicle, since the model is, essentially, a mechanical analog of the full-scale structure. From a highly simplified design standpoint, it would appear that a scale model could be constructed from full-scale

drawings with dimensions reduced by the scale factor. This is not true, however, since such factors as material fabrication properties, machine processes, cost and time considerations, and practical limits on material tolerances must be weighed against alternative design procedures and their effect on the test objectives. The results of this process of trade-off and compromise will establish the degree of allowable deviation from exact miniature duplication and will set the requirements which simulated components or properties must satisfy.

The selection of a scale factor for replica model construction must also be made on the basis of other salient factors. The practical questions of facilities to house and test the model, and logistical support considerations, such as handling and mechanical assembly of model stages, will determine some maximum model size which is economically attractive. Technical questions of thin-gage metal fabrication, component miniaturization possibilities, transducer size limits as compared with model structure, and test program objectives will determine a minimum model size.

From a review of the prototype on the basis of manufacturing state of the art in thin-gage metals, it was concluded that although advancements in the state of the art would be required, a replica model with a scale factor of 1:10 would be not only feasible but economical since the facilities and logistical systems necessary to support and test a model of this size were available at the Langley Research Center. It was, however, established that the geometric duplication of the Apollo spacecraft was not economically attractive. Consequently, the boost stages of the Apollo/Saturn V replica model were designed from a scale factor of 1:10 with minor deviations but only the flexural rigidity, mass distribution, and nominal external dimensions of the spacecraft were scaled. Even this limited approach could not be applied to the LM portion of the spacecraft where only the correct mass location and method of attachment to the LM adapter were scaled.

#### Planned Deviations from Direct Scaling

As noted earlier, some deviations from the direct geometric scaling of the prototype were felt to be necessary, both from a fabrication and an economic viewpoint. These planned deviations are summarized for each of the principal structural areas.

The model propellant tank bulkheads were spun from single sheet stock rather than fabricated from gores. Prototype gore weld lands were represented in the model by built-up sections at the land location or by increasing the total bulkhead thickness. Likewise, the waffle patterns on the bulkheads were represented in the model by equivalent skin thickness.

For the unpressurized skirts, the use of doublers to effect hat-section stringer geometry changes were permitted. Also, spot welds were used in lieu of rivets to fabricate the skin-stringer assemblies.

The prototype shear-type joints were geometrically scaled wherever possible; however, deviations would be permitted in the fasteners. Spot welds on the model were deemed acceptable in lieu of prototype mechanical fasteners.

The prototype tension joints were geometrically scaled wherever practical in the model. Although fewer fasteners were permitted, the net cross-sectional area was scaled.

Scaling of only the elastic properties of tank-bulkhead-to-cylinder-wall joints and common-bulkhead-to-aft-bulkhead joints was required. Deviations from full-scale fabrication and manufacturing techniques were permitted.

The model engines and engine actuators were scaled only elastically from the prototype; however, all gimbal joints were scaled duplications of prototype hardware.

Secondary structures such as plumbing, flight instrumentation, thrust structure heat shields, insulation, and control systems were included in the model as ballast weights.

The use of simulated liquid propellants was permitted in all tanks. No cryogenic liquids were considered. Water was deemed suitable for simulation of the RP-1 in the S-IC stage and the LOX in all stages. The simulation of the LH<sub>2</sub> in the upper stages was considered to be a major problem since the simulant must have the correct mass density, be noncryogenic, be easily added or removed from the tanks, and not be mechanically attached to the structure. It was therefore concluded that some type of granular material would be acceptable as the LH<sub>2</sub> simulant.

### Model-Prototype Parameter Relationships

The adoption of direct geometric scaling with a ratio of 1:10 and the use of similar materials between prototype *p* and model *m* dictate the following model to prototype relationships:

Poisson's ratio, $\nu$	$\nu_m/\nu_p = 1$
Material density, $\rho$	$\rho_m/\rho_p = 1$
Modulus of elasticity, $E$	$E_m/E_p = 1$
Longitudinal stiffness, $EA$	$(EA)_m/(EA)_p = 10^{-2}$
Bending stiffness, $EI$	$(EI)_m/(EI)_p = 10^{-4}$
Torsional stiffness, $GJ$	$(GJ)_m/(GJ)_p = 10^{-4}$
Mass, $m$	$m_m/m_p = 10^{-3}$
Mass moment of inertia, $I'$	$I'_m/I'_p = 10^{-5}$
Length, $l$	$l_m/l_p = 1/10$
Diameter, $d$	$d_m/d_p = 1/10$
Shell frequency, $\omega_{shell}$	$\omega_{shell}_m/\omega_{shell}_p = 10$
Bending frequency, $\omega_{bending}$	$\omega_{bending}_m/\omega_{bending}_p = 10$
Slosh frequency, $\omega_{slosh}$	$\omega_{slosh}_m/\omega_{slosh}_p = 10^{1/2}$

## MODEL DESCRIPTION AND FABRICATION TECHNIQUES

### Model Description

The 1/10-scale Apollo-Saturn V dynamic model was built to NASA specifications by the Los Angeles Division of North American Aviation, Inc., and consists of five basic units, representing the S-IC, the S-II, the S-IVB, and the instrument unit of the Saturn V launch vehicle and the Apollo spacecraft. The Apollo spacecraft is composed of the lunar module, service module, command module, and launch escape system. Figure 6 is a sketch of the complete model with all internal and external joints. Separation stations at which disassembly may be conveniently accomplished are symbolically identified in the figure. The circled identification symbols are used to designate particular joints which are discussed in detail in a later section. The complete model, as built, is shown in figure 7, supported in the test facility by a 4-cable suspension system designed to provide the proper simulation for free-free longitudinal vibration response studies.

Wherever possible, primary load-carrying structures on the launch vehicle have been geometrically scaled in the model. The lunar module adapter has been similarly scaled. Although the external dimensions of the model structure above the LM adapter have been scaled, the type of construction and materials used differ from the prototype. Except for the LM, which has only the mass characteristics of its full-scale counterpart, this structure does have the properly scaled bending stiffness. The mass and stiffness properties of the model are presented in table I and figures 8 and 9. Table I lists the incremental weights and section centers of gravity as calculated from the model drawings. Figure 8 is a graphic comparison of the model bending stiffness distribution with that calculated for the prototype. The longitudinal stiffness of the model as indicated by the calculated material area values is shown graphically in figure 9.

S-IC stage.- Figures 10 to 14 illustrate some of the steps during assembly of the thrust structure of the model S-IC stage. Figure 10 shows the center engine support beam assembly. Figure 11 shows the cross-beam assembly with the lower ring frame, thrust posts, and holddown posts attached. The intermediate, variable-thickness ring frames are added as shown in figure 12. The welding fabrication of the skin-stringer skirt structure is shown in figure 13. The spot-welding technique used to join the formed hat-section stringers to the skin is typical of the construction of the other skin-stringer areas on the model. Figure 14 shows the assembly of the thrust structure section with the skin fastened around the skeleton structure and mechanically attached.

An end view of the first-stage tail-section assembly with fuel tank attached is shown in figure 15, prior to engine installation. The engine actuator support structures and engine fairings are shown at the four locations, 90° apart on the assembly. Fins, not shown in the figure, are mounted on each of the four fairings.

Three of the five simulated first-stage engine assemblies are shown in figure 16. One of these assemblies is mounted to the thrust pad at each of four locations around the lower ring frame. The fifth assembly is attached at the junction of the thrust structure cross beams. Each assembly consists of a gimbal assembly, which is geometrically scaled from the prototype; a tubular structure which provides the required stiffness; added weights for proper mass and inertia distribution; actuator attachment brackets; and a nonstructural foamed plastic fairing. The test transducer masses were included in the simulated engine design. Three simulated transducers are shown in figure 16. During tests any or all the simulated transducers may be replaced by working units without altering the engine mass and inertia properties.

The lower bulkhead of the first-stage fuel tank is shown in figure 17. This aluminum-alloy bulkhead was spin formed to an ellipsoidal shape. Five cutouts were made in the bulkhead to provide for the installation of the five LOX suction duct tunnels. Two smaller cutouts were capped and fittings were installed to accommodate two inboard fuel lines. The bulkhead was chemically milled to the required thickness. Thickened areas simulating the gore weld lands in the prototype can be seen in the figure. The tube shown is a part of the model fill and drain line. The Y-section ring which joins the bulkhead to the fuel-tank cylindrical skin section and to the lower tail section assembly is shown welded to the bulkhead equator. The Y-ring was machined from an aluminum-alloy forging.

One of the four cylindrical skin sections of the first-stage fuel tank is partially shown in figure 18 prior to being rolled into cylindrical shape. Each section has 51 integrally milled tee-section stiffeners. The skin thickness is tapered from 0.017 inch (0.043 cm) at the forward end to 0.019 inch (0.048 cm) at the aft end.

Figure 19 shows an interior view of the partly assembled fuel tank. The four skin sections were rolled to the proper curvature and joined by four longitudinal welds. The seven ring-type antislosh baffles shown were spotwelded and clipped to the stringers. Straps connecting the ring baffle assemblies are shown being spotwelded into place. Another view of the interior of the fuel tank is shown in figure 20. Three of the five simulated LOX suction duct tunnels can be seen in place. Each of these tunnels has a basic inside diameter of 2.50 inches (6.2 cm) and is stiffened externally by integrally milled rings.

A single simulated LOX suction duct was installed in the center tunnel. This duct is shown in figure 21 prior to installation in the model. Identified in the figure are centering, or holdoff, springs which maintain the orientation of the duct with respect to the tunnel, the simulated pressure-volume compensator (PVC), the bellows which simulate complex gimbal or sliding joints in the full-scale duct, and the attachment bracket which is a scaled replica of the full-size structure. The duct does not extend all the way to the

engine, but is capped off by a closure plate immediately aft of the simulated PVC. Hence, no coupled engine-pump—liquid responses of the model are possible.

The upper bulkhead of the fuel tank is shown in figure 22. Five cutouts are provided for the installation of the five simulated LOX suction duct tunnels. The tank vent line fitting is also shown. The weld lands of the prototype are simulated here by an increased uniform thickness of the bulkhead. The Y-section ring which connects this bulkhead to the cylindrical skin section and to the intertank section is shown welded to the bulkhead equator.

The model tank, fixture, and welding equipment for the fuel tank final circumferential welding is shown in figure 23.

An interior view of the intertank section is presented in figure 24. The corrugated skin was formed in four panels from aluminum-alloy sheet and was chemically milled to provide the required skin-thickness variation. Five intermediate I-section ring frames are mechanically attached to the skin. The connection at the corrugated skin section to upper and lower ring frames is made with 432 channel-shaped fittings.

An interior view of the oxidizer tank is presented in figure 25. The design and construction of this tank is similar to that used on the fuel tank. Each of the four skin sections which compose this tank has 42 integrally milled tee-section stringers. The final skin thickness tapers from 0.019 inch (0.5 cm) forward to 0.025 inch (0.6 cm) aft. The ring-type slosh baffles shown were spotwelded and clipped to the stringers. The ballast weights shown in this view represent the mass characteristics of helium bottles used as ullage pressure sources and the mass characteristics of other secondary structures on the prototype.

The upper bulkhead of the S-IC LOX tank is visible in figure 26 along with part of the S-IC forward skirt. The S-IC forward skirt has a skin thickness of 0.010 inch (0.25 cm) and is constructed similar to the skin assembly on the thrust structure. The complex ring frame at the forward station has its inner flange supported by 18 equally spaced diagonal struts and is identical to the prototype joint.

S-II stage.— Figure 27 shows the model S-IC/S-II interstage structure. This interstage has the typical skin-stringer construction previously described. The skin thickness is 0.007 inch (0.018 cm). The joint at model station 156.4 simulates the separation joint on the prototype and has 216 small tension straps spot welded to the hat-section stringers on each side of the joint.

The aft skirt-thrust structure assembly of the second stage is shown in figure 28. The aft skirt is a cylindrical section with typical skin-stringer construction and a skin thickness of 0.007 inch (0.018 cm). Doublers bonded to the 216 hat-section stringers provide the required variation in cross-sectional area. The conical section of the thrust

structure is of similar construction. The skin has a compound tapering thickness. A pair of thrust longerons are spotwelded to the inside face of the skin at each of the four outboard engine locations. The modified center engine support assembly consists of four beams placed in a cross arrangement and spliced at the stage center line.

Figure 29 shows the assembly of the thrust-cone—aft-skirt structure and the inter-stage section. The thrust longerons and internal ring frames can be seen.

The five model second-stage engines are shown in figure 30. These simulated J-2 engines consist basically of a steel gimbal assembly and a tube assembly having actuator attach fittings, simulated or actual transducers, and required ballast weights.

The common bulkhead which separates the model second-stage oxidizer and fuel tanks is shown under construction in figure 31. This structure is of honeycomb sandwich construction consisting of 0.012-inch- (0.03 cm) thick aluminum face sheets bonded to a 0.480-inch- (1.22 cm) thick aluminum honeycomb core. Near the bulkhead equator, the honeycomb is terminated and is replaced by a putty filler whose thickness tapers to 0.05 inch (0.0129 cm) at the equator. The aft skin is an ellipsoid. Both face sheets are bonded to a closeout ring at the equator to complete the assembly. In the figure, a plywood support ring is attached to the periphery of the lower face sheet. Figure 32 shows the complete common bulkhead with the bolting-ring section assembly attached. The bolting-ring section has integral longitudinal and circumferential stiffeners machine-milled on the outside with a resulting rectangular grid pattern.

Figure 33 shows the second-stage oxidizer-tank—bolting-ring assembly. The lower bulkhead is ellipsoidal in shape and is fusion welded to the common bulkhead. A 4-inch-diameter (10.16 cm) cutout is provided for access.

An internal view of the fuel tank subassembly consisting of the upper bulkhead and the cylindrical tank wall section is shown in figure 34. The bulkhead is ellipsoidal in shape and is fusion-welded to the cylindrical skin section. The skin section has integral longitudinal and circumferential stiffeners, machined milled on the inside surface to a rectangular grid pattern while in the flat condition. Four longitudinal welds are used to assemble the shell.

The second-stage forward-skirt assembly has the typical skin-stringer construction and is not shown. The skin was chemically milled on the inside surface to provide a varying thickness of 0.004 to 0.012 inch (0.01 to 0.03 cm).

The fully assembled second stage is shown in figure 35. The openings in the skirt areas are scaled duplicated of those on the prototype.

S-IVB stage.— Figure 36 shows the second-stage—third-stage adapter. This inter-stage structure is a truncated cone of typical skin-stringer construction. The skin

thickness is 0.004 inch (0.01 cm). Longitudinal members, or intercostals, are spot-welded to the skin and ring frames at discrete points on the periphery.

The third-stage aft skirt of typical skin-stringer construction is shown in figure 37.

The common bulkhead of the third stage is shown, partially assembled, in figure 38. Outer and inner face sheets, having thicknesses of 0.004 and 0.006 inch (0.01 and 0.015 cm), respectively, were spin formed and bonded to a 0.185 inch (0.46 cm) thick, 1/8-inch (0.31 cm) cell, 0.0007 inch (0.0018 cm) wall aluminum honeycomb core. The edge of the bulkhead was closed out with an aluminum ring which was mechanically attached to the locally thickened face sheets and bonded to the core material. This joint is discussed more fully in a subsequent section.

Figure 39 shows part of the third-stage thrust cone and engine assembly, including the gimbal joint. The plastic tubing is part of the ullage pressurization system. The fully assembled third stage is shown in figure 40.

Apollo payload.- The simulated lunar module (LM) is shown in figure 41. The internal ballast mass used to achieve proper mass and center of gravity can be seen. Four tubular support assemblies form the attachment truss necessary to connect the model LM to the LM adapter structure which is shown partially constructed in figure 42. An aluminum ring, shown near the base of the adapter cone, supports the model LM. The adapter is a truncated cone of honeycomb sandwich construction. The face sheets are 0.0017-inch (0.004 cm) thick aluminum. The core thickness varies from 0.150 inch (0.38 cm) forward to 0.25 inch (0.635 cm) aft. The honeycomb core is of 1/8-inch (0.32 cm) hexagonal cell with wall thickness of 0.0015 inch (0.0038 cm). Figure 43 shows the LM mounted in the adapter structure.

The simulated Apollo service and command modules and the launch escape system are shown assembled in figure 44. The simulated service module is a cylindrical shell consisting of a single aluminum sheet of varying thickness, bonded to a 1.33-inch (3.38 cm) thick foamed plastic section. The simulated command module is a truncated cone of similar construction. The simulated launch escape system is a machined aluminum tube having a constant inside diameter of 2.54 inches (6.45 cm) and a varying thickness.

#### Examples of Solutions to Model Design and Construction Problems

Some typical model structural components and assemblies are shown in figures 45 to 49. These figures serve to illustrate manufacturing and assembly processes which, although not identical to processes utilized in prototype construction, result in equivalent hardware. These figures also are indicative of the complexity of the model and the detail to which the full-scale vehicle was reproduced in the model.

Hat-shaped stringers.- Perhaps the most commonly encountered deviation from true geometric scaling for this model lay in the treatment of the variable cross-section, hat-shaped external stringers found on most of the unpressurized compartment skins. The prototype stringers were extruded hat sections of varying cross section both longitudinally and circumferentially and were riveted to the skin. The model stringers were formed from sheet stock, similarly proportioned to those on the prototype, but with constant cross section to which flat doubler sheets were added to provide the required variations in area and inertia. This procedure is illustrated in figure 45 which shows a typical variable-cross-section stringer designed from direct geometric scaling and the same stringer as found on the model.

Ring frames.- Another example of deviation from true geometric scaling is illustrated in figure 46. The figure shows two variations of the same substructure, one of the intermediate ring frames in the first-stage tail section. Figure 46(a) depicts a scaled duplication of full-scale hardware in which each of the eight sections of the ring has a constant longitudinal dimension, or thickness, and a circumferentially varying radial dimension, or width. The design of figure 46(b) results in a dynamically equivalent substructure with a considerable reduction in fabrication time and cost. It consists of eight sections each of which is of constant width but with circumferentially varying thickness. This more economical design was chosen for the 1/10-scale model and is shown pictorially in figure 12.

In the fabrication of all constant-cross-section ring frames in the model, an alternate manufacturing procedure was utilized which produced geometrically similar structural components with fewer and less intricate machine processes. This procedure is illustrated in figure 47. Direct duplication of prototype ring frames would require individual shaping of five separate parts and then welding of these parts into a single unit as shown in figure 47(a). The typical model design shown in figure 47(b) eliminates much of the machining and fabrication work by machining the ring as a single piece from a forging and then adding a formed one-piece stiffener. The resultant structure has the same structural dynamic properties as the more complex exact miniaturization of the full-scale structure.

Structural joints.- In a few instances, alternate designs were required in order to permit assembly of the structural components. A typical design variation of this type is illustrated in figure 48. The structure depicted is the S-IVB aft-bulkhead—common-bulkhead joint. In the full-scale structure, shown in figure 48(a), the joint is fabricated with rivets and welds. This method of construction was impossible in the model structure because of the inaccessibility of the LOX tank interior. Consequently, a joint design was adopted for incorporation into the 1/10-scale model which permits the final closure to be effected externally. This design is shown as figure 48(b). The bulkhead structure near the joint was locally modified by adding a relatively heavy adapter ring to which the

bulkhead was riveted. This ring was then bolted to the skin from the outside and a bead of sealant compound was applied at the intersection of the common bulkhead and the LH<sub>2</sub> tank wall. The resultant joint is therefore not a true representation of the full-scale component.

Perhaps one of the most graphic indications of the complexity of the model and the degree to which the prototype is duplicated is obtained by examination of other structural joints employed in the model. Details of several of these joint areas are presented in figure 49. The location of these joints is shown in figure 6 by the lettered circles on the left-hand side of the model drawing. The joints which appear in figure 49 carry corresponding letter identifications.

Figure 49(a) is the junction of the S-IC fuel tank and the intertank section. The fuel-tank upper bulkhead, the fuel tank wall, and the intertank section are joined by a Y-ring assembly. There exists a deviation from replica scaling in that one leg of the Y-ring is attached by a bolted flange to allow access to the intertank interior areas. The intertank—Y-ring connection is an unusual joint, made necessary by the complex corrugated intertank skin, and consists of channeled strips attached alternately to the inside and outside surfaces of the Y-ring leg from the corrugated intertank surface. Part of this joint is also shown photographically in figure 24. A similar joint (fig. 49(b)) is used at the intersection of the lower LOX tank-bulkhead—LOX-tank-wall and intertank structure. This joint, however, is closed by a weld rather than by the bolted flange connection. At the junction of the S-IC LOX tank upper bulkhead and the tank-wall—forward-skirt interface shown in figure 49(c), a variation in fabrication procedure was utilized in the model structure. In order to complete the final weld in the joint, the Y-ring was fabricated in two pieces and the shorter leg was spotwelded to the locally thickened forward-skirt skin. The closure was then effected by an external weld. The resultant hardware has the same basic dimensional properties as would have resulted from direct geometric scaling.

The model joints shown in figures 49(d) and 49(e), respectively, are scaled duplicates of prototype joints with the exception that the number of fasteners used in the model is less than the number required on the prototype. The fasteners, however, were sized so that the total fastener area was a scaled quantity. The application of replica scaling to the joint shown in figure 49(d) was judged to be the most expedient approach since considerable engineering time would have been required to design properly a more easily manufactured connection with comparable dynamic properties. Further, the scaling laws applicable to a joint of this type are not sufficiently defined to permit evaluation of any alternate design, particularly the effect of the pinned-truss ring frame braces.

The remaining structural joints shown in figures 49(f) to 49(l) are essentially scaled duplicates of the full-scale structure with the exceptions of previously noted deviations in ring-frame and bulkhead constructions.

Fabrication problem areas.- Other fabrication problems, not classified as design deviations, include machining process, metal forming procedures, machine and chemical milling tolerances, fastening methods, and welding techniques. Not only can the solution of these problems dictate the degree to which a given launch vehicle can be reproduced to a specified reduced scale, but they also can be significant factors in establishing the economic feasibility of acquiring a dynamic model such as the 1/10-scale Apollo/Saturn V. If the resulting fabrication limitations are practical, it may be possible to duplicate the full-scale, or prototype, structure at a predetermined reduced size at less cost than would be needed to simulate the structure by employing corresponding expensive engineering time. In addition, it is inevitable that as additional models are designed and constructed and as compatible parallel fabrication techniques are developed, the state of the art of producing lightweight structures must improve and thus allow a possible increase in scale factor and a model having correspondingly more refined details.

Refined structures, such as the 1/10-scale Apollo/Saturn V dynamic model, should be fabricated and assembled by specialists who are familiar with handling extremely lightweight and thin-skinned materials as specified by the design. In addition, shaping and attaching the components needed for the subassemblies require the employment of specialized machinery and equipment and can, in fact, even dictate the need for development of a new generation of fabrication processes. Nominal machine and fabrication shop practices, as employed in the manufacture of present-day airframes and launch vehicles, are adequate for the heavier gage full-scale structures; but the production of the involved model was greatly aided by the use of modified metal cutting machines and by the use of unique forgings from which model components could be machined. The forging, in this case, consisted of a large hollow cylindrical piece having an inside diameter of about 39 inches (99.06 cm) and an outer diameter of about 42 inches (106.68 cm) from which many ring frames could be machined at a significant cost reduction without any sacrifice of machining accuracy.

Although the nominal tolerances, as accepted for standard machine shop work, cannot be scaled in the same ratio as the model scale factor, care can be taken to insure that the machinery used will restrict the variation of dimensions to an acceptable level. Care can also be exercised to control the more significant dimensions with a greater tolerance than allowed in the less critical areas. For example, when designing for the bending stiffness of a given tank section, the thickness of the skin panel is more critical than the dimensions of the associated integrally milled stiffeners. In addition, it is also noted that in general as related to panel thickness, tolerances accepted for chemical milling processes cannot have any greater accuracy than exist for the required preparatory machine milling processes. With proper component design, equipment preparation, and careful fabrication procedures, the efficiency and accuracy of the machine work can be maintained with satisfactory results.

Another specific fabrication problem was encountered when forming the second- and third-stage waffle pattern skins. It was necessary to develop a method of rolling or forming the individual tank wall panels in a fashion which would not result in a local failure caused by the strong region of stiffness introduced by the integrally milled waffle construction. It was found that by filling the many pockets with an epoxy, covering the entire panel with a relatively soft thin aluminum panel (not attached) and then rolling to the prescribed curvature, a very satisfactory waffle pattern tank wall panel could be formed. The epoxy could be removed with relative ease simply by applying heat to the structure.

Another factor found to be beneficial for fabricating the Apollo/Saturn V model included the methods employed to make required assembly attachments. The full-scale vehicle is fabricated with appropriate weldments, bolts, nuts, and rivets. Obviously, the smaller model must be assembled by other methods because of the impracticability of the reduced-scale attachment hardware. There must be a compromise both in the type and the number of simulated fasteners. Also, it is generally accepted that whenever an effort is made to approximate the structural dynamic properties of a complex structure, the detail design of the joints and attachment hardware should be conservative with a resulting excessively stiff component since any effort to scale directly the size and number of bolts or rivets would be impractical both from a manufacturing and an assembly viewpoint. In addition, although it is true that there can be some conservative distortion of the joint stiffness properties, there can be little hope of achieving any degree of success in reproducing desired damping characteristics, in particular, and this limitation includes skin-stringer construction, when the rivets or bolts are replaced by spot welds. Generally, bolted joints can be represented by using convenient, commercially available fasteners, such as 0-80 screws, a lesser number of fasteners being used, the number of which is determined from the correctly scaled fastener area. This design approximates the proper stiffness and damping. However, for the case where rivets are replaced by spot welds, as with the 1/10-scale model skin-stringer construction, economic feasibility can be the controlling factor. A spot-welding machine to mass produce many consistently uniform nuggets had to be developed and only then could the cost of the model be significantly reduced without appreciable degradation of the model similitude.

#### Quality Assurance and Structural Reliability

In order to assure that the model hardware does indeed meet the design requirements, it was necessary that the design assumptions be verified by test data and that adherence to the manufacturing and fabrication tolerances be carefully controlled. Design loads were calculated by utilizing handbook values for material strengths, weld characteristics, mechanical fastener properties, and bonding material specifications. Random samples of materials to be used in the model were subjected to tests in order to assure a minimum of variance from nominal handbook properties. Failure characteristics of lap

welds, lap bonds, spot welds, and fusion welds were determined for sample specimens corresponding to model configurations.

In areas wherein fabrication procedures were employed which differ from prototype techniques, care was exercised to assure that the resultant components were not structurally degraded by the model fabrication technique. For example, the hat-section stiffeners on the prototype are extruded shapes whereas those on the model are formed from sheet stock. Therefore, the model stringers are subject to local deformations and stress concentrations. Since the 1g inertia loads on the model are only one-tenth those acting on the prototype, there is an inherently large safety factor for the model in spite of any potential degradation of the model structure.

In several instances, it was necessary to substitute different alloys of the same material in order to take advantage of superior metal forming and fabrication properties of the alternate alloys. The gross effects of such substitutions on model integrity must be evaluated. For example, on the prototype, the first-stage tankage is formed with 2219-T87 aluminum and the second- and third-stage tankage is made from 2014-T6 aluminum. The superior weldability of the 2219-T87 alloy led to its employment in all three stages of the model. The 2219-T87 alloy, however, has lower tensile strength than the 2014-T6 alloy; consequently, the allowable pressure capability of the second and third stages is slightly degraded from prototype values. This lower allowable pressure is greater than any anticipated environmental operating pressure and the design pressure requirement for the upper stages was thereby reduced; thus, a safety margin comparable to the prototype was preserved. Verification of the design-pressure load capability was accomplished by hydrostatically testing each of the tanks. In addition, the common bulkheads of the second and third stages were subjected to external hydrostatic pressure tests to insure proper collapse resistance. For the protection of both the model and the test personnel, relief valves were installed in the external gas pressurization system which will prevent operating pressures from approaching the proof test pressures.

One requirement imposed on the model which does not exist for the prototype is the ability of the tankage to survive long-term exposure to potentially corrosive liquids. To satisfy this requirement, the interior of each tank was spray coated with a film of polyurethane with a nominal thickness of 0.002 inch. Test samples of tank material were similarly coated and showed no corrosive degradation with long-term exposure to tap water. Further minimization of corrosion danger was achieved by specifying the use of de-ionized water during test operations. A more comprehensive discussion of the corrosion problem in model space vehicles is given in reference 12.

## Associated Model Components

Replica scaling, where the primary load-carrying structure is geometrically reproduced at one-tenth the size of the prototype, could not be employed in model areas where fabrication limitations and necessary associated component requirements dictated either items for which full-scale hardware design was not complete, which were impossible to manufacture, or which were unique to the model. Sections of the model where full-scale definition and fabrication capabilities limited duplication of full-scale components included the Apollo spacecraft and secondary, or nonload carrying, structure of the booster stages. Associated test components include simulation of liquid propellants, plumbing, suspension system, support fixtures, and instrumentation attachments.

Propellant simulation.- The full-scale Saturn V launch vehicle has RP-1 and liquid oxygen in its first-stage propellant tanks and liquid oxygen and liquid hydrogen in the second- and third-stage propellant tanks. These propellants, with the exception of the first-stage fuel (RP-1), are cryogenic fluids with physical properties that were impractical to accommodate in the design of the 1/10-scale dynamic model. In addition, because of the extremely low temperatures of liquid oxygen and liquid hydrogen, the launch vehicle must have relatively heavy tank wall insulation that is considered nonstructural and can only be considered as added distributed mass along the tank walls. The specific gravity of the onboard liquids with the exception of the LH<sub>2</sub> could be approximated with water which has a specific gravity between the value 0.80 for RP-1 and the value 1.14 for LOX. Proper control of tank water levels then permits the representation of the correct propellant weight but results in some deviation in mass distribution along the vehicle length. The low specific gravity of the hydrogen propellant dictated an extremely lightweight simulant having a specific gravity of 0.07. Small, hollow, styrene plastic balls with a specific gravity of 0.07 were procured as the LH<sub>2</sub> simulant.

Some launch-vehicle propellants and potential-model simulated-propellant specific gravities are indicated in figure 50. The propellants are shown on the left-hand side and the simulants are tabulated on the right-hand side.

Propellant plumbing system.- A schematic view of the necessary plumbing system for handling the simulated liquid propellants of the model is shown in figure 51. Water is gravity fed from a source above the model through appropriate plumbing to the various tanks of the vehicle stages. The simulated propellant supply line can be disconnected from the model after the proper amount of simulant has been added to the various tanks. The water in the tanks, which is used to simulate the true propellant, is buffered and pressurized with nitrogen gas. It was necessary to introduce the water into the tank through the bottom to avoid erosive damage to the tank walls, baffles, and lower bulkhead.

Suspension systems.- A variety of suspension systems may be used in the testing of a model such as the 1/10-scale Saturn V. Several such systems are shown in figure 52

and discussed in reference 13. The choice of a particular system must be based upon the physical properties of the model to be tested, the boundary conditions to be simulated, and the method of introducing the input force. The 1/10-scale Saturn V cannot be suspended with a one-cable system since the model will fail in tension under its own weight. For boundary restraints corresponding to base-cantilevered or simulated prelaunch hold-down, the base-restraint system may be used with properly designed restraint springs. For simulated free-free vibration, adaptations of the harness system were selected for both lateral and longitudinal response tests. For employment of the harness, a light-weight cradle was constructed which served both as support for the model and as an attachment device for the vertical cables. For lateral tests, a two-cable support system with lateral restraint as shown in figure 52(e) was chosen and for longitudinal tests a four-cable system with turnbuckles in each of the four vertical cables. Cable lengths and diameters were selected from static load requirements and to yield model rigid body frequencies during longitudinal tests which will be at least an order of magnitude lower than the lowest structural frequency.

#### CONCLUDING REMARKS

A 1/10-scale structural model of the Apollo-Saturn V launch vehicle was constructed for studies of vehicle dynamics at the Langley Research Center. The project objectives were to provide structural dynamic data for evaluation and improvement of analyses of launch vehicles, to produce data pertinent to the dynamics of the Saturn V vehicle, and to advance the state of the art in the design and fabrication of dynamic models. This paper outlines the design philosophy, presents a limited description of the model as it relates to the prototype, and documents solutions to some design and fabrication problems which were encountered.

Replica scaling of the main load-carrying structural components, which necessitated an extension of the state of the art in fabrication techniques, was employed and resulted in a model which duplicates the full-scale structure to a high degree. Extreme full-scale design details, such as hat-section stringers, corrugated intertank sections, and scaled joint reproduction, were duplicated in the fabrication of the 1/10-scale model. During the model development phase, it was necessary to improve fabrication procedures substantially, to obtain better control of machining and chem-milling tolerances, to gain a better understanding of curvature forming techniques, and to develop the use of aluminum forgings for machining of complex ring frames.

A careful analysis of the prototype structural details was required to ascertain the practical and economic feasibility of duplicating component hardware to the chosen scale factor. In instances where dimensional analysis could adequately define the model requirements, secondary structural elements were simulated rather than replically

scaled. For the primary structure where the model component designs dictated sizes too small to be duplicated, an acceptable design required that only the correct mass and stiffness distributions be retained in the model. Such items as instrumentation black boxes, bottles containing pressurization gases, heat shields, and other secondary nonload-carrying structures were simulated. Other model sections, such as those in the payload, which have skin gages too thin to be duplicated at the selected scaled size were also simulated. Some joints and similar sections could not be adequately defined by the most rigorous present-day dimensional analysis and therefore were built as scaled duplicates of the full-scale members. Other sections, although of secondary importance from a dynamics viewpoint, were replicaly scaled because they required less expenditure of effort with duplicate fabrication than for dynamic simulation. All substitutions were carefully considered, however, lest their inclusion degrade the usefulness of the total structure through either introduction of misleading response data or the suppression of critical responses. In addition, transducers and subsystems, which are integral to the model during the test program but which have no counterpart in the full-scale vehicle, were incorporated into the model design.

With proper care in the selection of the scale factor and methods of manufacture and with judicious evaluation of deviations from direct scaled duplication, replica models are considered technically and economically feasible for studies of the structural dynamic characteristics of large complex launch vehicles. It is believed that this model represents advancements in the state of the art of dynamic modeling and exemplifies the current limit of practical accomplishment in dynamic model design and construction.

Langley Research Center,

National Aeronautics and Space Administration,

Langley Station, Hampton, Va., May 4, 1967,

124-11-05-11-23.

## REFERENCES

1. Brooks, George W.: The Application of Models to Helicopter Vibration and Flutter Research. American Helicopter Society, Inc. (Proc. Ninth Annual Forum, Washington, D.C., May 14-17, 1953.)
2. Regier, Arthur A.: The Use of Scaled Dynamic Models in Several Aerospace Vehicle Studies. Paper presented at ASME Colloquium on Use of Models and Scaling in Simulation of Shock and Vibration (Philadelphia, Pa.), Nov. 1963.
3. Garrick, I. E.: Some Concepts and Problem Areas in Aircraft Flutter. S.M.F. Fund Paper No. FF-15, Inst. Aero. Sci., Mar. 1957.
4. Runyan, H. L.; Morgan, H. G.; and Mixson, J. S.: Use of Dynamic Models in Launch-Vehicle Development. AGARD Rept. 479, May 1964.
5. Mixson, John S.; Catherine, John J.; and Arman, Ali: Investigation of the Lateral Vibration Characteristics of a 1/5-Scale Model of Saturn SA-1. NASA TN D-1593, 1963.
6. Mixson, John S.; and Catherine, John J.: Experimental Lateral Vibration Characteristics of a 1/5-Scale Model of Saturn SA-1 With an Eight-Cable Suspension System. NASA TN D-2214, 1964.
7. Mixson, John S.; and Catherine, John J.: Comparison of Experimental Vibration Characteristics Obtained From a 1/5-Scale Model and From a Full-Scale Saturn SA-1. NASA TN D-2215, 1964.
8. Catherine, John J.: Torsional Vibration Characteristics of a 1/5-Scale Model of Saturn SA-1. NASA TN D-2745, 1965.
9. Chang, C.: Experimental Damping Studies. HREC/0088-1, LMSC/HREC A712619 (Contract NAS8-20088), Lockheed Missiles and Space Co., Jan. 6, 1966.
10. Thompson, William M., Jr.: An Investigation of the Response of a Scaled Model of a Liquid-Propellant Multistage Launch Vehicle to Longitudinal Excitation. NASA TN D-3975, 1967.
11. Jaszlics, Ivan J.; and Morosow, George: Dynamic Testing of a 20% Scale Model of the Titan III. AIAA Symposium on Structural Dynamics and Aeroelasticity, Aug.-Sept. 1965, pp. 477-485.
12. Powell, Clemans A., Jr.; and Scholl, Harland F.: Corrosion Problems With Simulated Fuel in Launch Vehicle Models. Materials Protection, vol. 5, no. 8, Aug. 1966, pp. 33-34.

13. Herr, Robert W.; and Carden, Huey D.: Support Systems and Excitation Techniques for Dynamic Models of Space Vehicle Structures. Proceedings of Symposium on Aeroelastic and Dynamic Modeling Technology. RTD-TDR-63-4197, Pt. I, Aerospace Ind. Assoc., Mar. 1964, pp. 249-277.

TABLE I.- CALCULATED SECTION MASSES AND CENTERS OF GRAVITY  
OF 1/10-SCALE APOLLO/SATURN V MODEL

Section boundaries				Mass of section		Section center-of-gravity model station	
From model station		To model station					
in.	m	in.	m	lbm	kg	in.	m
-11.50	-0.2921	36.48	0.9266	193.1115	87.5954	12.77	0.3243
36.48	.9266	38.48	.9774	1.4426	.6544	37.29	.9472
38.48	.9774	40.48	1.0231	1.4465	.6561	39.37	.9999
40.48	1.0231	42.48	1.0790	1.4560	.6604	41.30	1.0490
42.48	1.0790	44.48	1.1298	1.4724	.6679	43.31	1.1001
44.48	1.1298	46.48	1.1806	1.5049	.6826	45.31	1.1508
46.48	1.1806	48.48	1.2314	1.5910	.7217	47.32	1.2019
48.48	1.2314	50.48	1.2822	1.2168	.5519	49.32	1.2527
50.48	1.2822	52.48	1.3330	1.2839	.5824	51.31	1.3033
52.48	1.3330	54.48	1.3838	1.4979	.6794	53.24	1.3523
54.48	1.3838	56.48	1.4346	1.5088	.6844	55.27	1.4038
56.48	1.4346	58.48	1.4854	1.5392	.6982	57.26	1.4544
58.48	1.4854	60.48	1.5362	1.2279	.5570	59.68	1.5159
60.48	1.5362	62.48	1.5870	4.6451	2.1070	61.65	1.5659
62.48	1.5870	64.48	1.6378	1.6759	.7602	63.26	1.6068
64.48	1.6378	66.48	1.6886	1.7506	.7941	65.36	1.6601
66.48	1.6886	68.48	1.7394	3.0654	1.3905	67.65	1.7183
68.48	1.7394	70.48	1.7902	1.7418	.7901	69.32	1.7607
70.48	1.7902	72.48	1.8410	2.0294	.9205	71.31	1.8113
72.48	1.8410	74.48	1.8918	2.5170	1.1417	73.50	1.8669
74.48	1.8918	76.48	1.9426	2.6906	1.2205	75.16	1.9090
76.48	1.9426	78.48	1.9934	2.3696	1.0748	77.66	1.9726
78.48	1.9934	80.48	2.0442	2.1661	.9825	79.37	2.0160
80.48	2.0442	82.48	2.0950	1.9728	.8949	81.38	2.0670
82.48	2.0950	84.48	2.1458	2.0687	.9384	83.47	2.1201
84.48	2.1458	86.48	2.1966	2.0163	.9146	85.57	2.1735
86.48	2.1966	88.48	2.2474	1.7345	.7868	87.58	2.2245
88.48	2.2474	90.48	2.2982	4.3466	1.9716	89.45	2.2720
90.48	2.2982	92.48	2.3490	1.3759	.6241	91.35	2.3203
92.48	2.3490	94.48	2.3998	1.1163	.5064	93.32	2.3703
94.48	2.3998	96.48	2.4506	1.7750	.8051	95.21	2.4183

TABLE I.- CALCULATED SECTION MASSES AND CENTERS OF GRAVITY  
OF 1/10-SCALE APOLLO/SATURN V MODEL - Continued

Section boundaries				Mass of section		Section center-of-gravity model station	
From model station		To model station					
in.	m	in.	m	lbm	kg	in.	m
96.48	2.4506	98.48	2.5014	1.4549	0.6599	97.28	2.4709
98.48	2.5014	100.48	2.5522	1.6761	.7603	99.23	2.5204
100.48	2.5522	102.48	2.6030	1.4081	.6387	101.28	2.5725
102.48	2.6030	104.48	2.6538	1.6625	.7541	103.26	2.6228
104.48	2.6538	106.48	2.7046	1.3752	.6238	105.29	2.6744
106.48	2.7046	108.48	2.7554	1.6123	.7313	107.27	2.7246
108.48	2.7554	110.48	2.8062	1.3700	.6214	109.29	2.7760
110.48	2.8062	112.48	2.8570	1.6054	.7282	111.29	2.8268
112.48	2.8570	114.48	2.9078	1.3597	.6168	113.29	2.8775
114.48	2.9078	116.48	2.9586	1.7642	.8002	115.32	2.9291
116.48	2.9586	118.48	3.0094	.8531	.3870	117.32	2.9799
118.48	3.0094	120.48	3.0602	1.0739	.4871	119.45	3.0340
120.48	3.0602	122.48	3.1111	.8497	.3854	121.48	3.0856
122.48	3.1111	124.48	3.1619	1.0424	.4728	123.45	3.1356
124.48	3.1619	126.48	3.2127	.7984	.3621	125.41	3.1854
126.48	3.2127	128.48	3.2635	1.0326	.4684	127.42	3.2365
128.48	3.2635	130.48	3.3143	.6825	.3096	129.48	3.2888
130.48	3.3143	132.48	3.6151	.8910	.4041	131.59	3.3424
132.48	3.6151	134.48	3.4159	.6863	.3113	133.48	3.3904
134.48	3.4159	136.48	3.4667	.9128	.4140	135.61	3.4445
136.48	3.4667	138.48	3.5175	.8392	.3807	137.47	3.4917
138.48	3.5175	140.48	3.5683	1.1657	.5288	139.70	3.5484
140.48	3.5683	142.48	3.6191	3.6721	1.6657	141.40	3.5916
142.48	3.6191	144.48	3.6699	1.3858	.6286	143.43	3.6431
144.48	3.6699	146.48	3.7207	1.5527	.7043	145.51	3.6960
146.48	3.7207	148.48	3.7715	1.3313	.6039	147.48	3.7460
148.48	3.7715	150.48	3.8223	1.7682	.8020	149.58	3.7993
150.48	3.8223	152.48	3.8731	1.6910	.7670	151.46	3.8471
152.48	3.8731	154.48	3.9239	2.5190	1.1426	153.53	3.9000
154.48	3.9239	156.48	3.9747	3.5949	1.6306	156.18	3.9670
156.48	3.9747	158.48	4.0255	2.3553	1.0684	157.38	3.9974

TABLE I.- CALCULATED SECTION MASSES AND CENTERS OF GRAVITY  
OF 1/10-SCALE APOLLO/SATURN V MODEL - Continued

Section boundaries				Mass of section		Section center-of-gravity model station	
From model station		To model station		lbm	kg	in.	m
in.	m	in.	m				
158.48	4.0255	160.48	4.0763	3.9940	1.8117	159.95	4.0627
160.48	4.0763	162.48	4.1271	3.8634	1.7524	161.80	4.1097
162.48	4.1271	164.48	4.1779	2.3824	1.0806	163.72	4.1585
164.48	4.1779	166.48	4.2287	12.4644	5.6538	165.65	4.2075
166.48	4.2287	168.48	4.2796	3.4325	1.5570	167.84	4.2631
168.48	4.2796	170.48	4.3304	3.2234	1.4621	169.34	4.3012
170.48	4.3304	172.48	4.3812	3.1670	1.4365	171.28	4.3505
172.48	4.3812	174.48	4.4320	3.2304	1.4653	173.20	4.3993
174.48	4.4320	176.48	4.4828	2.7129	1.2306	175.42	4.4557
176.48	4.4828	178.48	4.5336	2.4135	1.0948	177.31	4.5037
178.48	4.5336	180.48	4.5844	2.5363	1.1505	179.34	4.5552
180.48	4.5844	182.48	4.6352	1.8184	.8284	181.37	4.6068
182.48	4.6352	184.48	4.6860	1.8081	.8201	183.64	4.6644
184.48	4.6860	186.48	4.7368	3.1176	1.4141	185.29	4.7064
186.48	4.7368	188.48	4.7876	3.1992	1.4512	187.49	4.7622
188.48	4.7876	190.48	4.8384	3.4350	1.5581	189.53	4.8140
190.48	4.8384	192.48	4.8892	3.0340	1.3762	191.41	4.8618
192.48	4.8892	194.48	4.9400	2.9514	1.3387	193.42	4.9129
194.48	4.9400	196.48	4.9908	2.9558	1.3408	195.47	4.9649
196.48	4.9908	198.48	5.0416	3.0574	1.3868	197.38	5.0134
198.48	5.0416	200.48	5.0924	.7545	.3422	199.57	5.0691
200.48	5.0924	202.48	5.1432	.6531	.2962	201.27	5.1122
202.48	5.1432	204.48	5.1938	.6537	.2965	203.31	5.1640
204.48	5.1938	206.48	5.2446	.6524	.2959	205.28	5.2141
206.48	5.2446	208.48	5.2954	.6492	.2945	207.28	5.2649
208.48	5.2954	210.48	5.3462	.6071	.2754	209.29	5.3160
210.48	5.3462	212.48	5.3970	.6785	.3078	211.33	5.3678
212.48	5.3970	214.48	5.4478	.6465	.2932	213.42	5.4209
214.48	5.4478	216.48	5.4986	.6620	.3003	215.33	5.4694
216.48	5.4986	218.48	5.5494	.7259	.3293	217.34	5.5204
218.48	5.5494	220.48	5.6002	.6922	.3140	219.23	5.5684

TABLE I.- CALCULATED SECTION MASSES AND CENTERS OF GRAVITY  
OF 1/10-SCALE APOLLO/SATURN V MODEL - Continued

Section boundaries				Mass of section		Section center-of-gravity model station	
From model station		To model station					
in.	m	in.	m	lbm	kg	in.	m
220.48	5.6002	222.48	5.6510	0.6390	0.2898	221.38	5.6230
222.48	5.6510	224.48	5.7018	.6519	.2957	223.28	5.6713
224.48	5.7018	226.48	5.7526	.6388	.2898	225.37	5.7244
226.48	5.7526	228.48	5.8034	.6388	.2898	227.28	5.7729
228.48	5.8034	230.48	5.8542	.6461	.2931	229.36	5.8257
230.48	5.8542	232.48	5.9050	.6232	.2827	231.24	5.8735
232.48	5.9050	234.48	5.9558	.5446	.2470	233.52	5.9314
234.48	5.9558	236.48	6.0066	.4752	.2156	235.48	5.9812
236.48	6.0066	238.48	6.0574	.7705	.3495	237.74	6.0386
238.48	6.0574	240.48	6.1082	1.1734	.5322	239.41	6.0810
240.48	6.1082	242.48	6.1590	.9813	.4451	241.46	6.1331
242.48	6.1590	244.48	6.2098	1.0450	.4740	243.41	6.1826
244.48	6.2098	246.48	6.2606	1.1297	.5124	245.54	6.2367
246.48	6.2606	248.48	6.3114	1.3481	.6115	247.37	6.2832
248.48	6.3114	250.48	6.3622	1.2580	.5706	249.35	6.3335
250.48	6.3622	252.48	6.4130	1.7811	.8079	251.65	6.3919
252.48	6.4130	254.48	6.4638	.9014	.4089	253.15	6.4300
254.48	6.4638	256.48	6.5146	.8393	.3807	255.11	6.4798
256.48	6.5146	258.48	6.5654	1.1525	.5228	257.27	6.5346
258.48	6.5644	260.48	6.6162	1.3880	.6296	259.63	6.5946
260.48	6.6162	262.48	6.6670	1.3525	.6135	261.92	6.6528
262.48	6.6670	264.48	6.7178	2.2489	1.0201	263.54	6.6939
264.48	6.7178	266.48	6.7686	.9846	.4466	265.52	6.7442
266.48	6.7686	268.48	6.8194	.4108	.1863	266.20	6.7615
268.48	6.8194	270.48	6.8702	2.0215	.9170	269.23	6.8384
270.48	6.8702	272.48	6.9210	.6648	.3015	271.62	6.8991
272.48	6.9210	274.48	6.9718	1.2165	.5518	273.50	6.9469
274.48	6.9718	276.48	7.0226	1.0095	.4579	275.25	6.9913
276.48	7.0226	278.48	7.0734	.6011	.2726	277.52	7.0490
278.48	7.0734	280.48	7.1242	2.0140	.9135	279.66	7.1033
280.48	7.1242	282.48	7.1750	1.5095	.6847	281.29	7.1448

TABLE I.- CALCULATED SECTION MASSES AND CENTERS OF GRAVITY  
OF 1/10-SCALE APOLLO/SATURN V MODEL - Concluded

Section boundaries				Mass of section		Section center-of-gravity model station	
From model station		To model station		lbm	kg	in.	m
in.	m	in.	m				
282.48	7.1750	284.48	7.2258	1.3969	0.6336	283.23	7.1940
284.48	7.2258	286.48	7.2766	.9029	.4096	285.26	7.2456
286.48	7.2766	288.48	7.3274	.7788	.3533	287.29	7.2971
288.48	7.3274	290.48	7.3782	.4761	.2160	289.27	7.3474
290.48	7.3782	292.48	7.4290	.4758	.2158	291.27	7.3982
292.48	7.4290	294.48	7.4798	.4756	.2157	293.27	7.4490
294.48	7.4798	296.48	7.5306	.4756	.2157	295.27	7.4998
296.48	7.5306	298.48	7.5814	.4312	.1956	297.22	7.5494
298.48	7.5814	300.48	7.6322	.3879	.1760	299.27	7.6014
300.48	7.6322	302.48	7.6830	.3883	.1761	301.27	7.6522
302.48	7.6830	304.48	7.7338	.3150	.1429	303.38	7.7058
304.48	7.7338	306.48	7.7846	.2830	.1284	305.48	7.7592
306.48	7.7846	308.48	7.8354	.2829	.1283	307.48	7.8100
308.48	7.8354	310.48	7.8862	.6955	.3155	309.85	7.8702
310.48	7.8862	312.48	7.9370	.4235	.1921	311.48	7.9116
312.48	7.9370	314.48	7.9878	.4741	.2150	313.25	7.9566
314.48	7.9878	316.48	8.0386	.3891	.1765	315.38	8.0106
316.48	8.0386	318.48	8.0894	.5955	.2701	317.19	8.0566
318.48	8.0894	320.48	8.1402	.7574	.3436	319.45	8.1140
320.48	8.1402	322.48	8.1910	1.0266	.4657	321.65	8.1699
322.48	8.1910	325.855	8.2767	3.6628	1.6614	324.01	8.2298
325.855	8.2767	359.455	9.1301	32.9750	14.9575	335.26	8.5156
359.455	9.1301	377.655	9.5924	49.3576	22.3886	366.73	9.3149
377.655	9.5924	384.055	9.7550	6.6470	3.0151	380.22	9.6576
384.055	9.7550	394.055	10.0090	1.4770	.6700	387.90	9.8527
394.055	10.0090	399.055	10.1360	1.0065	.4565	396.56	10.0726
399.055	10.1360	404.055	10.2630	2.2288	1.011	401.56	10.1996
404.055	10.2630	409.055	10.3900	1.7914	.8126	406.56	10.3266
409.055	10.3900	414.055	10.5170	1.1803	.5354	411.56	10.4536
414.055	10.5170	419.055	10.6440	.7549	.3424	416.56	10.5806
419.055	10.6440	424.055	10.7710	.2816	.1277	420.72	10.6863

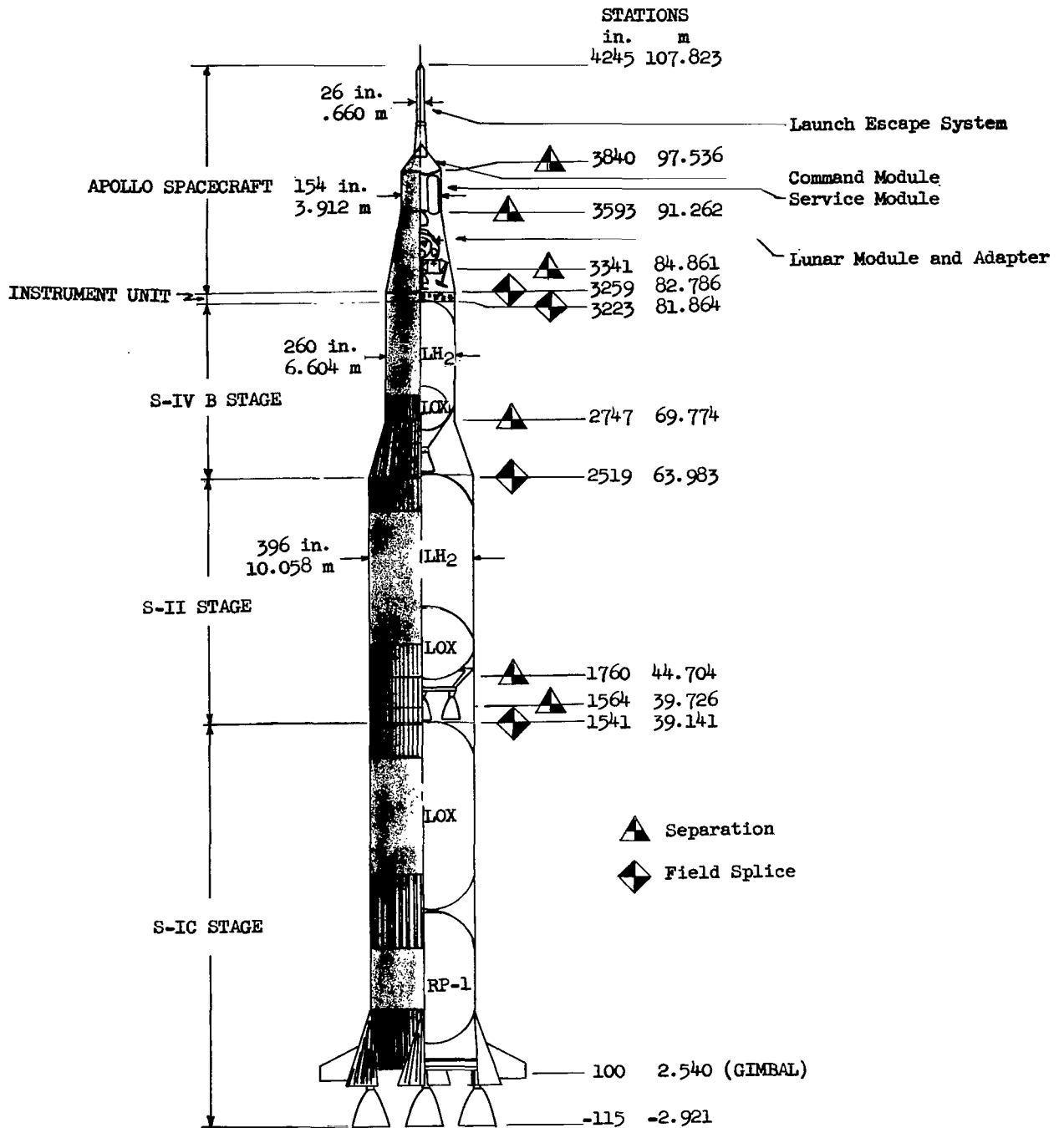


Figure 1.- Schematic of Apollo/Saturn V flight vehicle configuration.

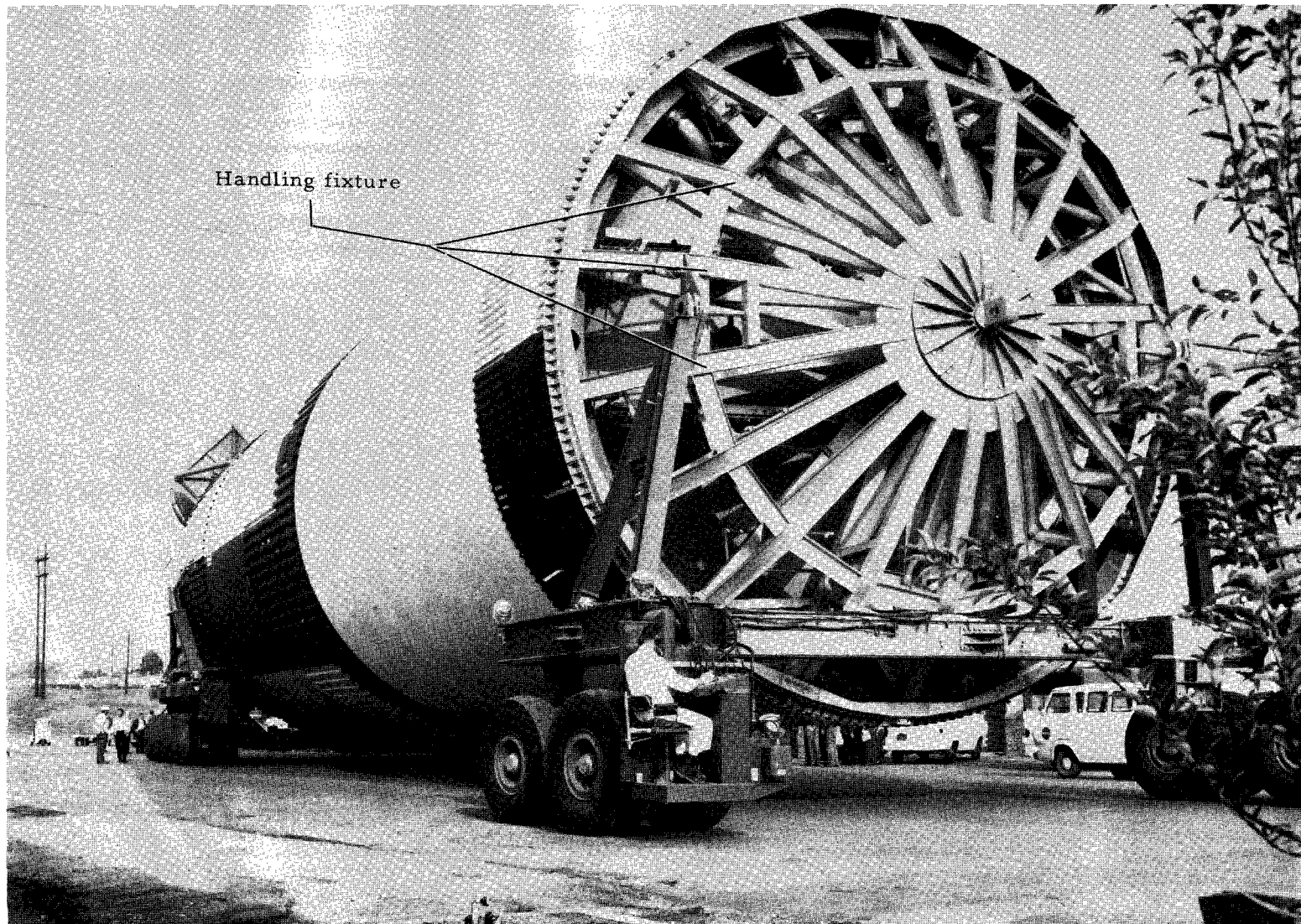


Figure 2.- Saturn V. S-IC stage.

L-67-1039

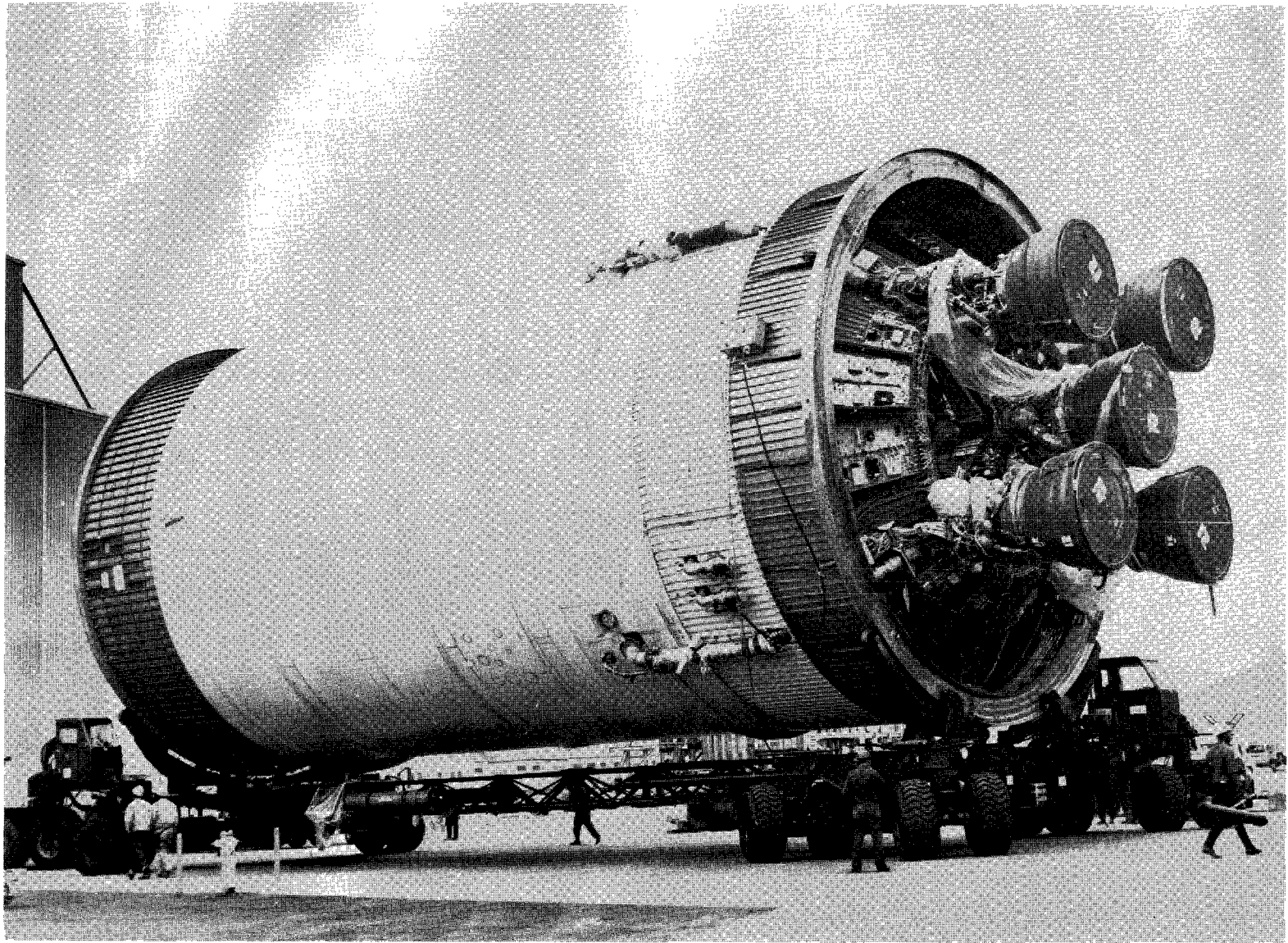


Figure 3.- Saturn V. S-II stage.

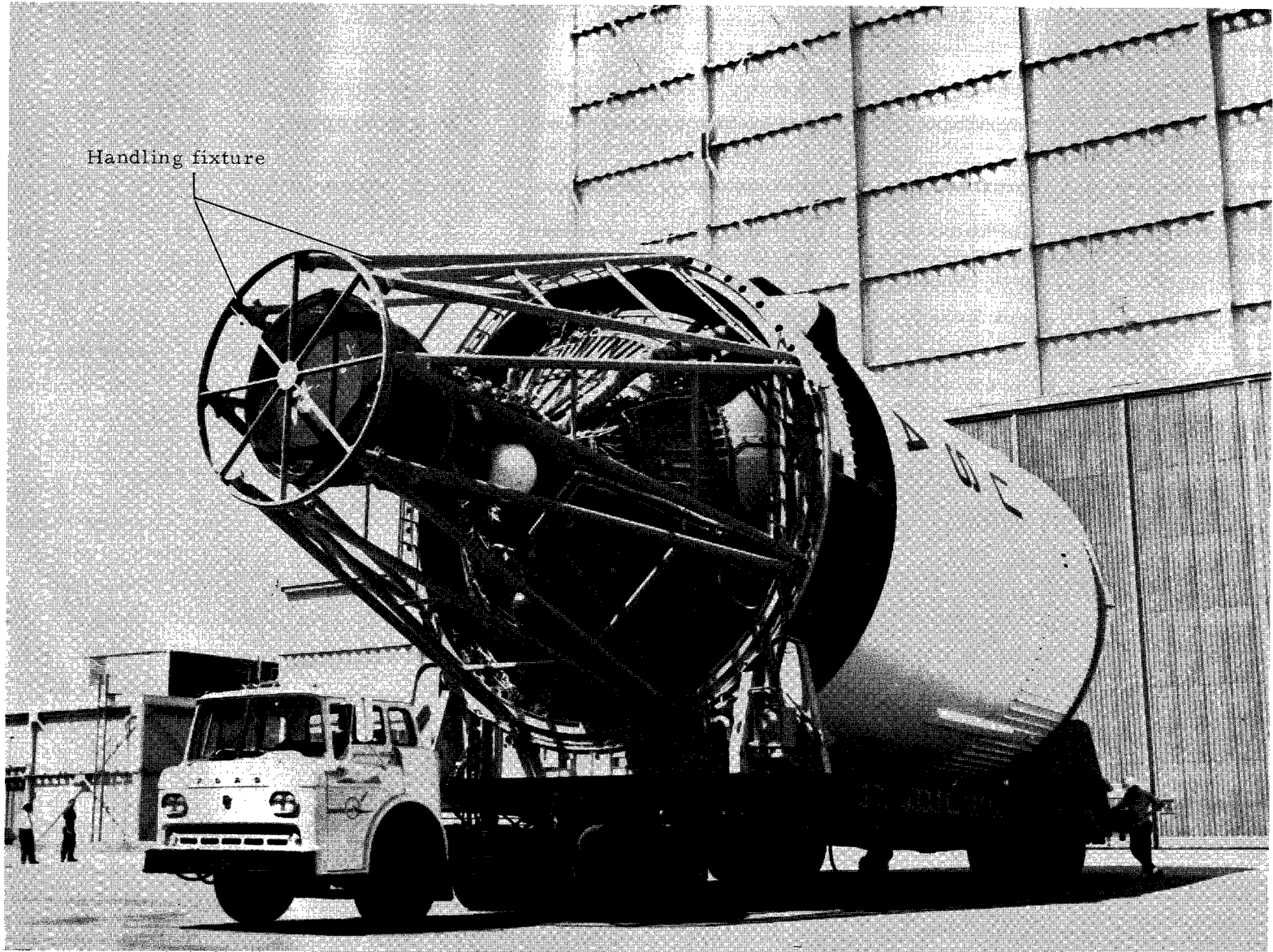


Figure 4.- Saturn V. S-IVB stage.

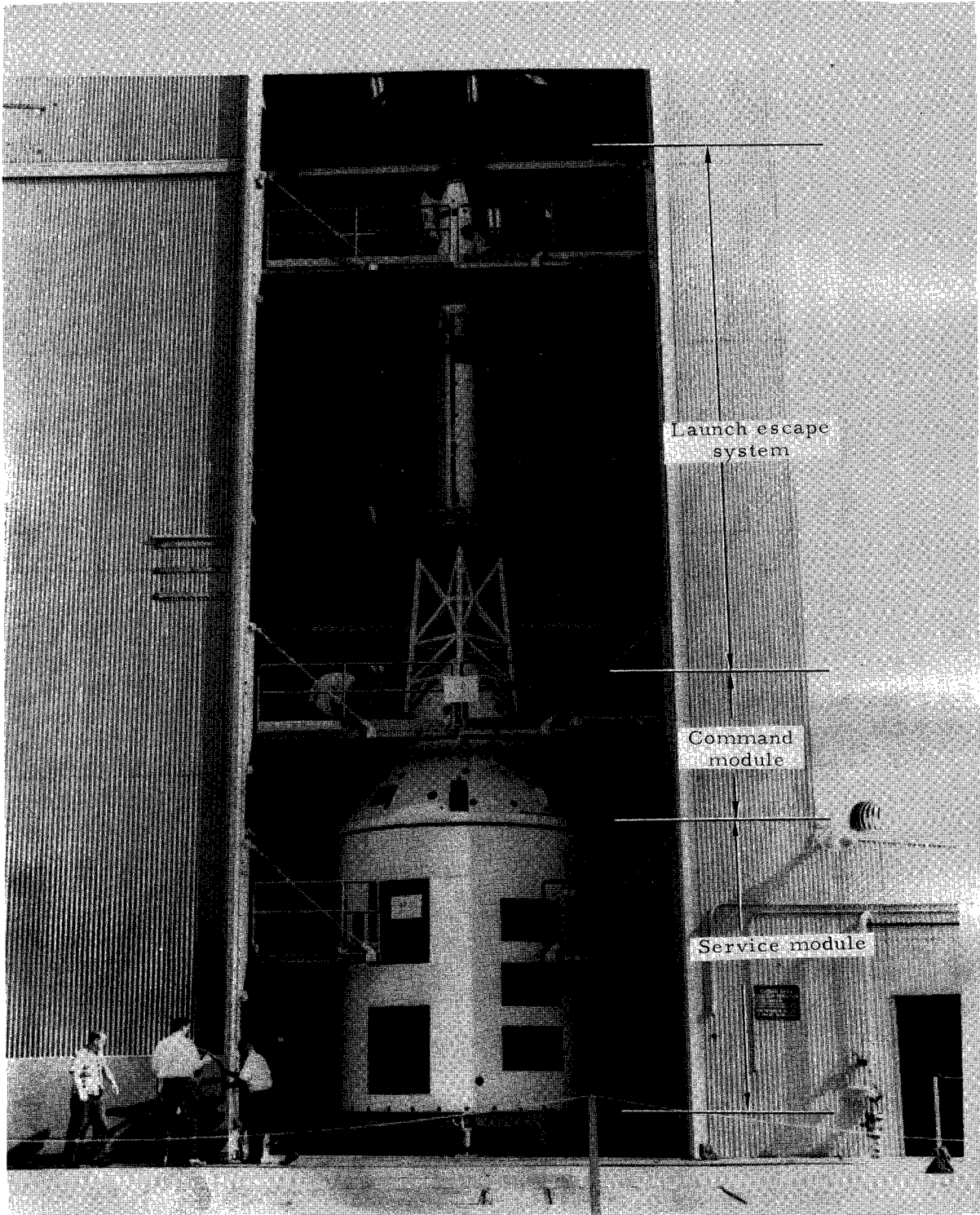


Figure 5.- Apollo spacecraft. Command and service modules and launch escape system.

L-67-1049

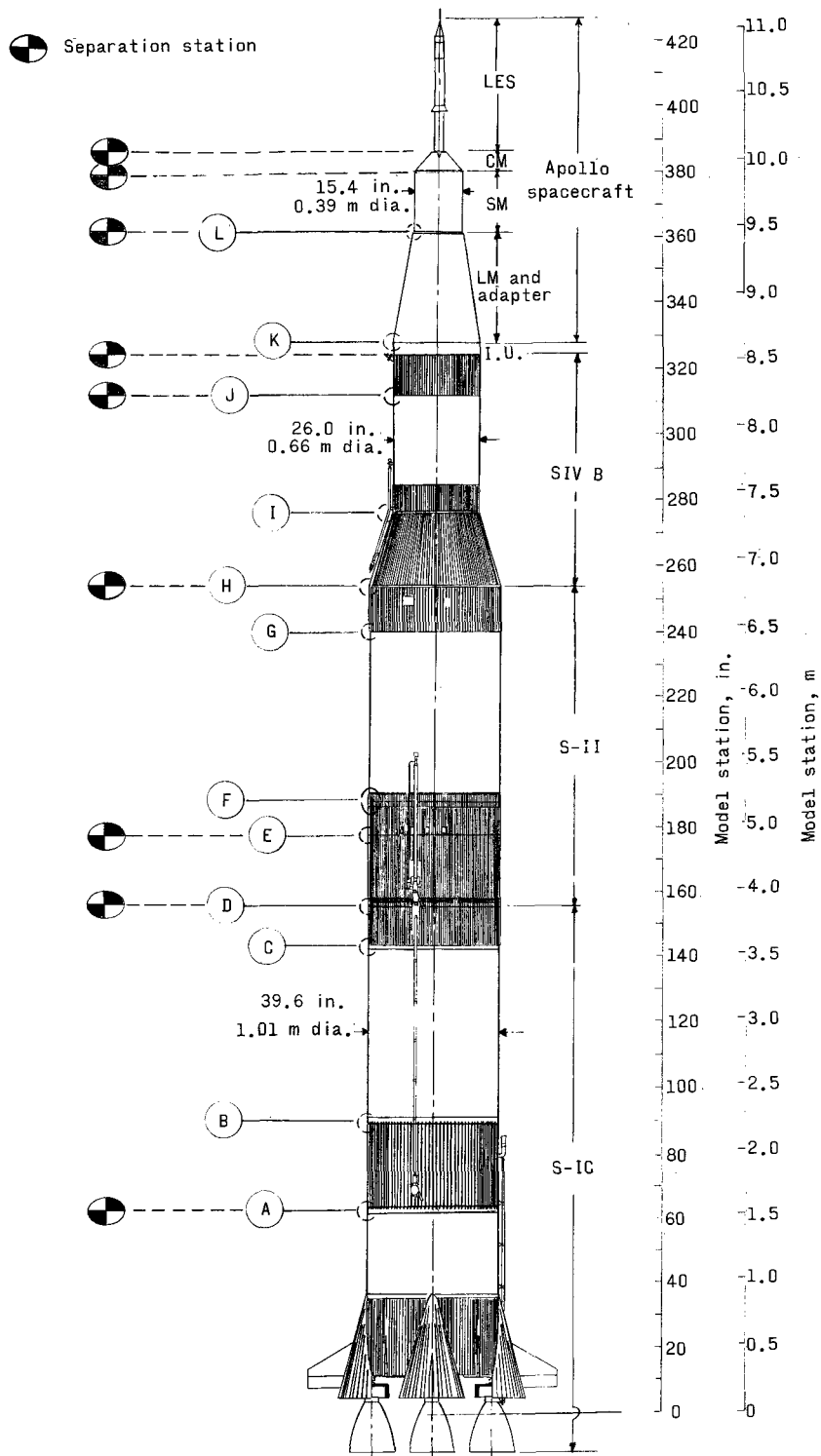


Figure 6.- Schematic of 1/10-scale Apollo/Saturn V model.

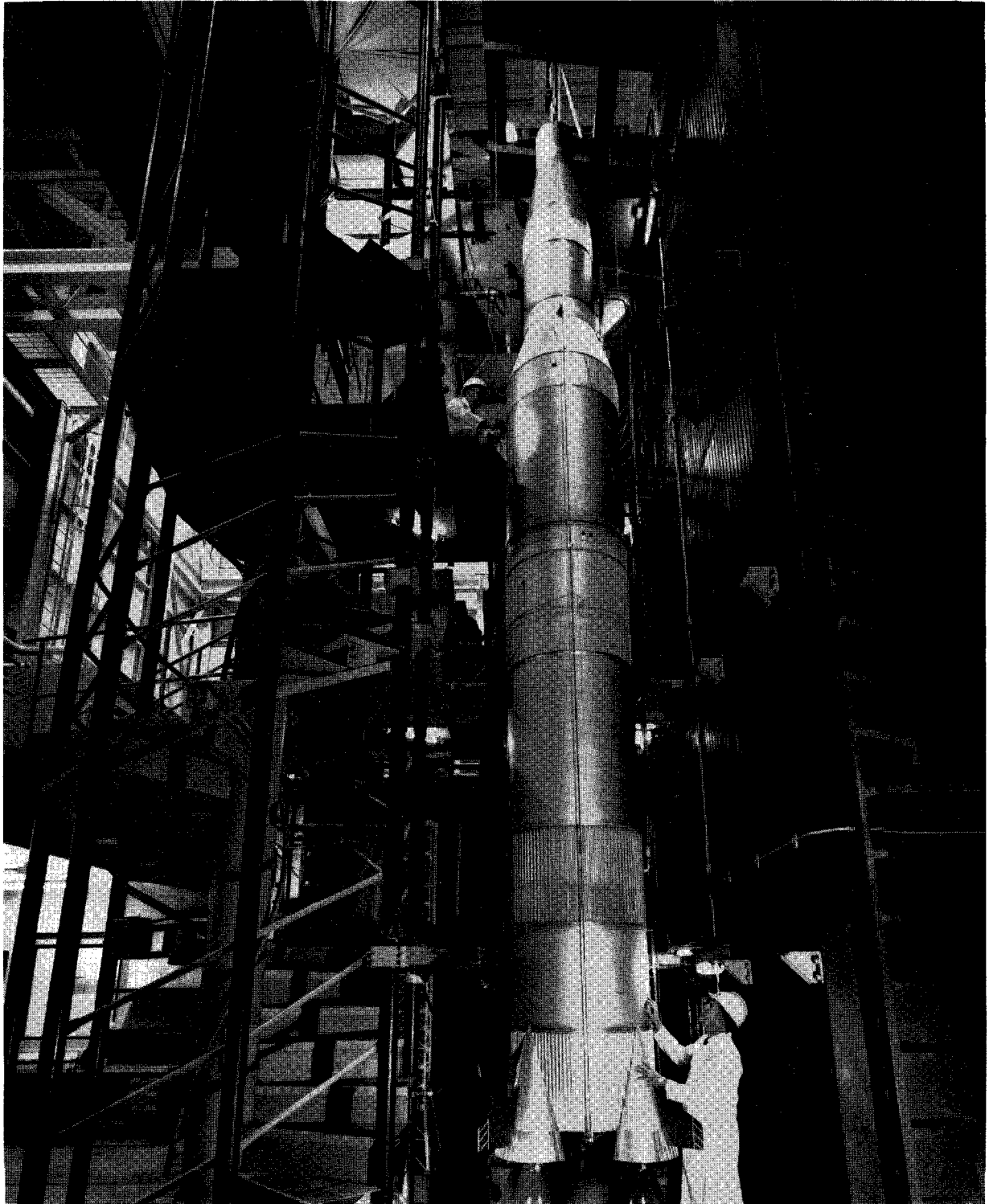


Figure 7.- 1/10-scale Apollo/Saturn V model in test stand.

L-65-8727

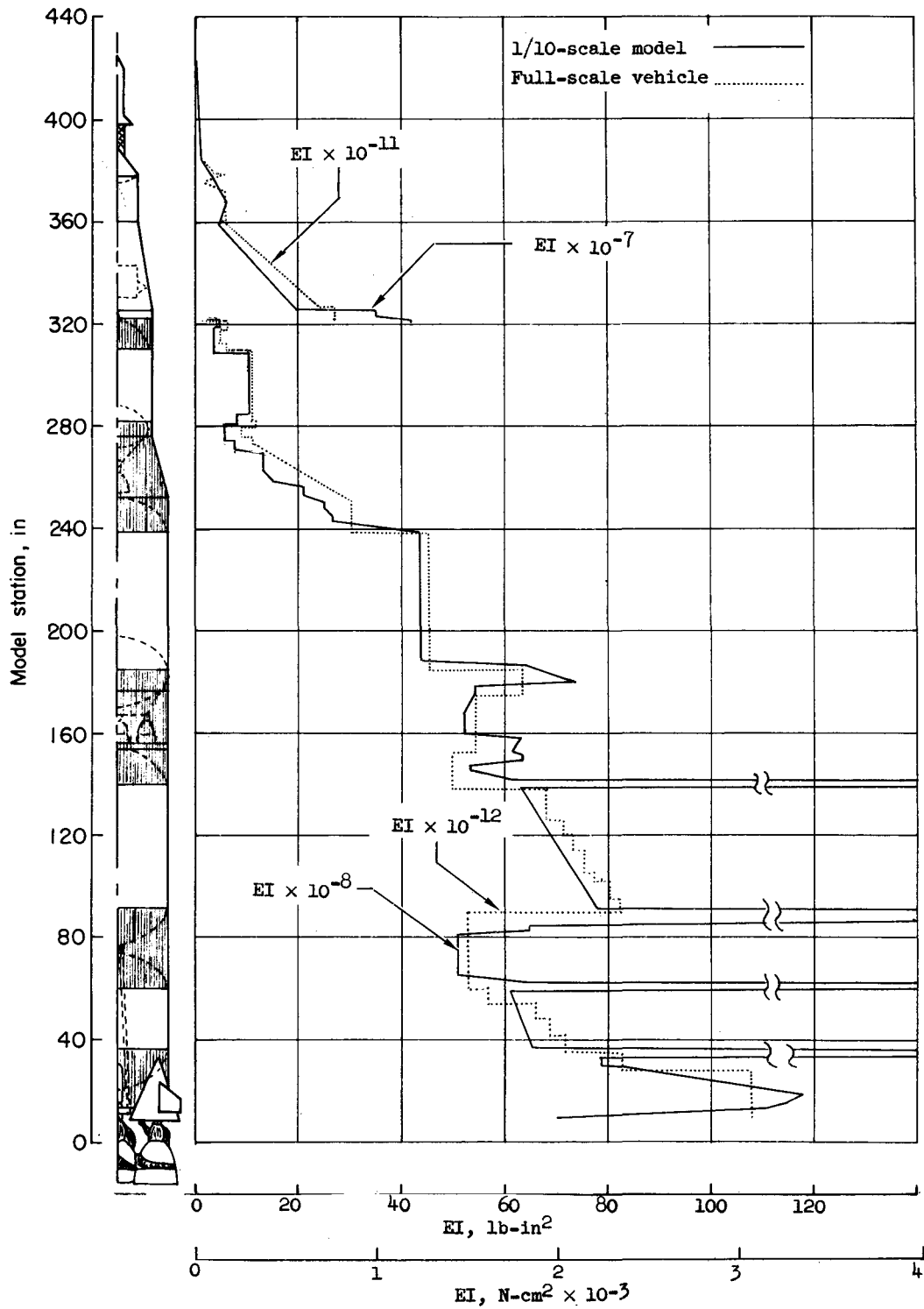


Figure 8.- Comparison of 1/10-scale model and full-scale vehicle bending stiffness.

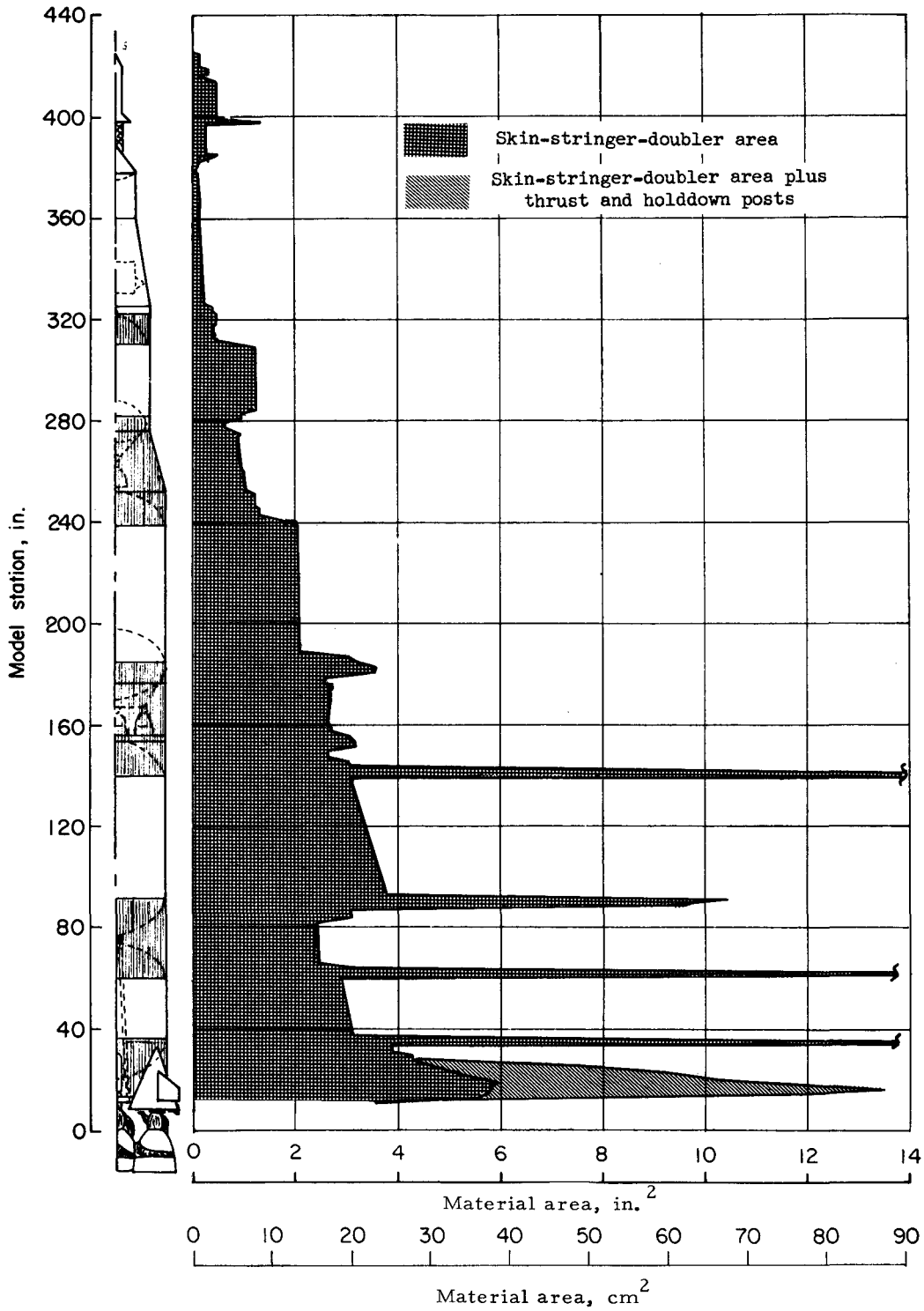


Figure 9.- 1/10-scale model material area (longitudinal stiffness proportional to area).

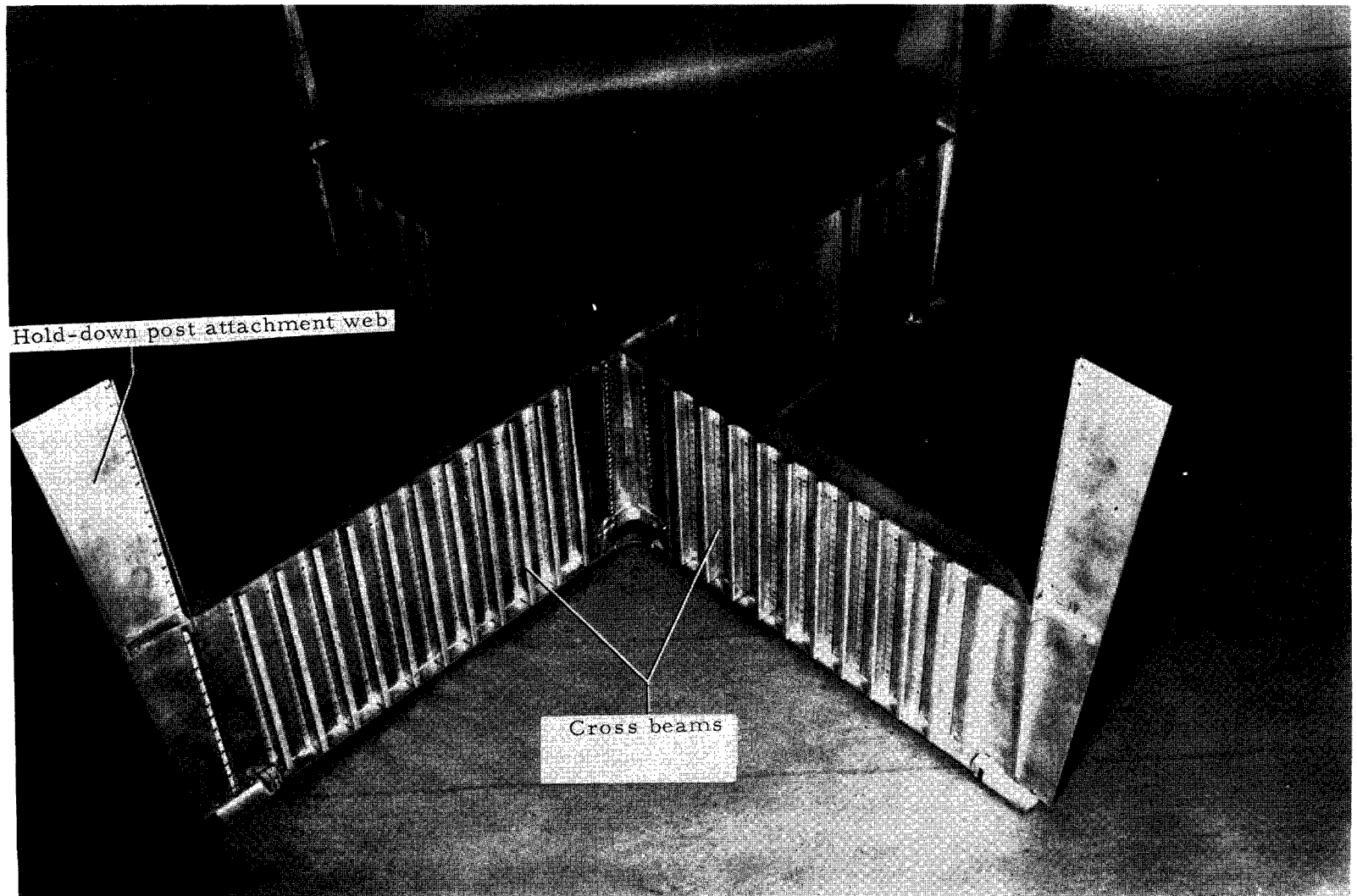


Figure 10.- S-1C center engine support beam assembly, 1/10-scale model.

L-67-1025

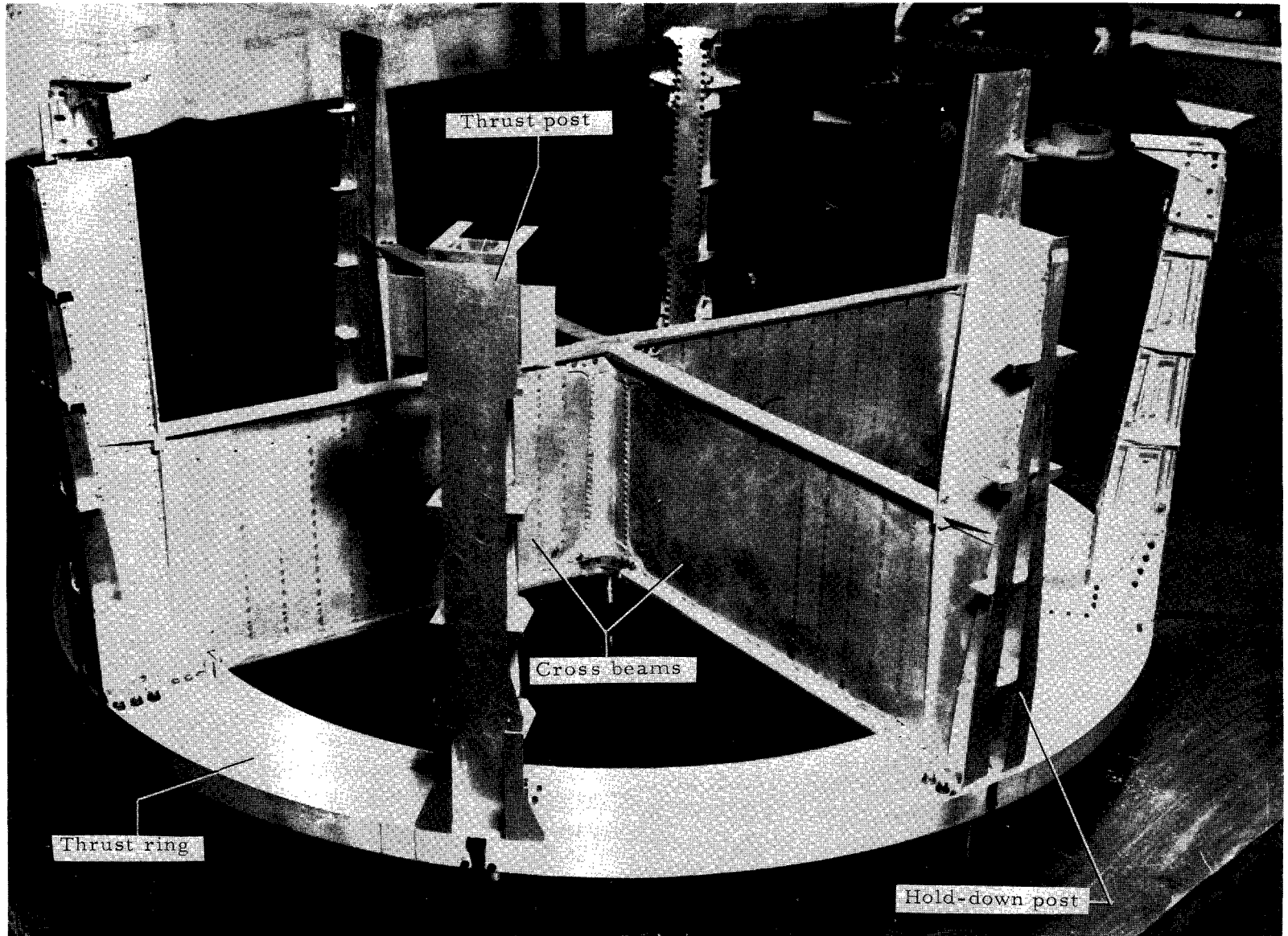


Figure 11.- S-IC thrust structure, partial assembly. 1/10-scale model.

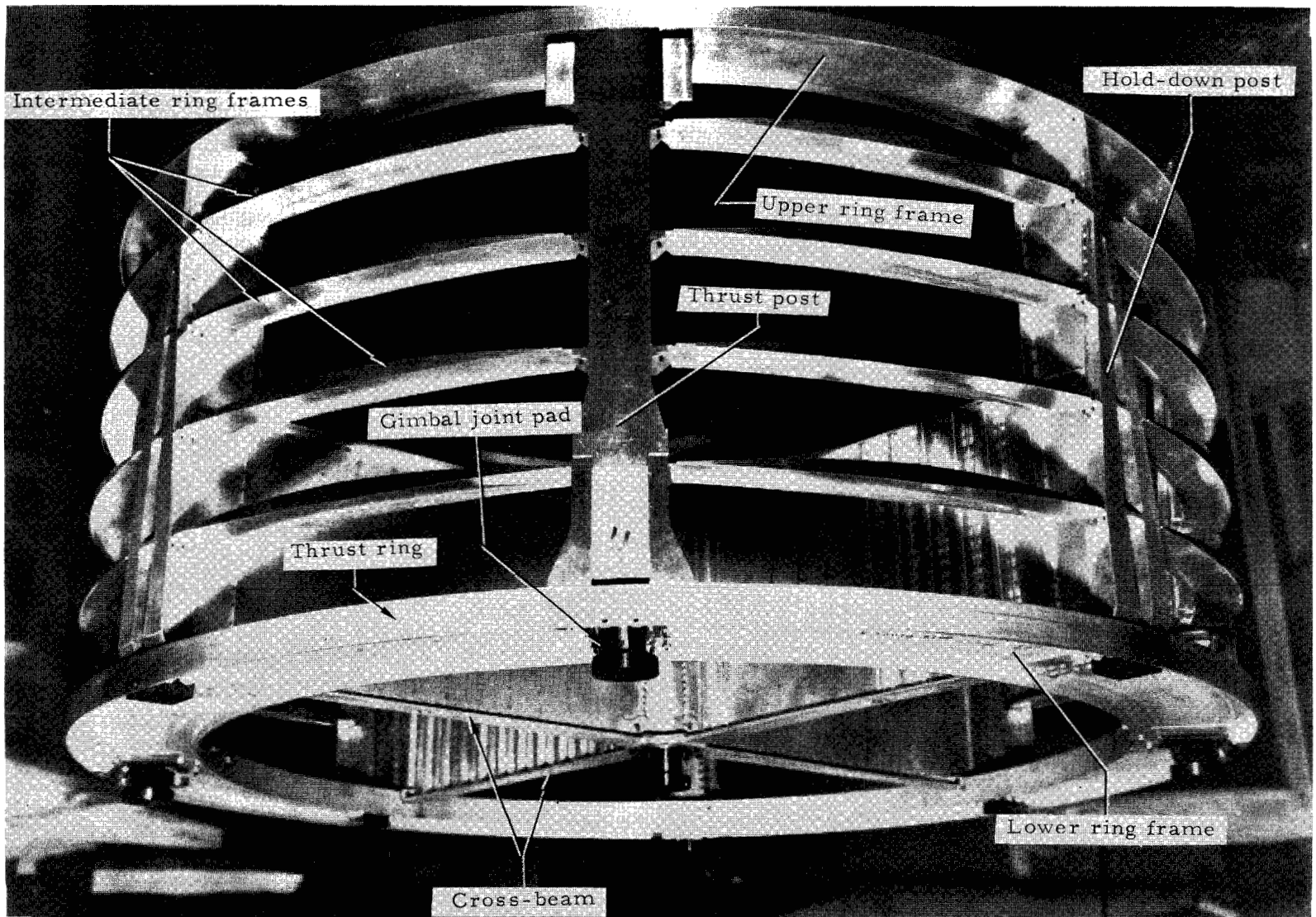


Figure 12.- S-IC thrust structure, partial assembly. 1/10-scale model.

L-67-1023



Figure 13.- Fabrication of skin/stringer structure. 1/10-scale model.

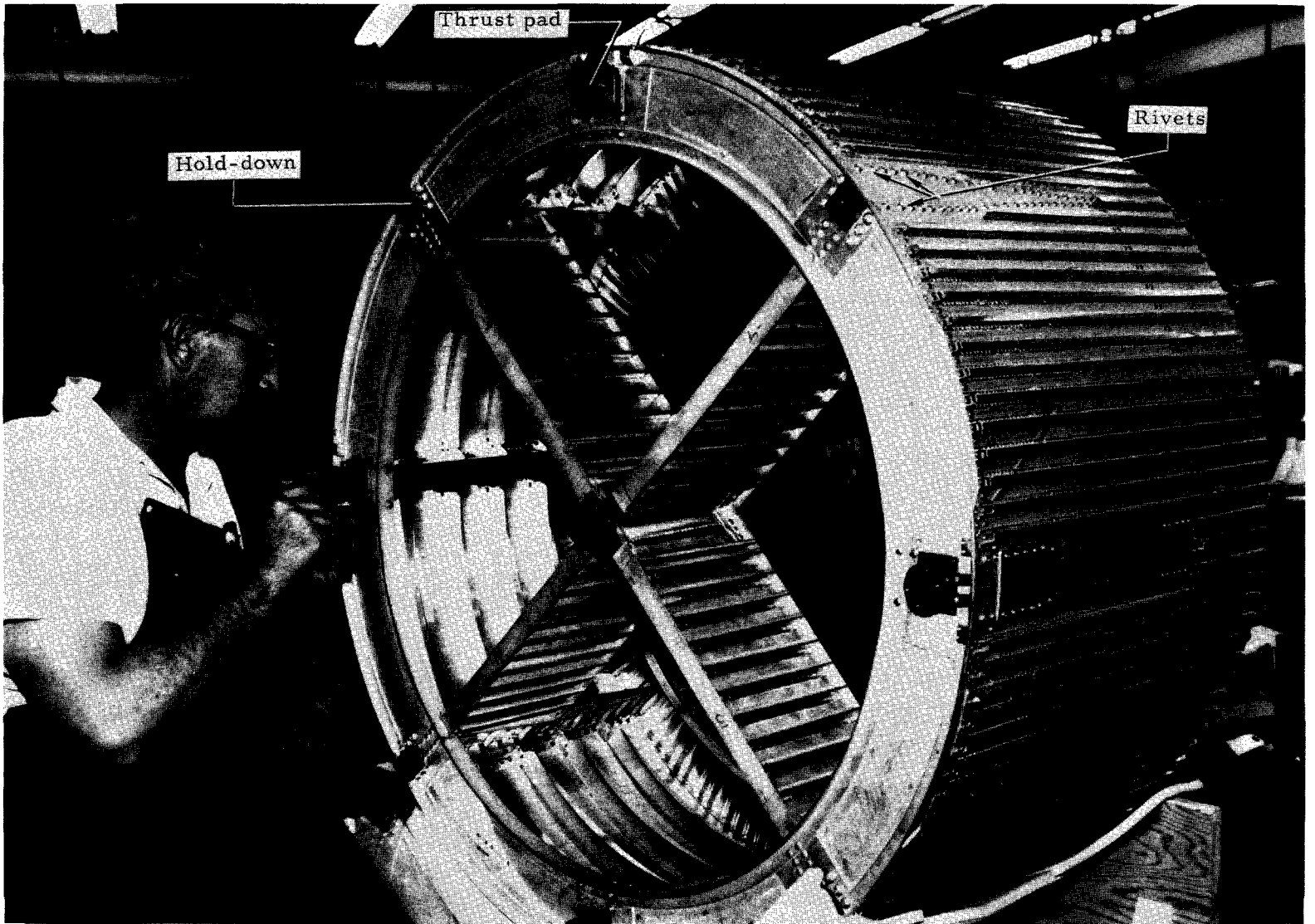


Figure 14.- S-IC thrust structure assembly. 1/10-scale model.

L-67-1031

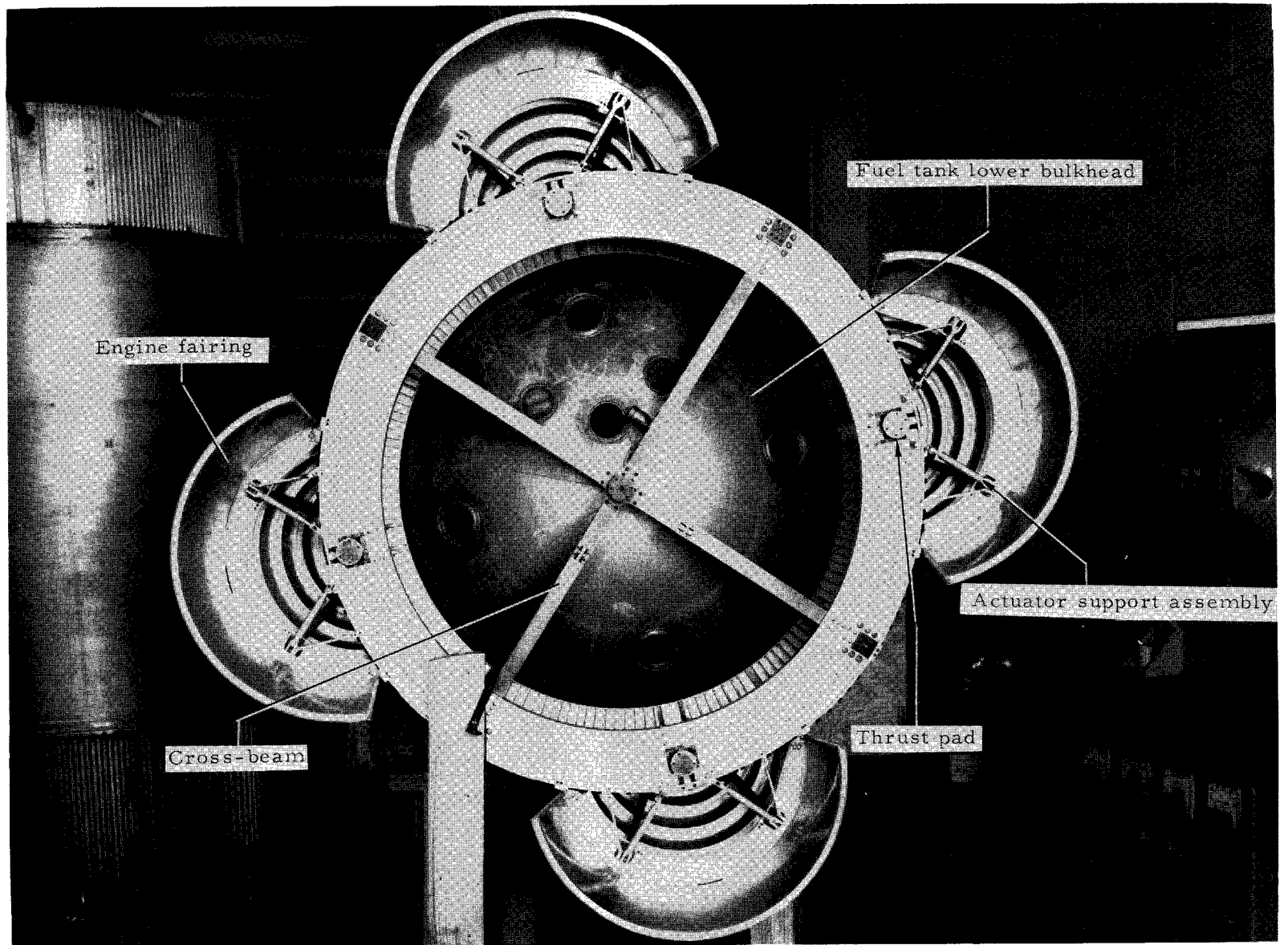


Figure 15.- Aft view of S-1C stage. 1/10-scale model.

L-64-9170.1

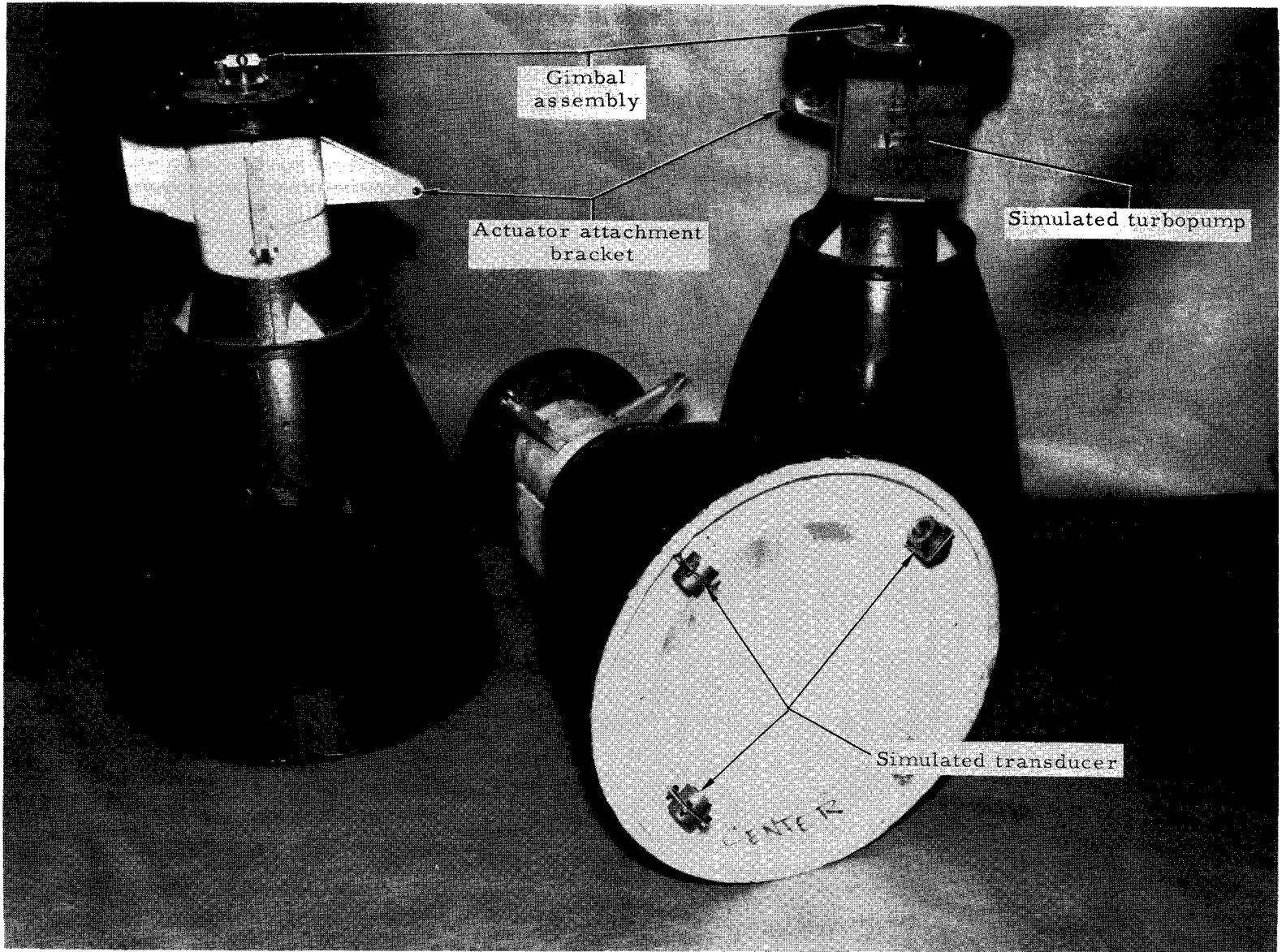


Figure 16.- Simulated F-1 engines. 1/10-scale model.

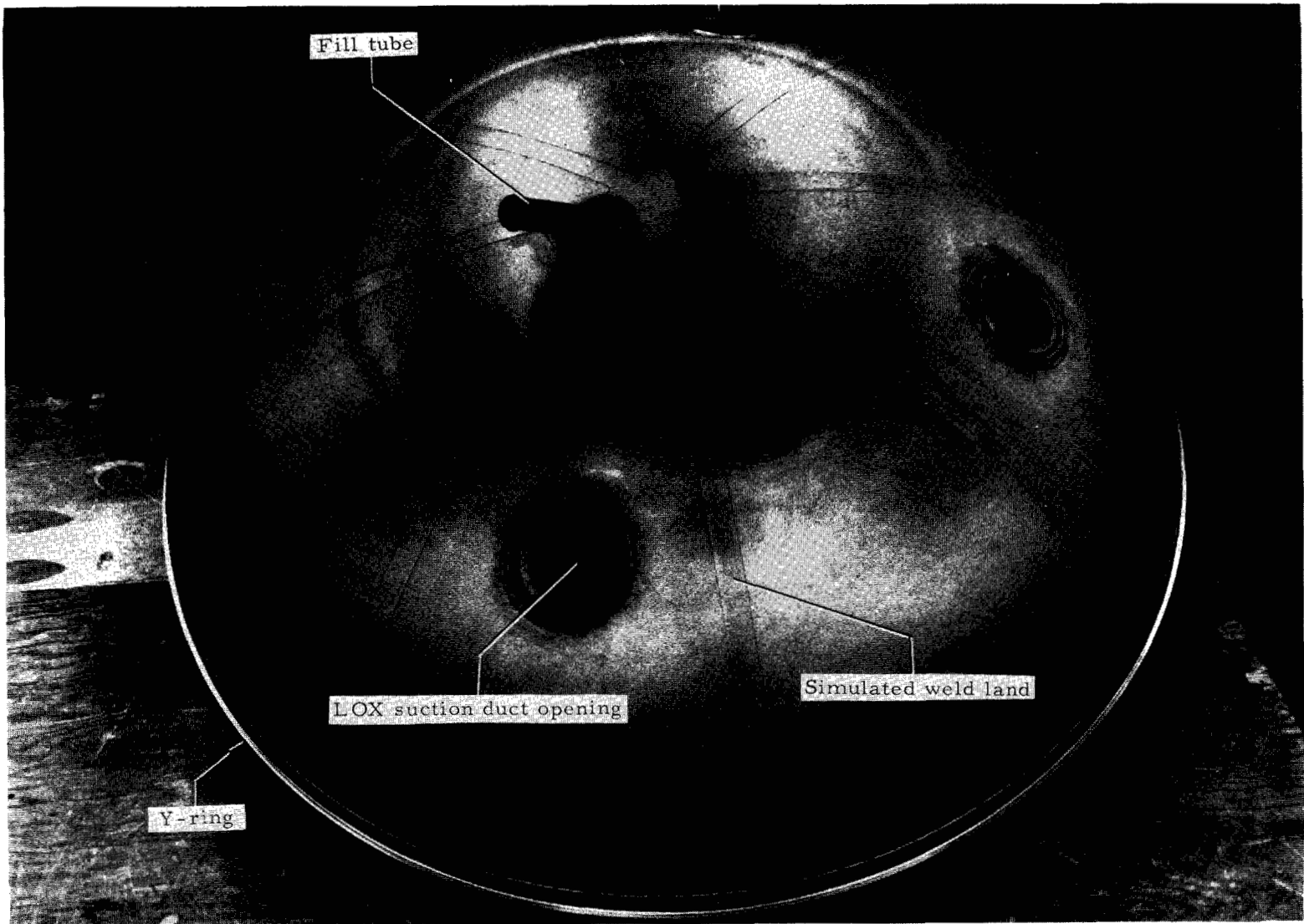


Figure 17.- S-1C stage, fuel tank lower bulkhead. 1/10-scale model.

L-67-1047



Figure 18.- S-IC stage, fuel tank skin section. 1/10-scale model.

L-67-1028

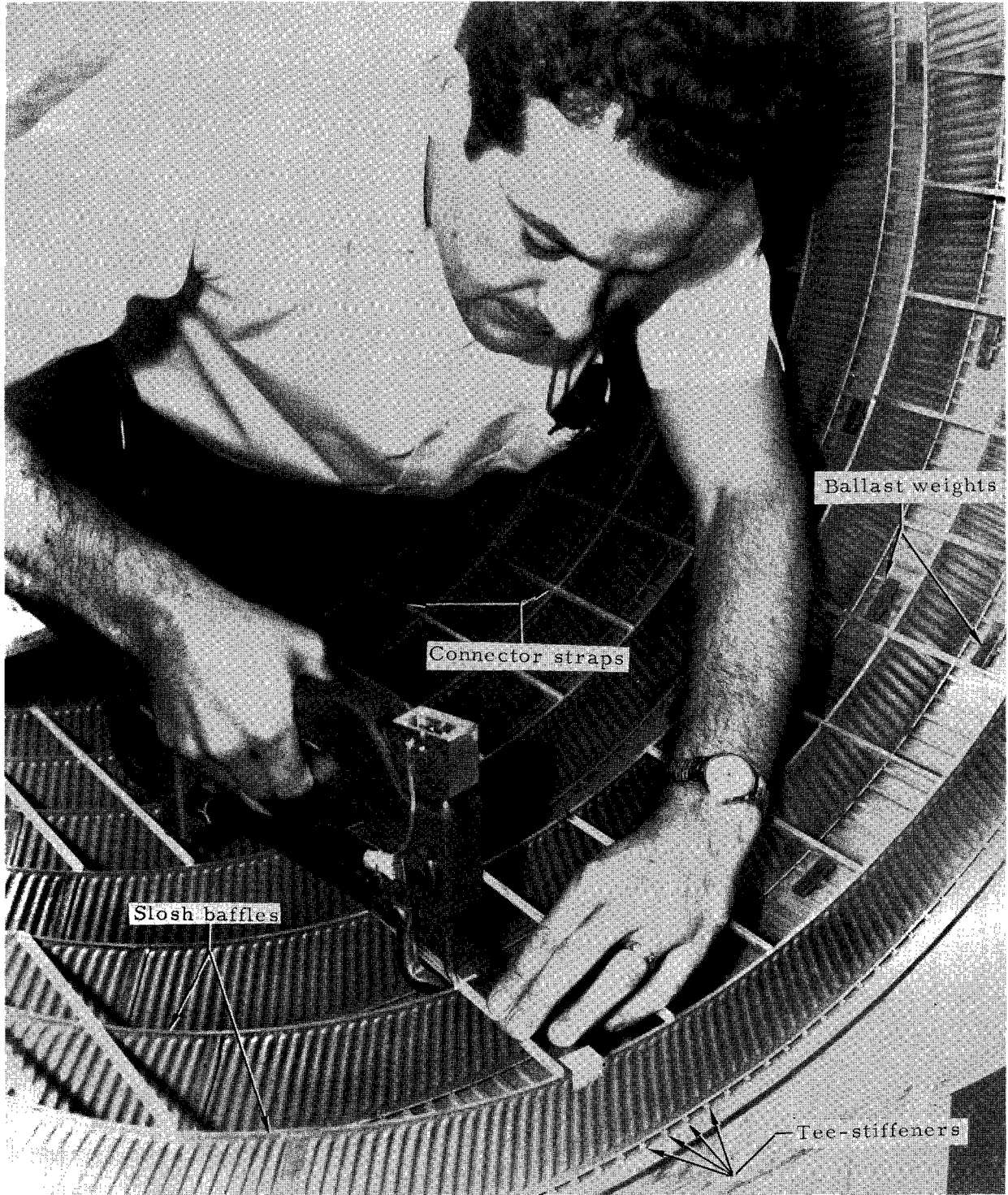


Figure 19.- S-IC stage. Installation of fuel tank slosh baffles. 1/10-scale model.

L-67-1024

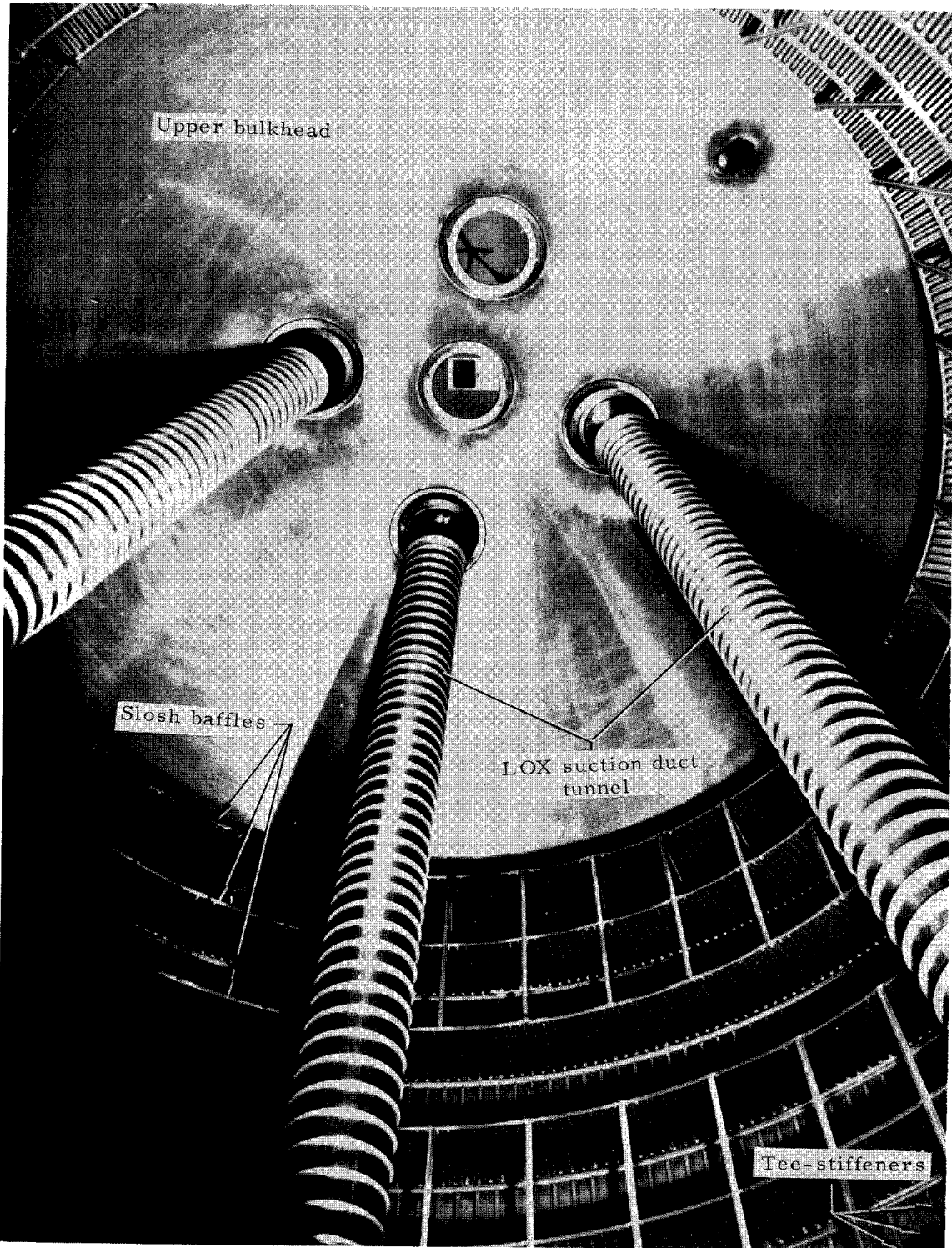


Figure 20.- S-IC stage. Interior of fuel tank. 1/10-scale model.

L-67-1040

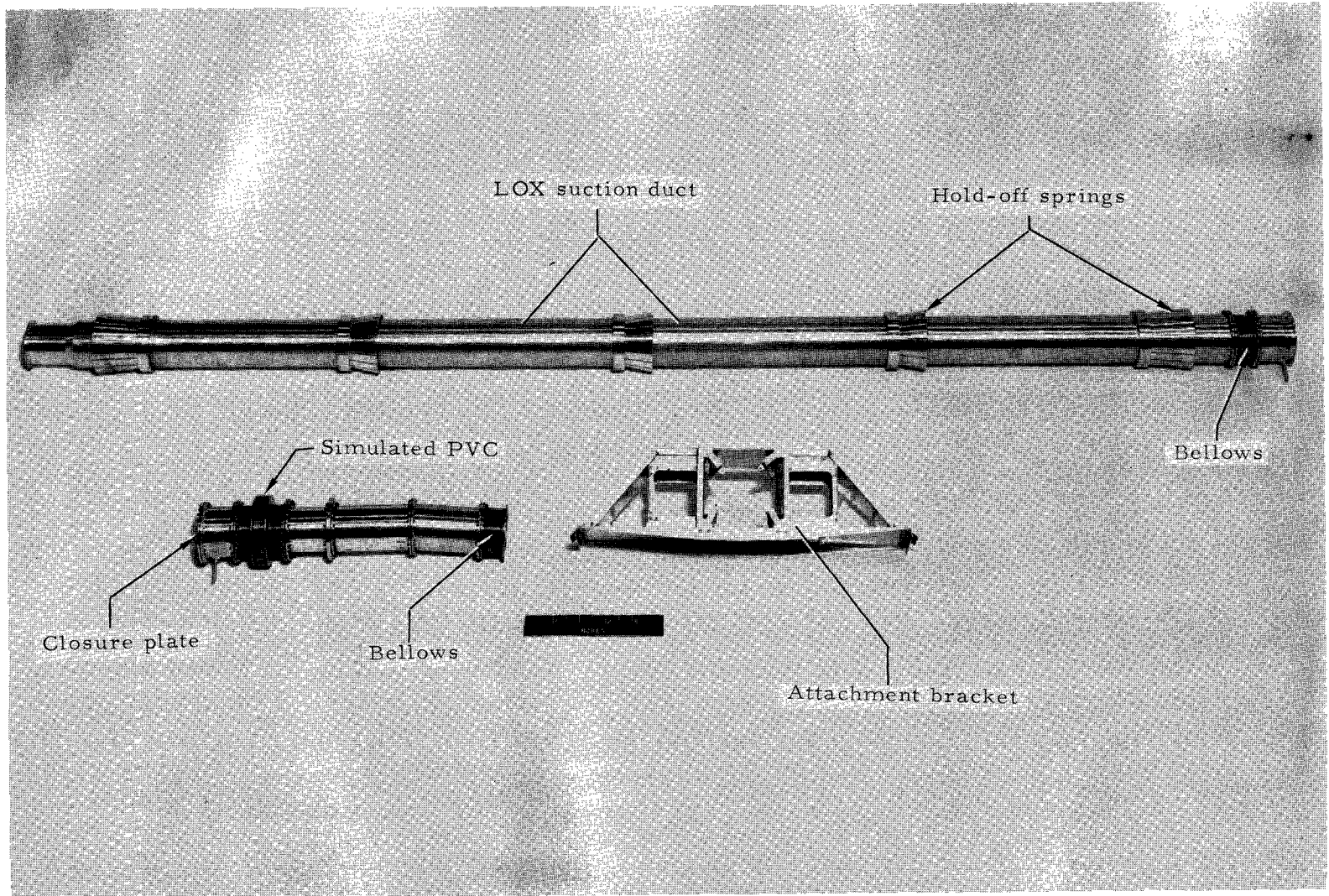


Figure 21.- S-IC stage. Simulated LOX suction duct. 1/10-scale model.

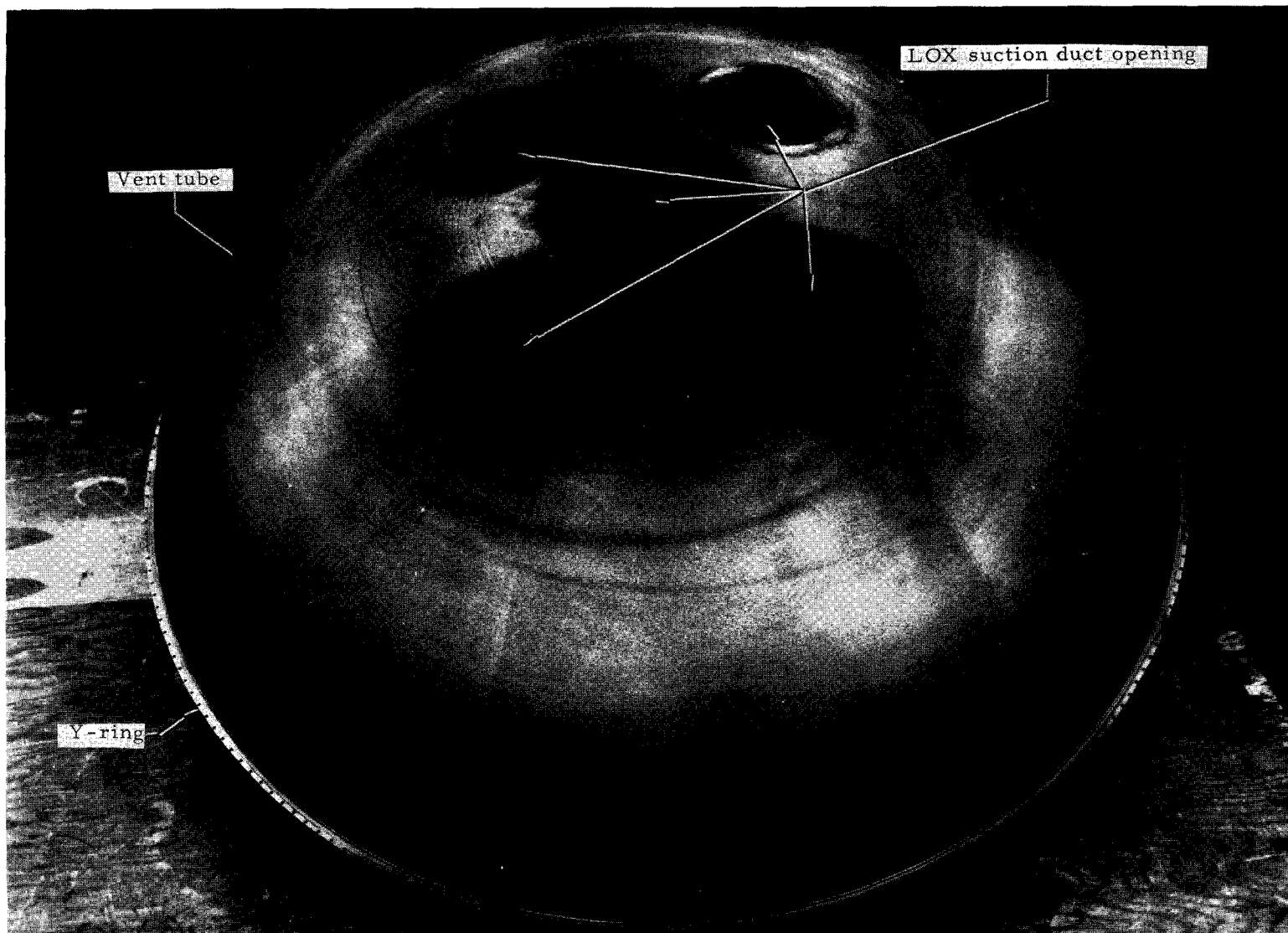


Figure 22.- S-1C stage. Fuel-tank upper bulkhead. 1/10-scale model.

L-67-1046

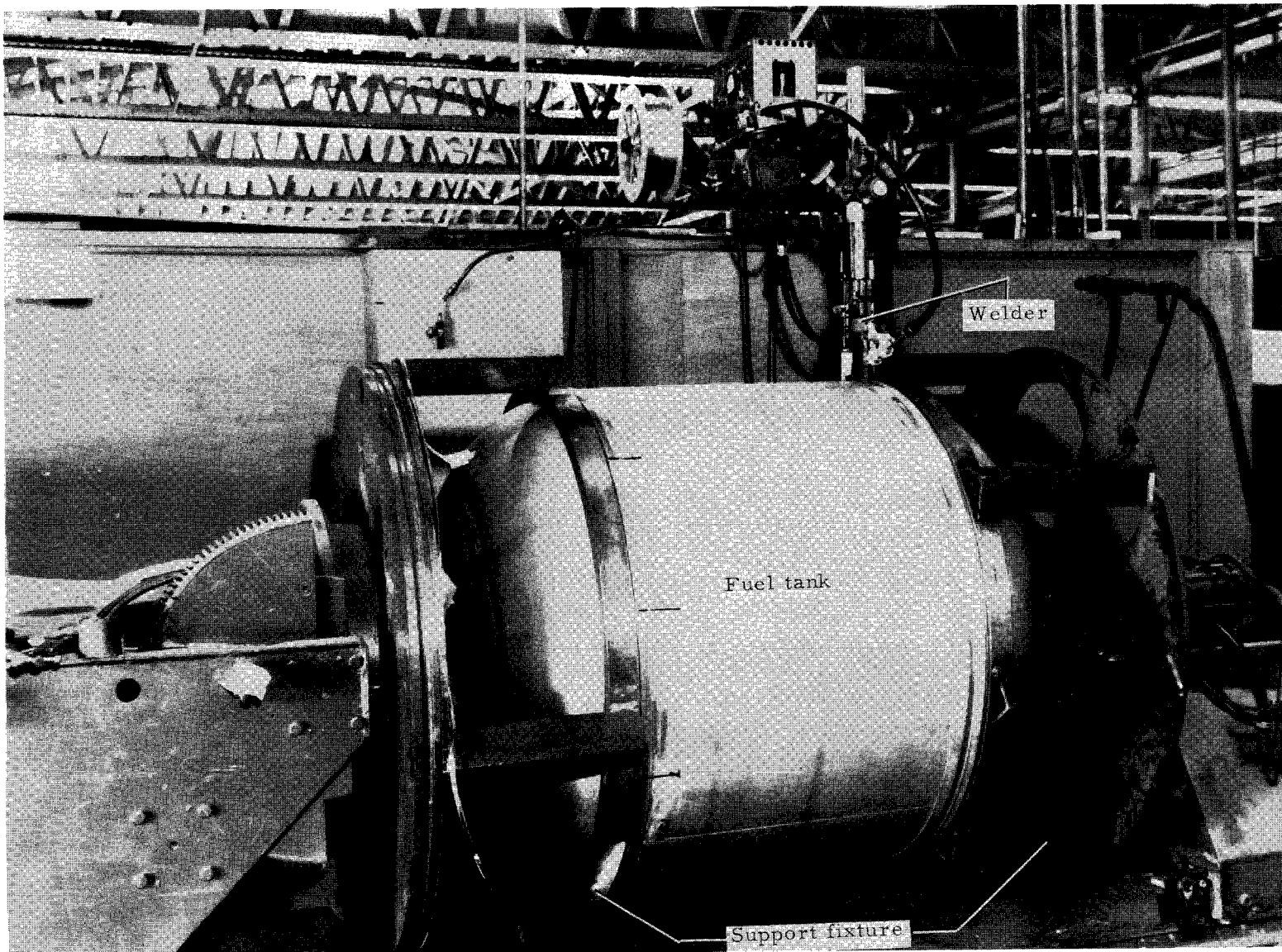


Figure 23.- S-IC stage. Fuel tank final assembly. 1/10-scale model.

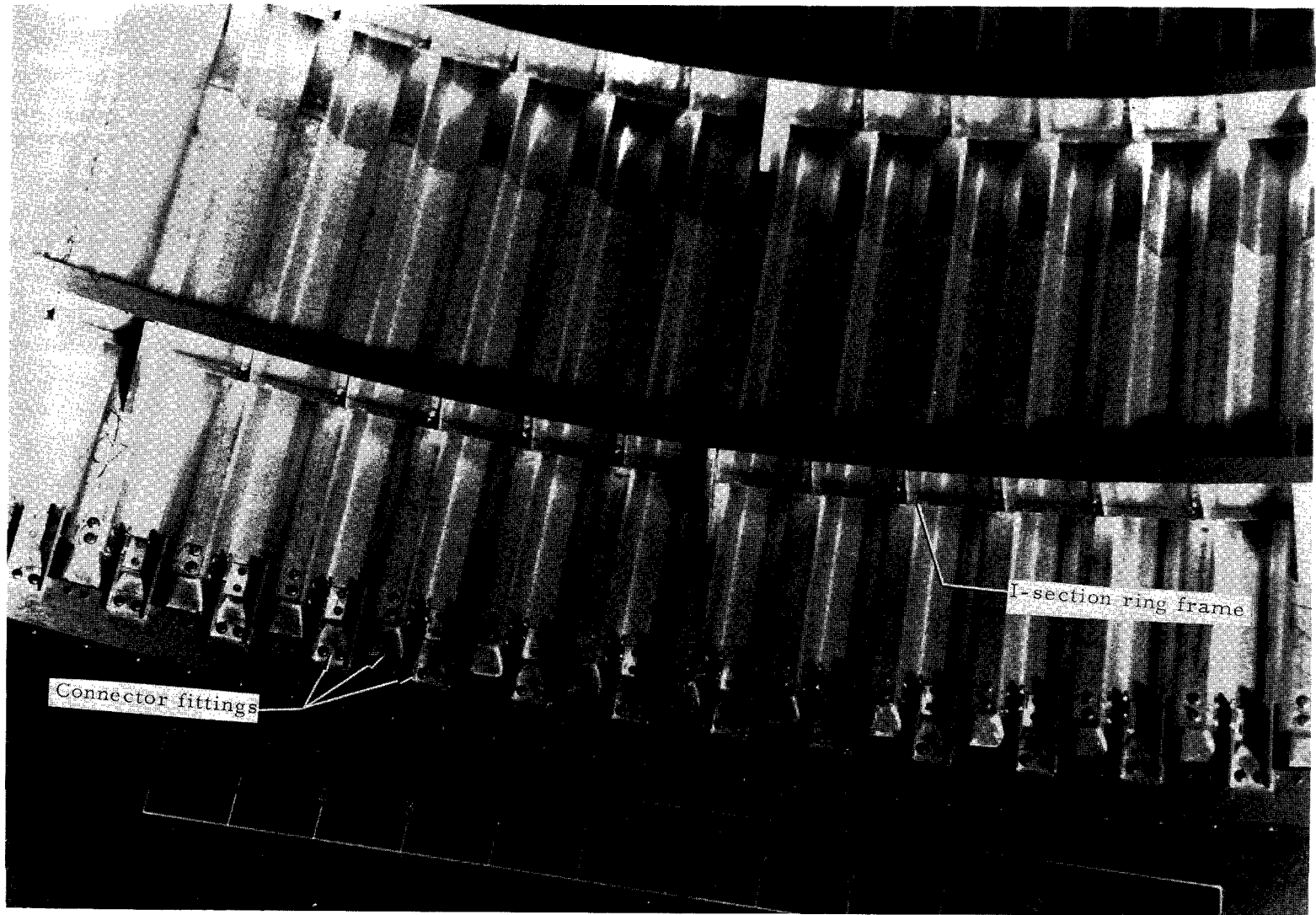


Figure 24.- S-1C stage. Intertank structure detail. 1/10-scale model.

L-67-1045

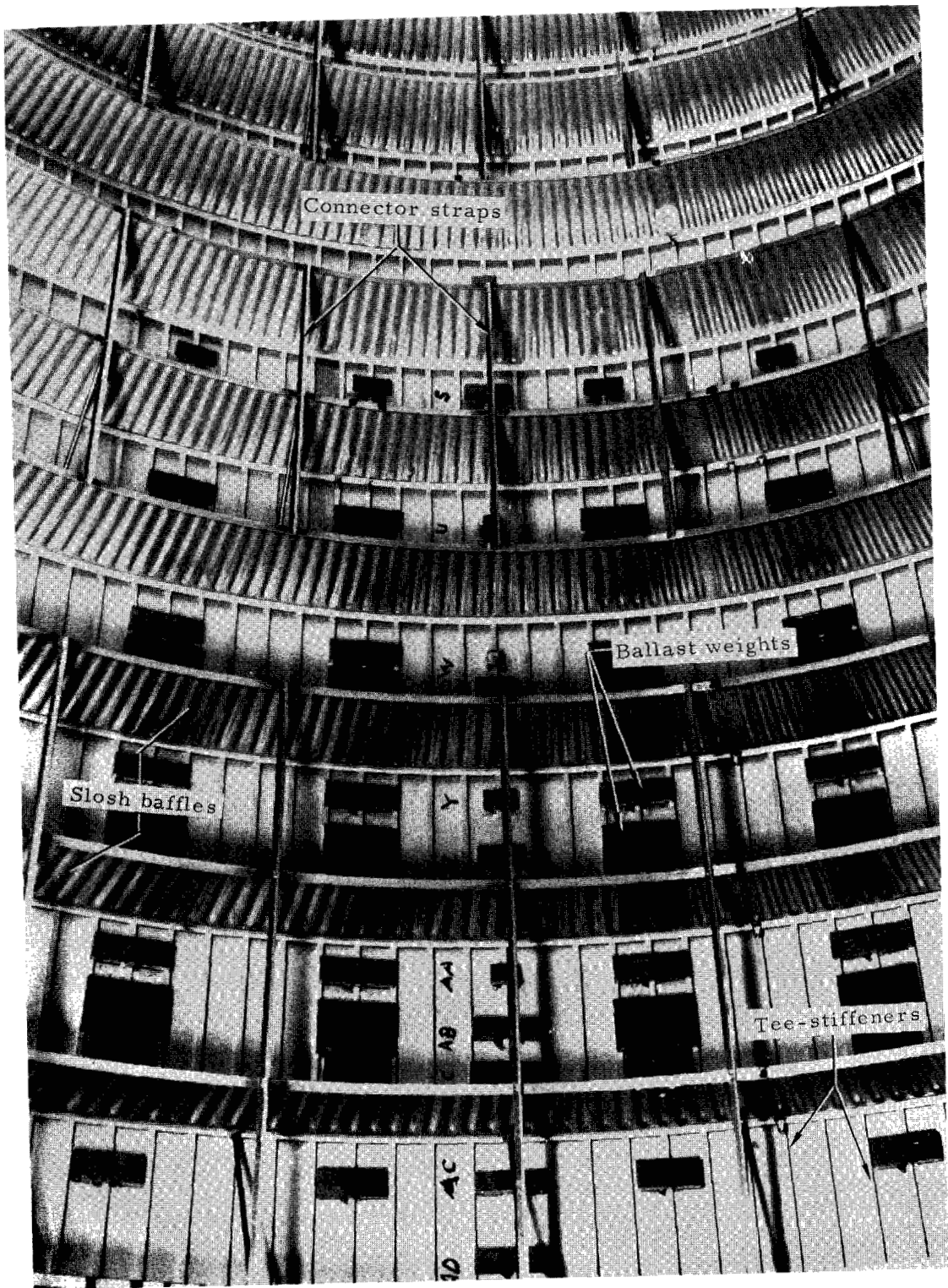


Figure 25.- S-IC stage. LOX tank interior. 1/10-scale model.

L-67-1041

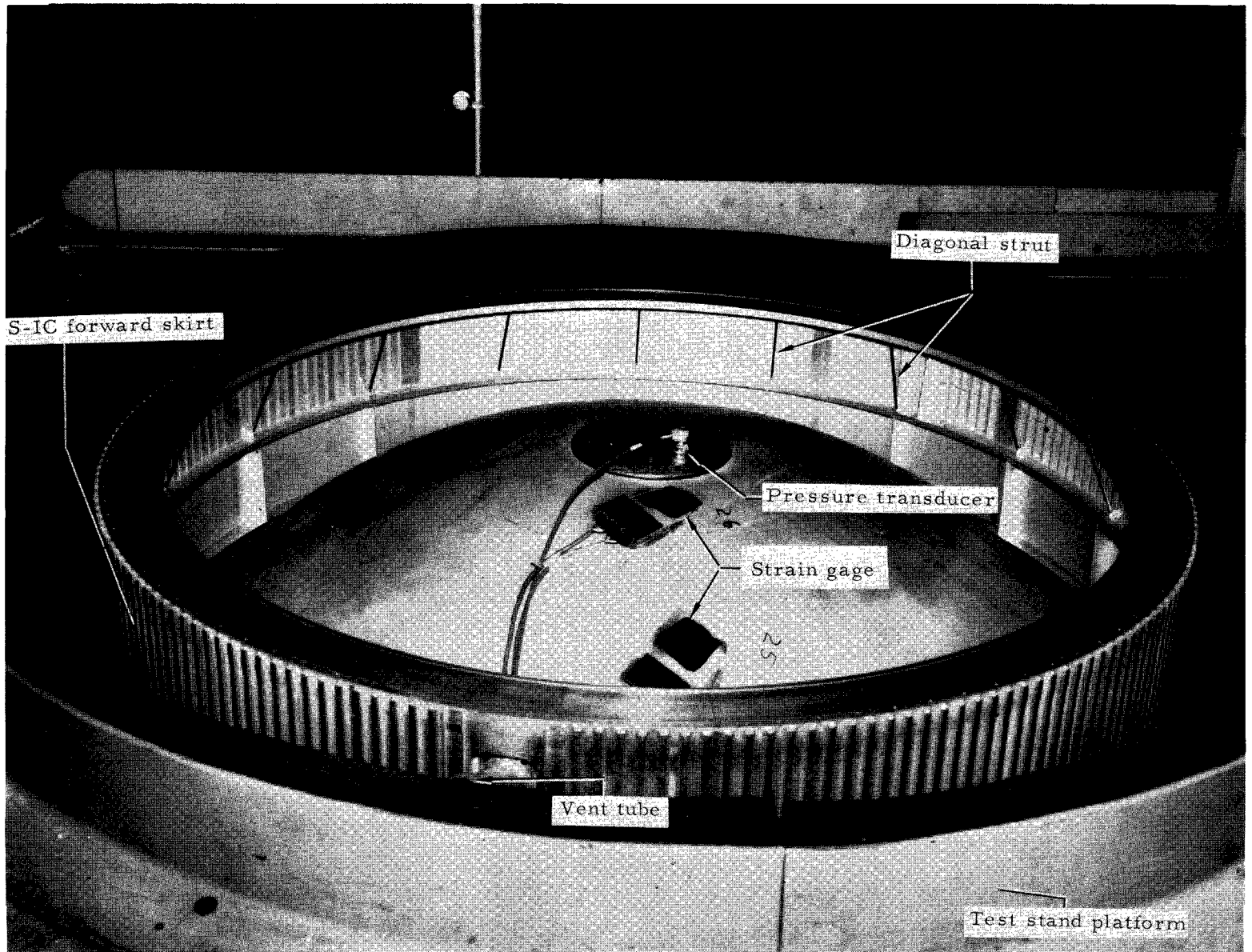


Figure 26.- Forward end of S-IC stage. 1/10-scale model.

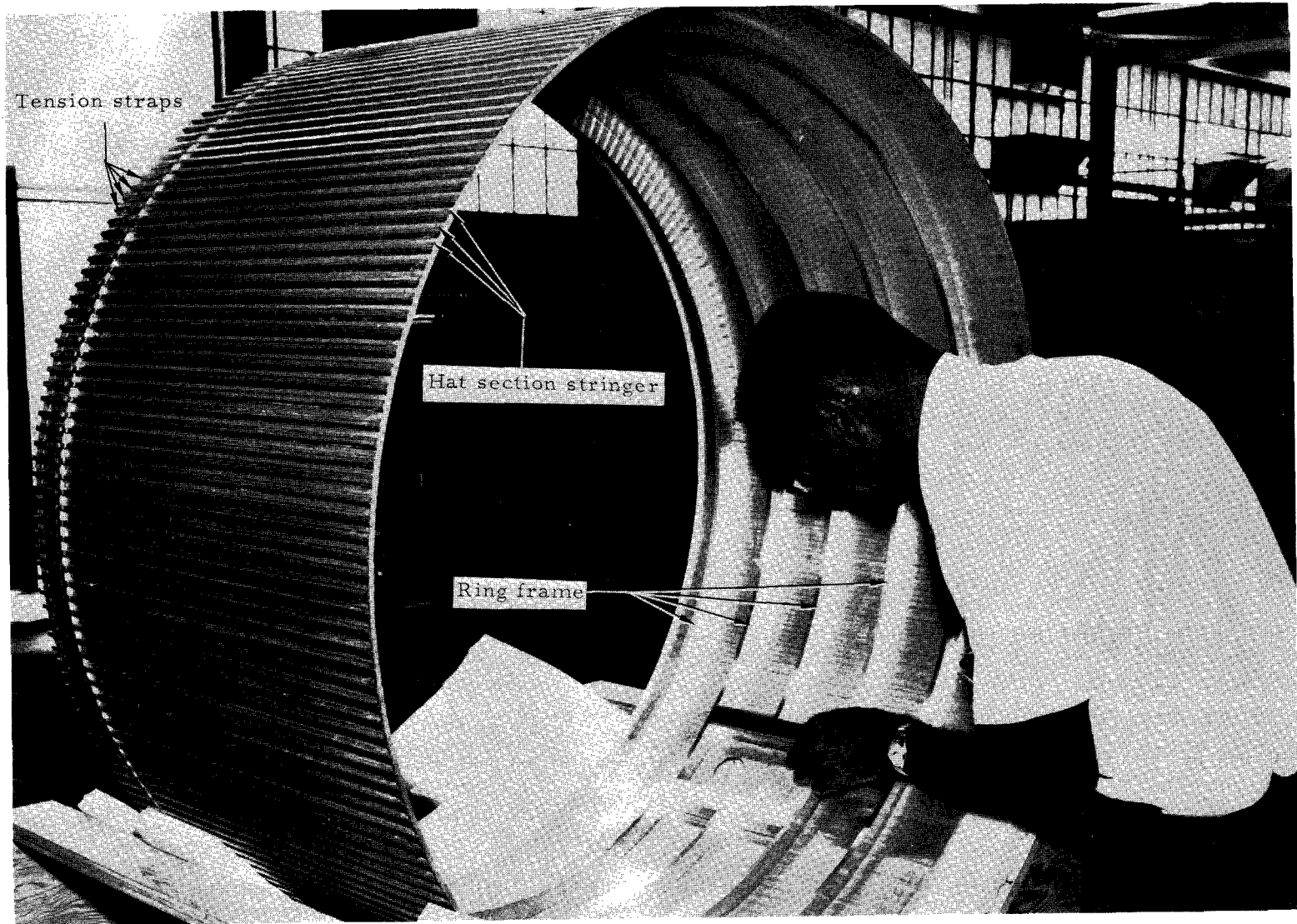


Figure 27.- S-IC/S-II interstage. 1/10-scale model.

L-67-1042

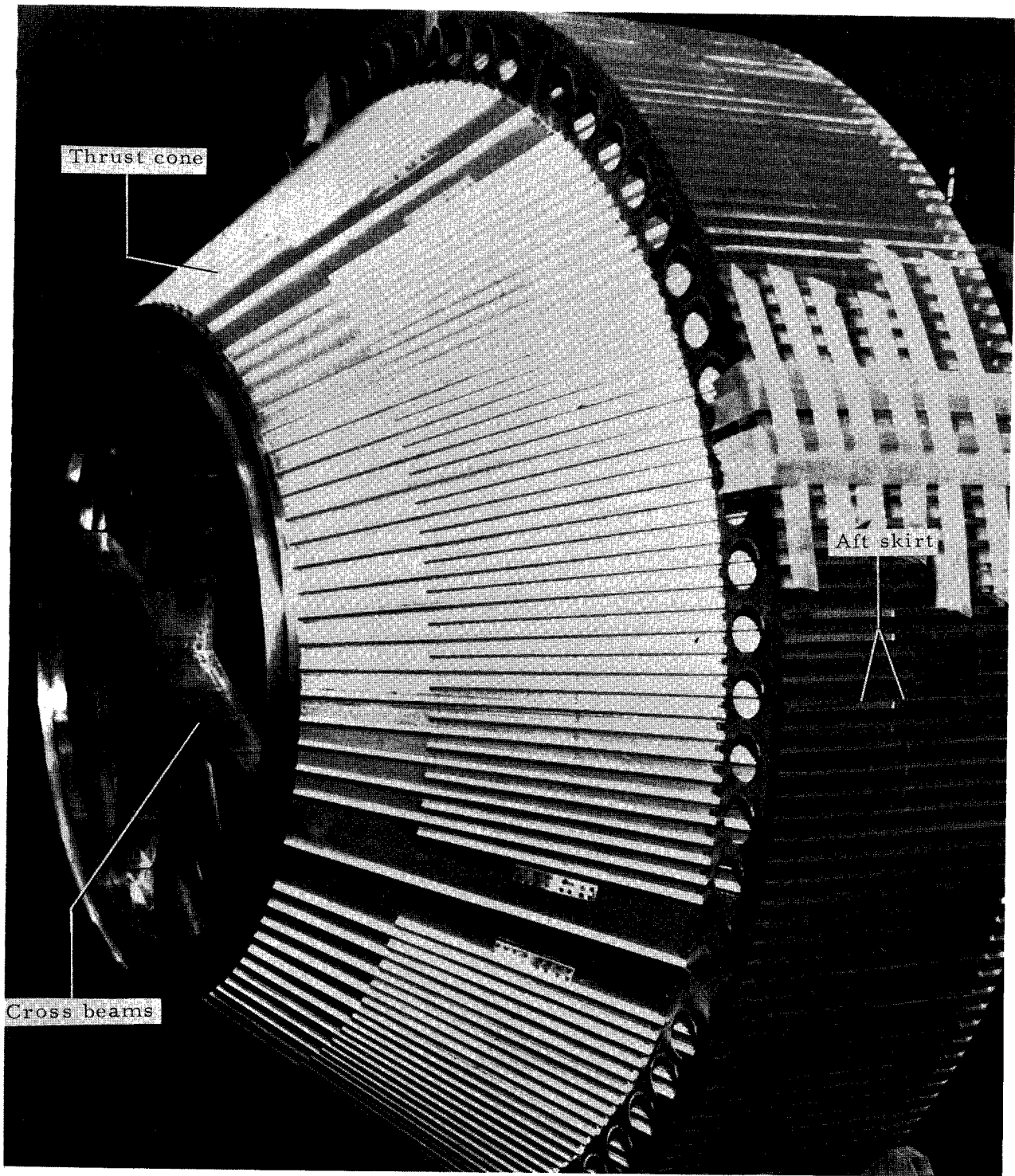


Figure 28.- S-II stage. Thrust structure and aft skirt assembly. 1/10-scale model.

L-67-1022

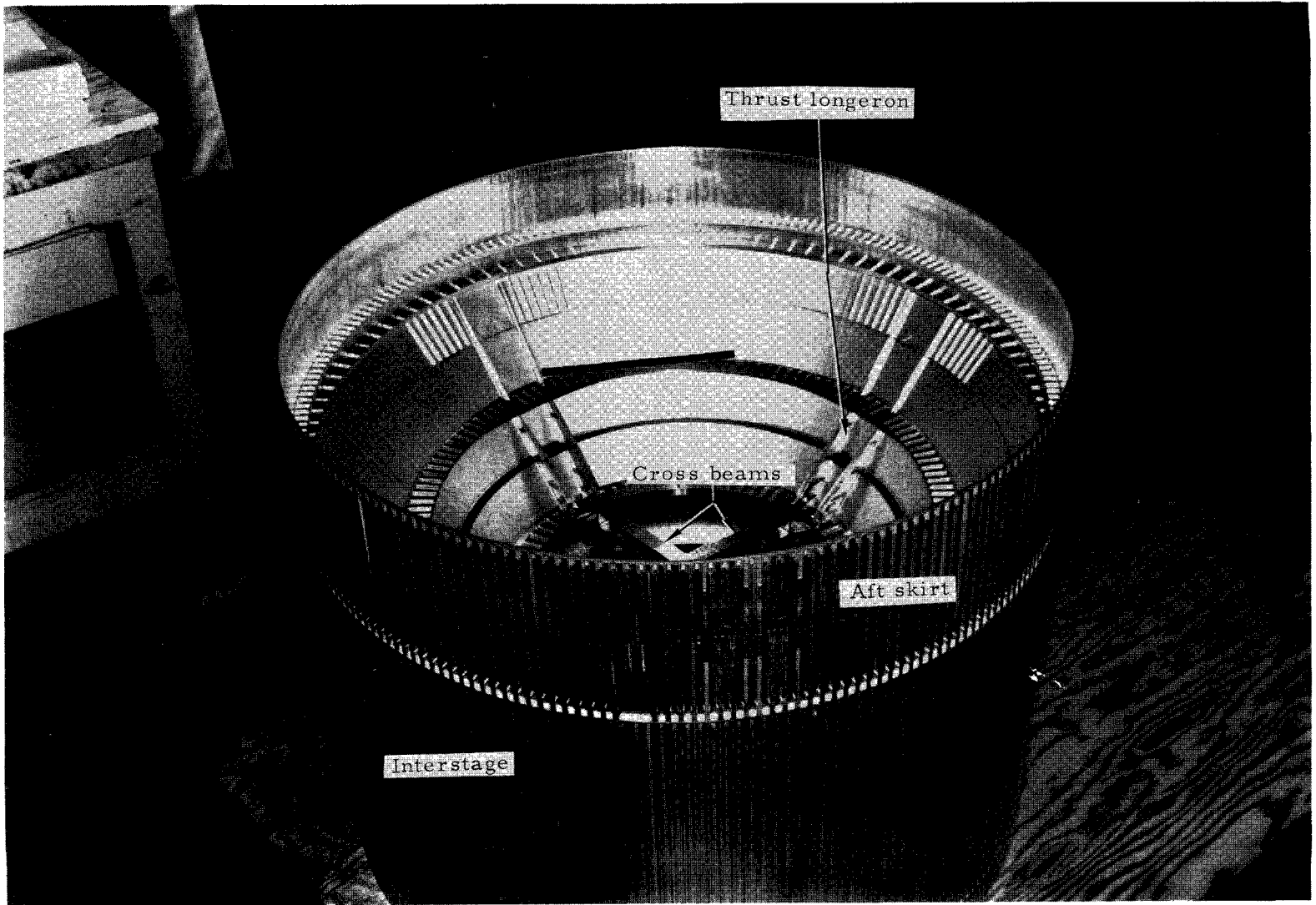


Figure 29.- S-11 stage. Thrust-cone-aft-skirt interstage assembly. 1/10-scale model.

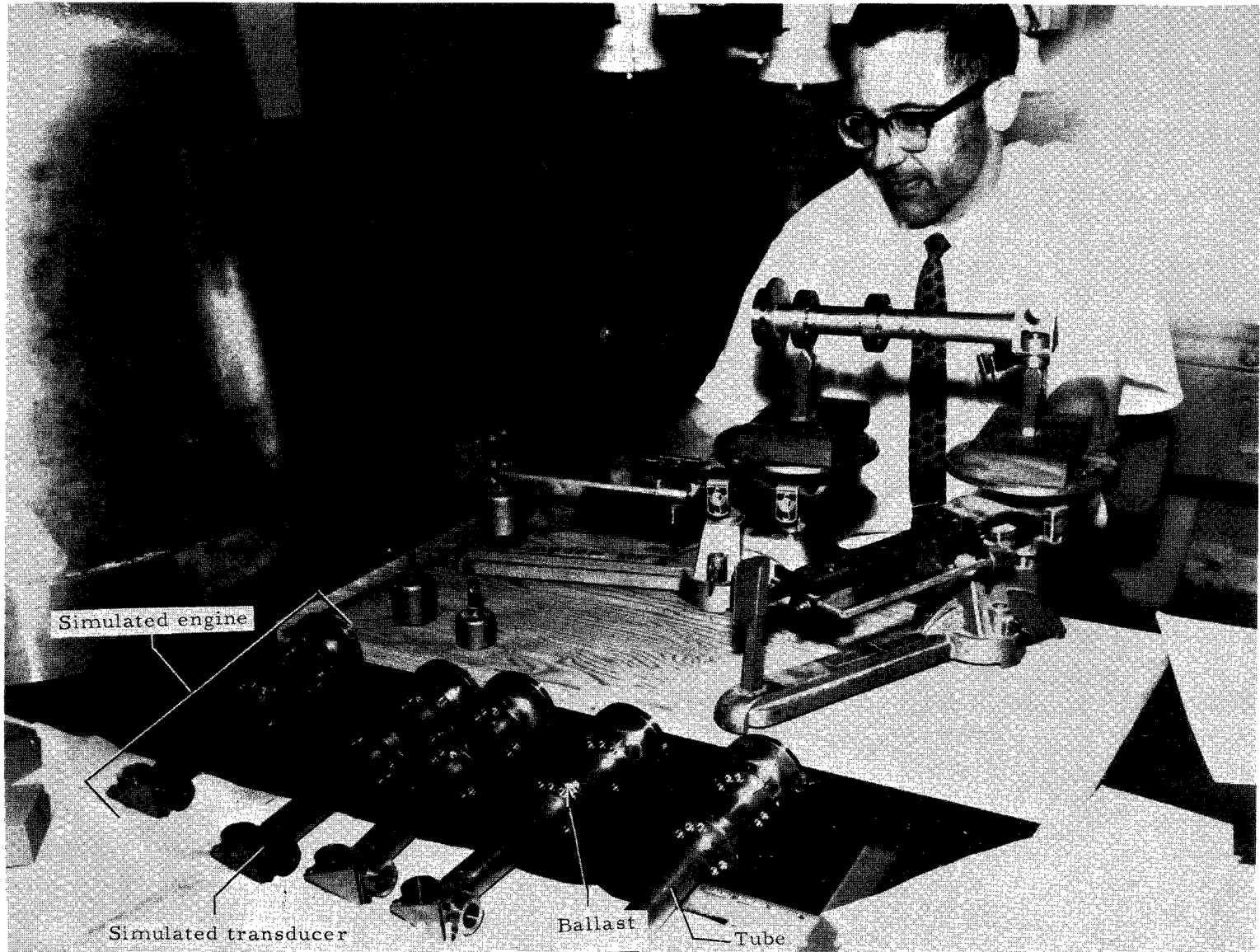


Figure 30.- Simulated J-2 engines. 1/10-scale model.

L-67-1044

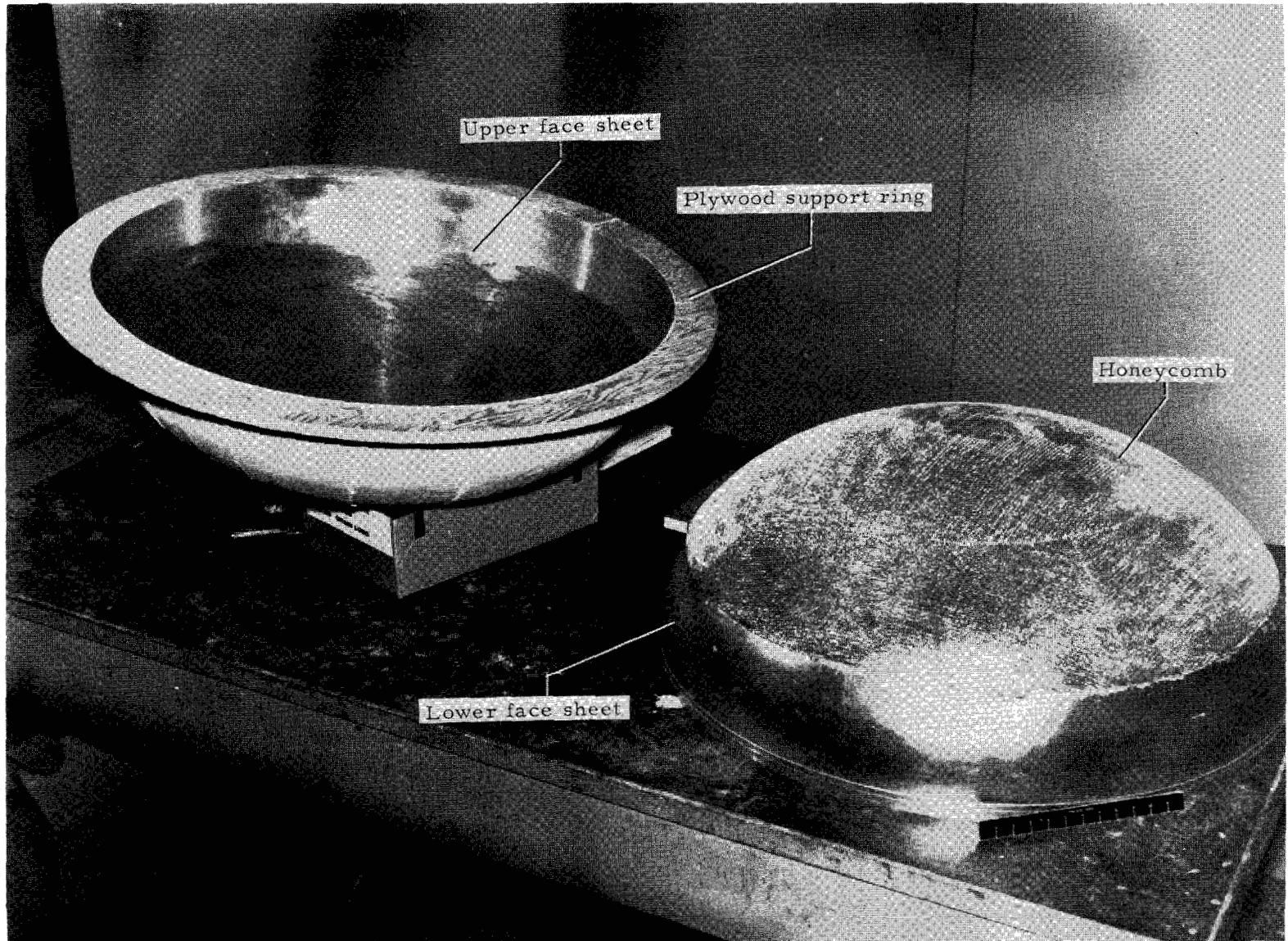


Figure 31.- S-II stage. Common bulkhead partially fabricated. 1/10-scale model.

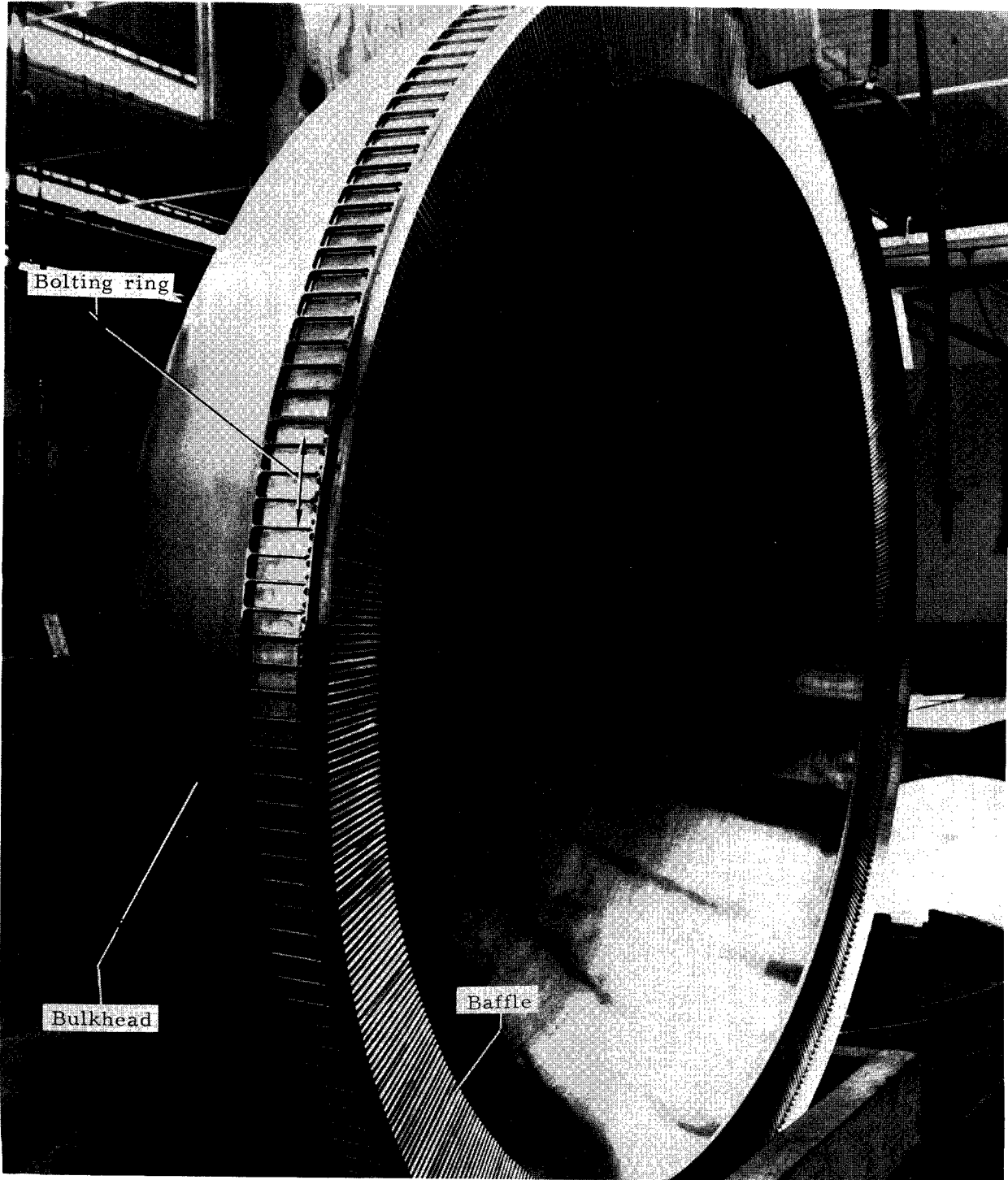


Figure 32.- S-II stage. Common-bulkhead-bolting-ring assembly. 1/10-scale model.

L-67-1027

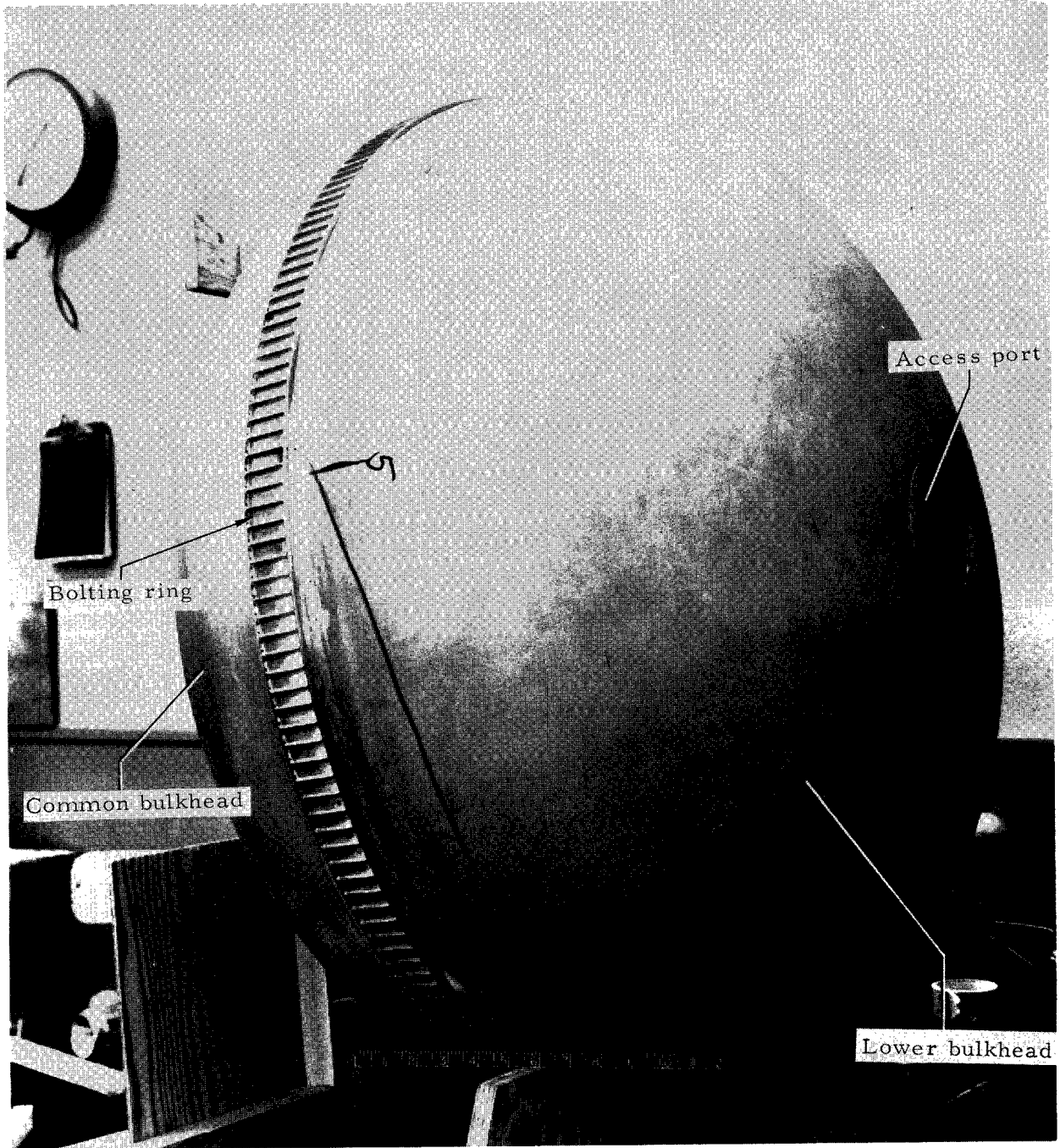


Figure 33.- S-II stage. LOX-tank—bolting-ring final assembly. 1/10-scale model.

L-67-1021

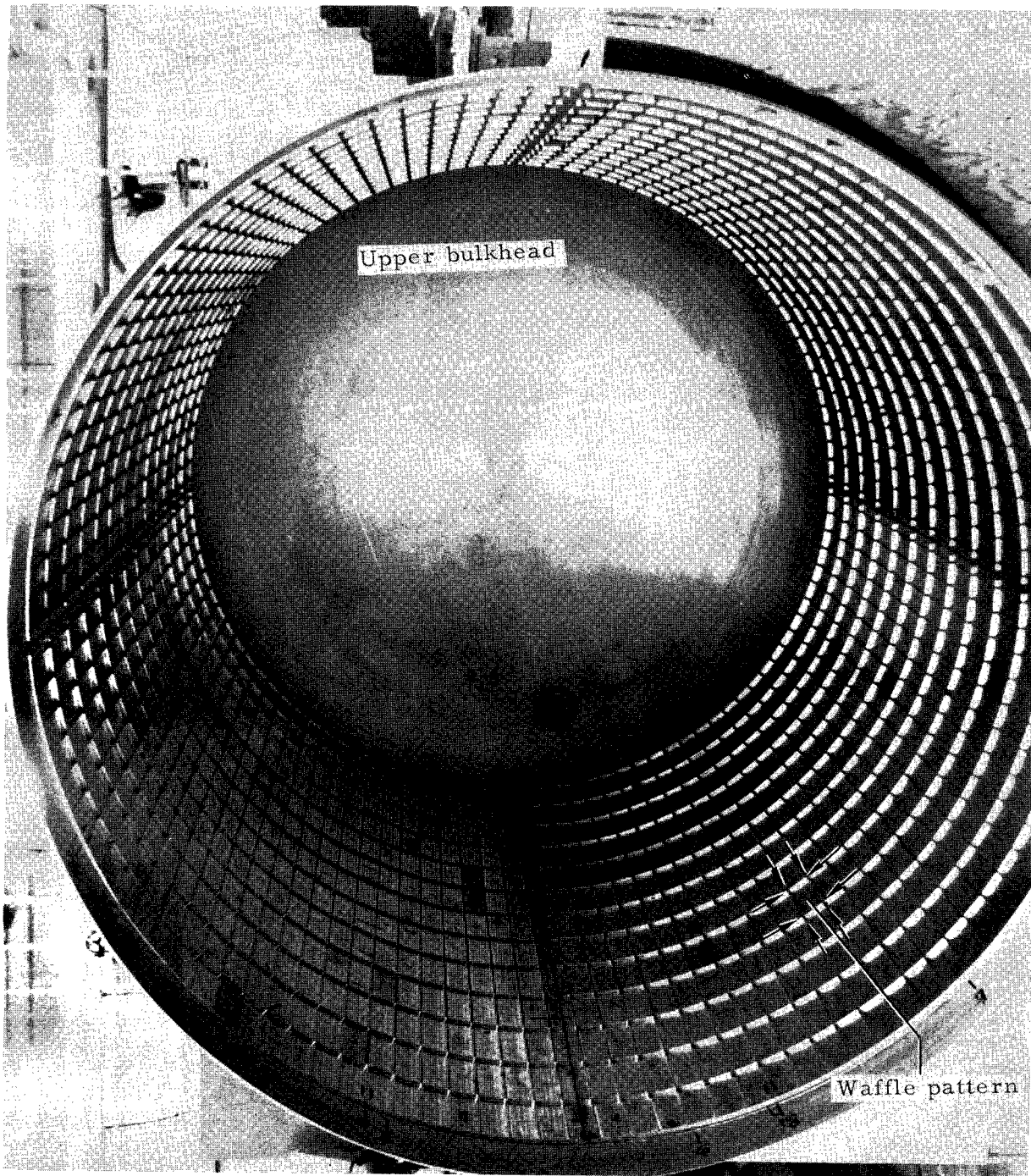


Figure 34.- S-II stage. Fuel tank interior. 1/10-scale model.

L-67-1020

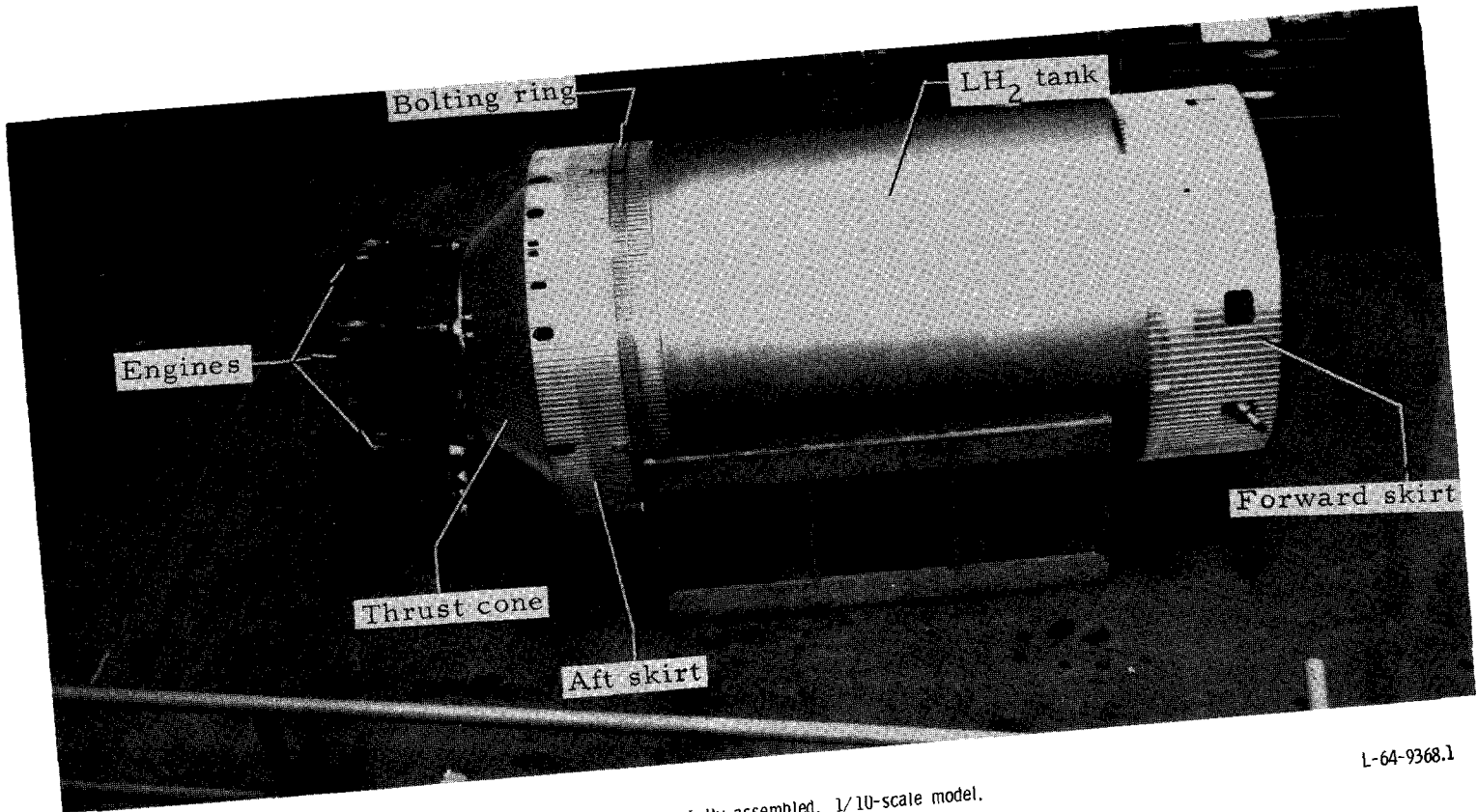


Figure 35.- S-II stage fully assembled. 1/10-scale model.

L-64-9368.1

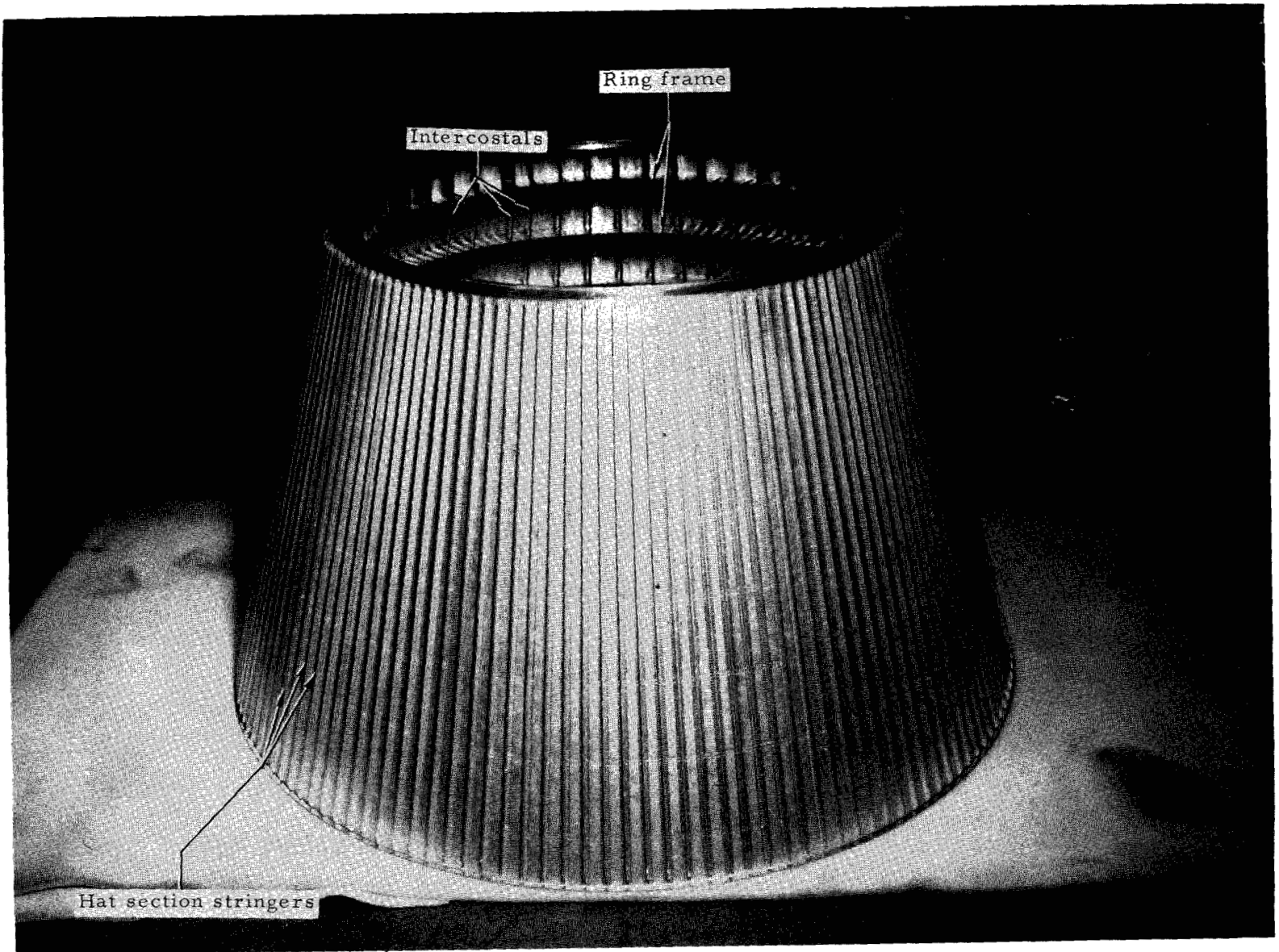


Figure 36.- S-11/S-IVB interstage. 1/10-scale model.

L-64-9369.1

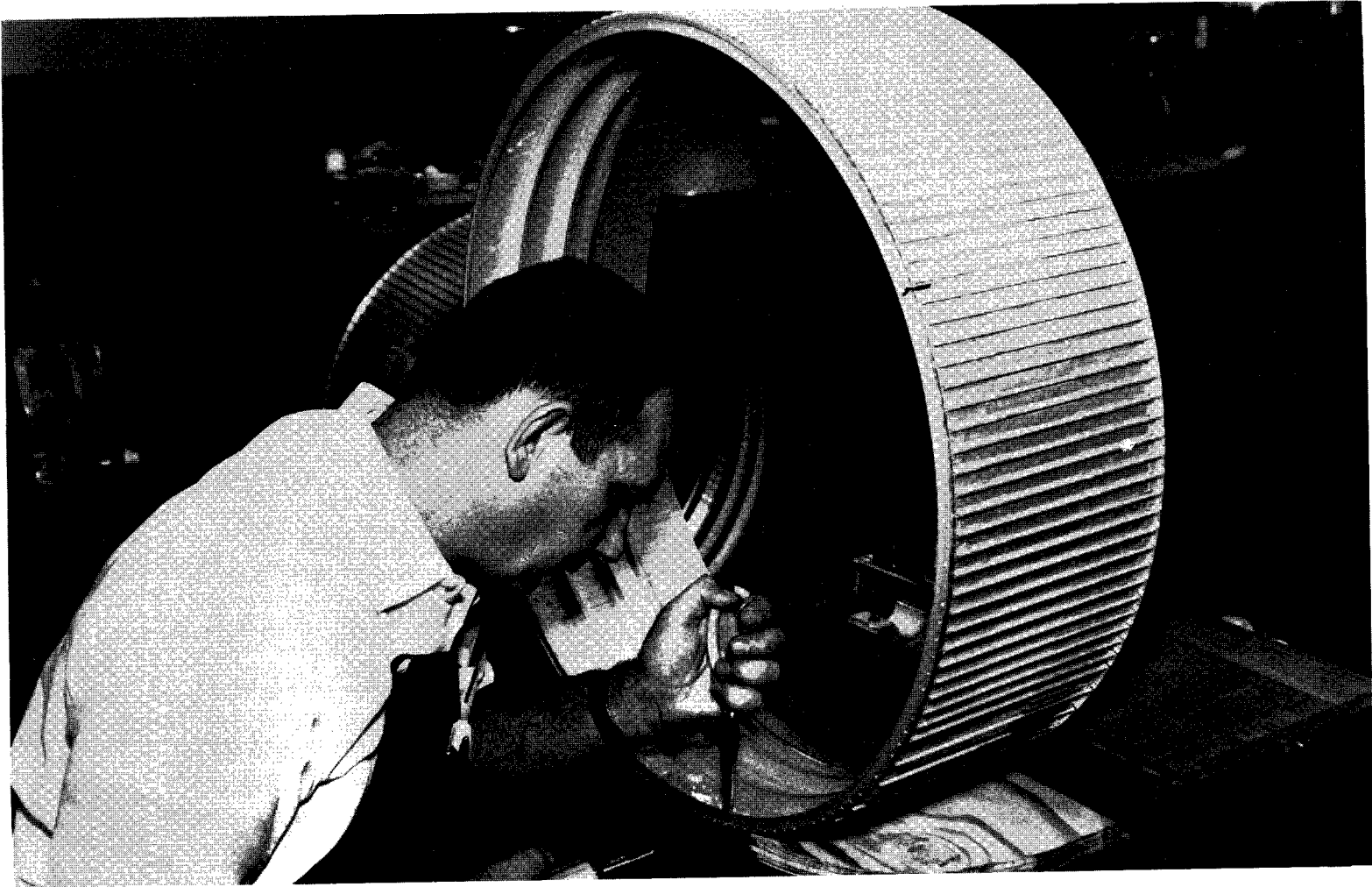


Figure 37.- S-IVB stage. Aft skirt. 1/10-scale model.

L-67-1048

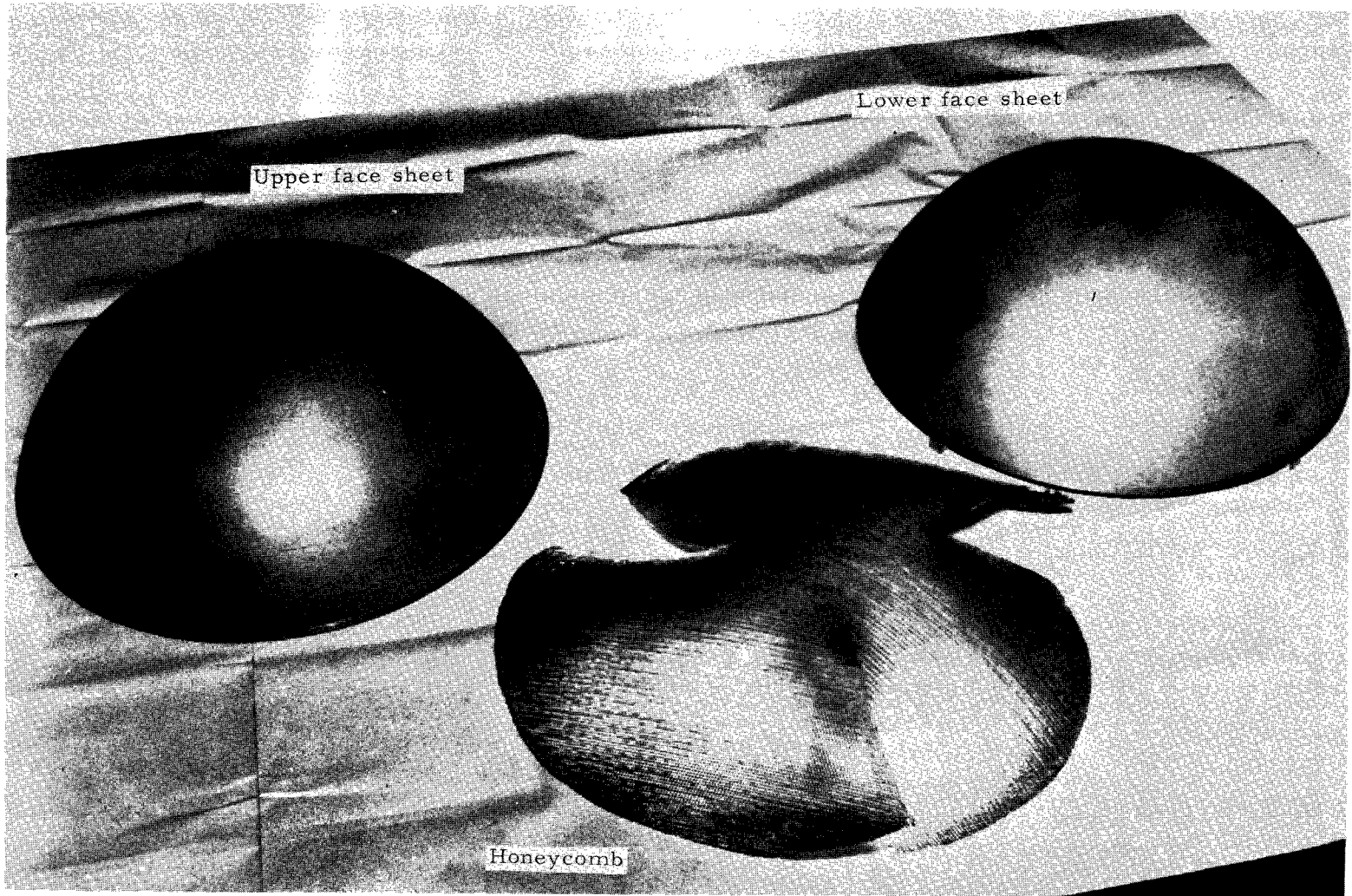


Figure 38.- S-IVB stage. Common bulkhead components before assembly, 1/10-scale model.

L-67-1043

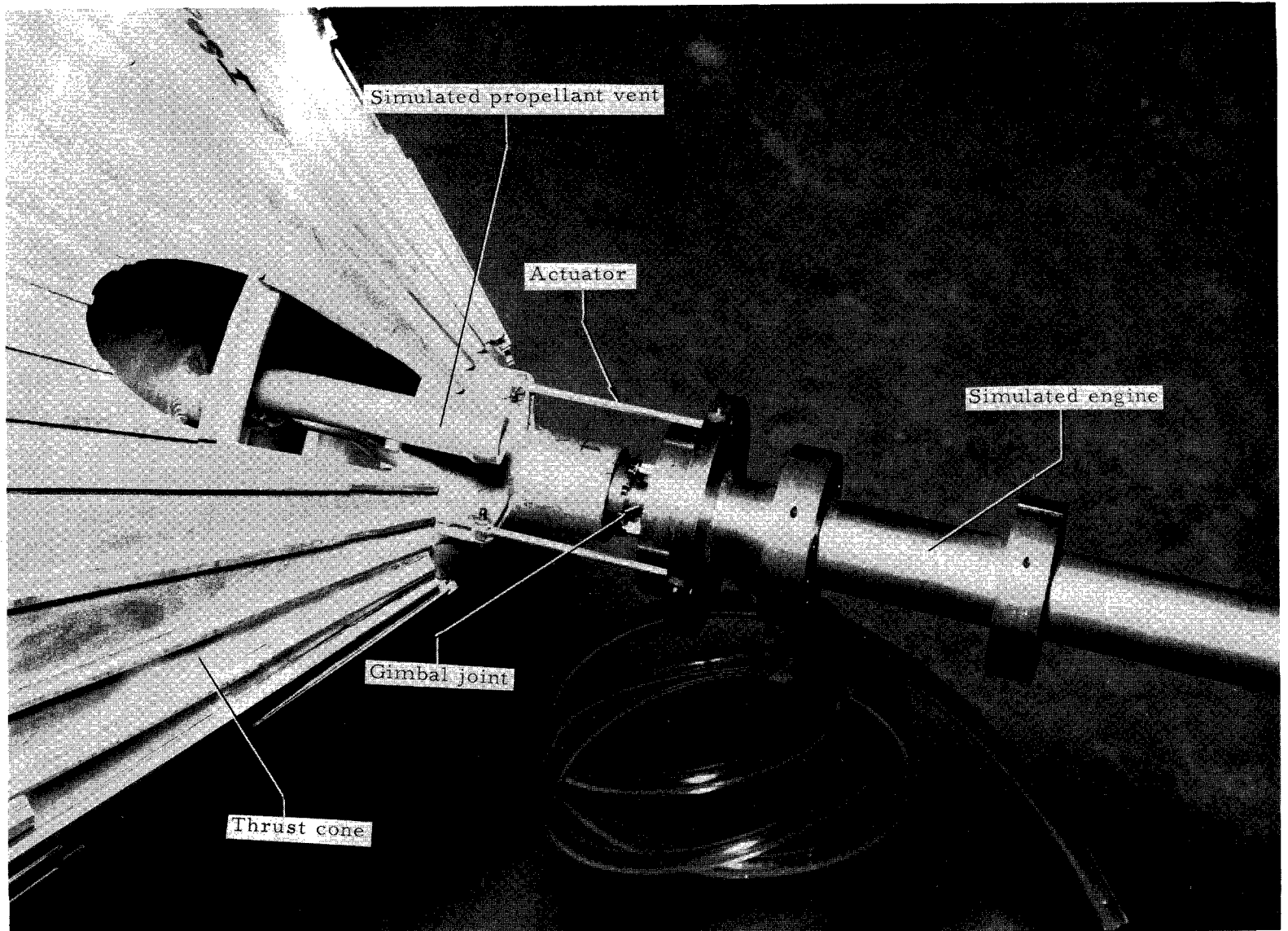


Figure 39.- S-IVB stage. Thrust cone and simulated engine. 1/10-scale model.

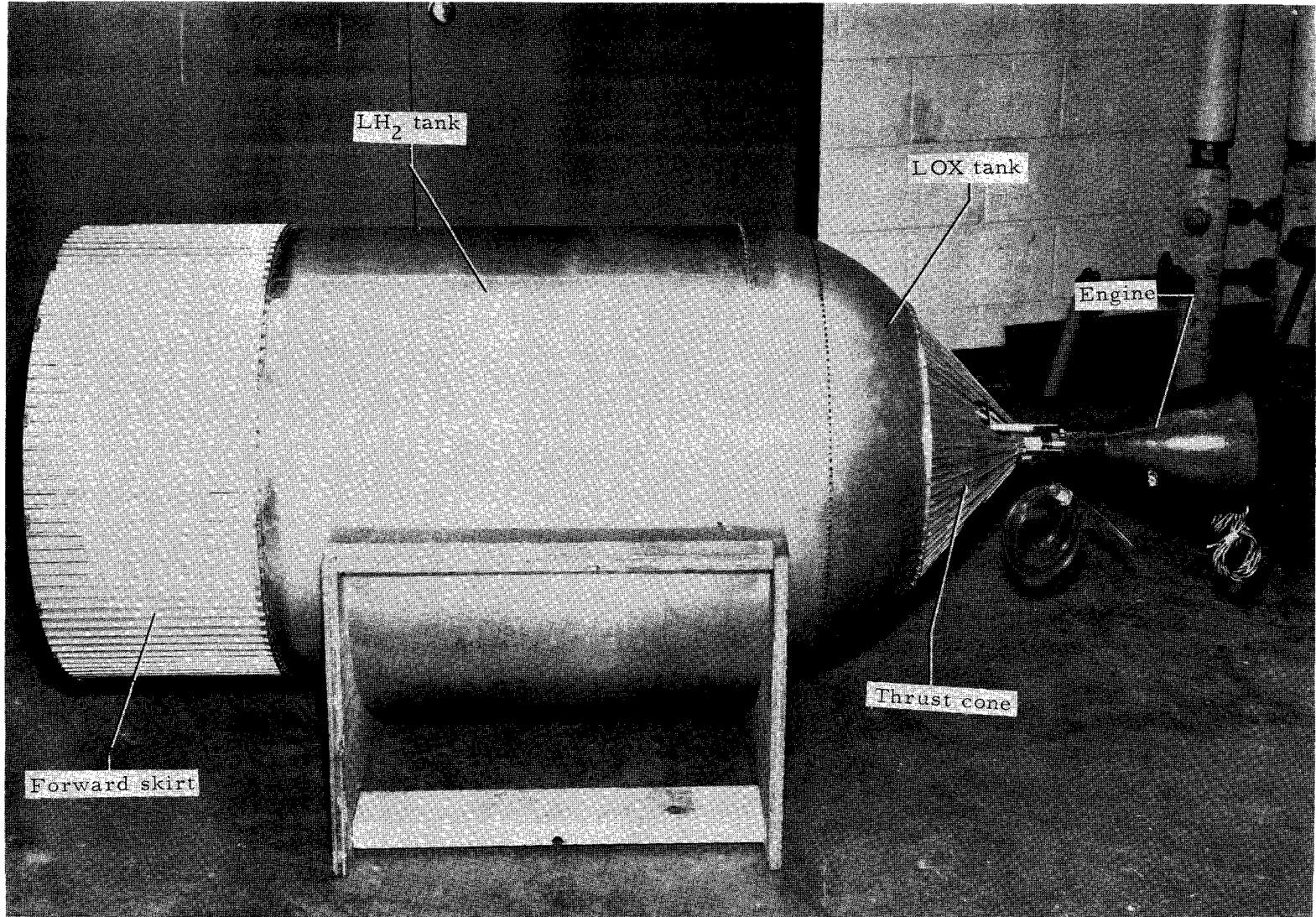


Figure 40.- S-IVB stage final assembly. 1/10-scale model.

L-64-9524.1

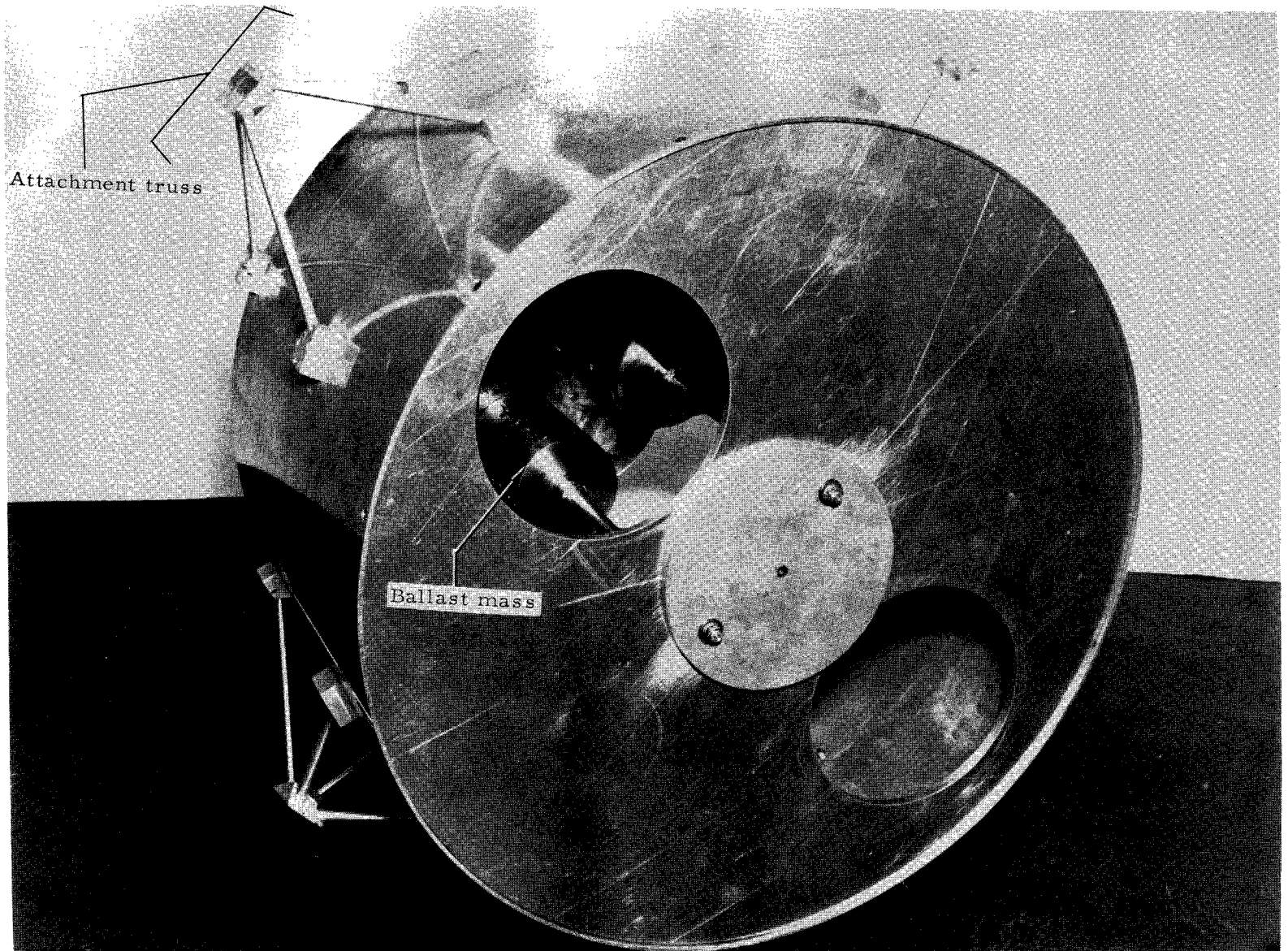


Figure 41.- Simulated lunar module, 1/10-scale model.

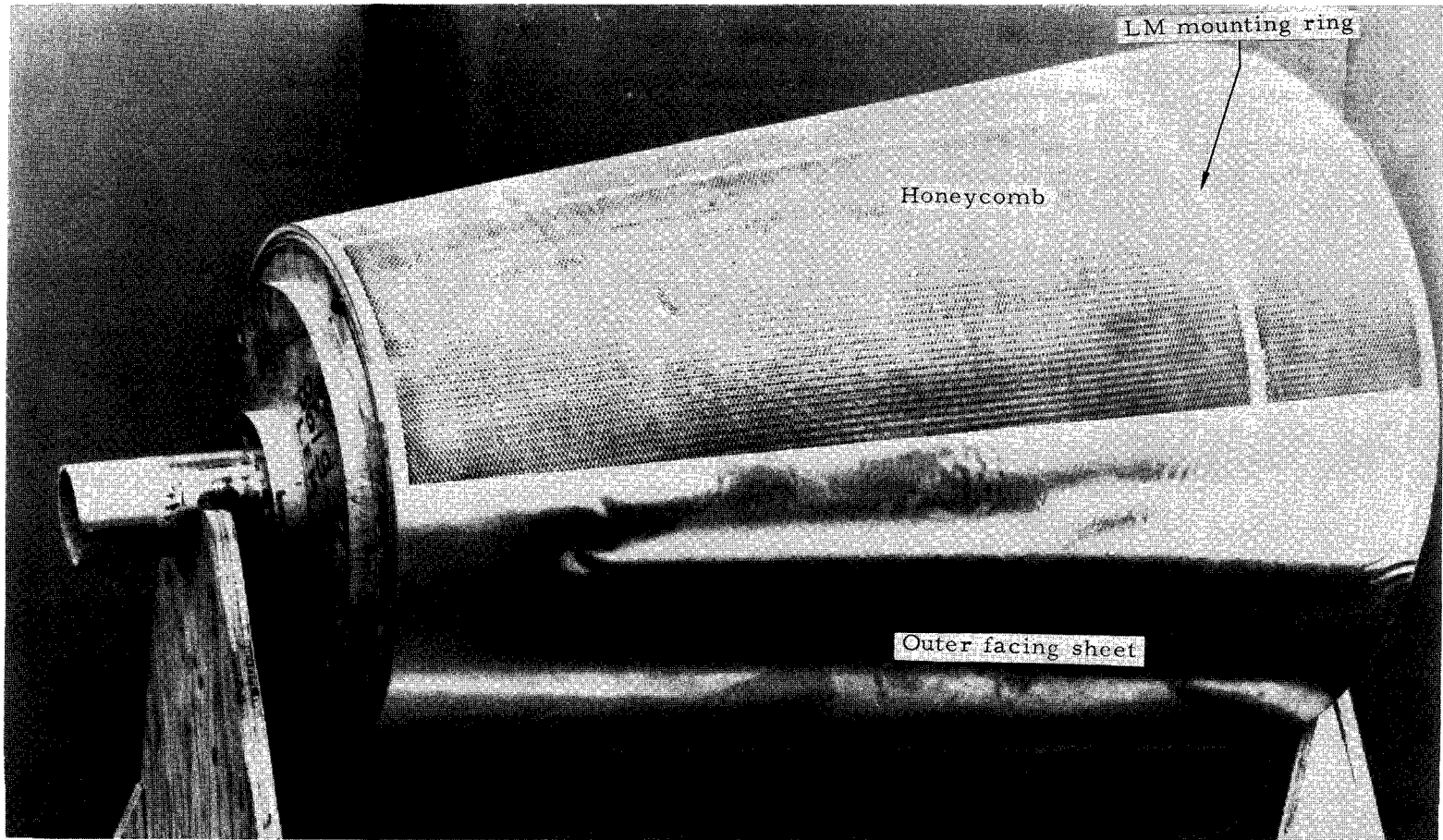


Figure 42.- Lunar module adapter under construction. 1/10-scale model.

L-67-1036

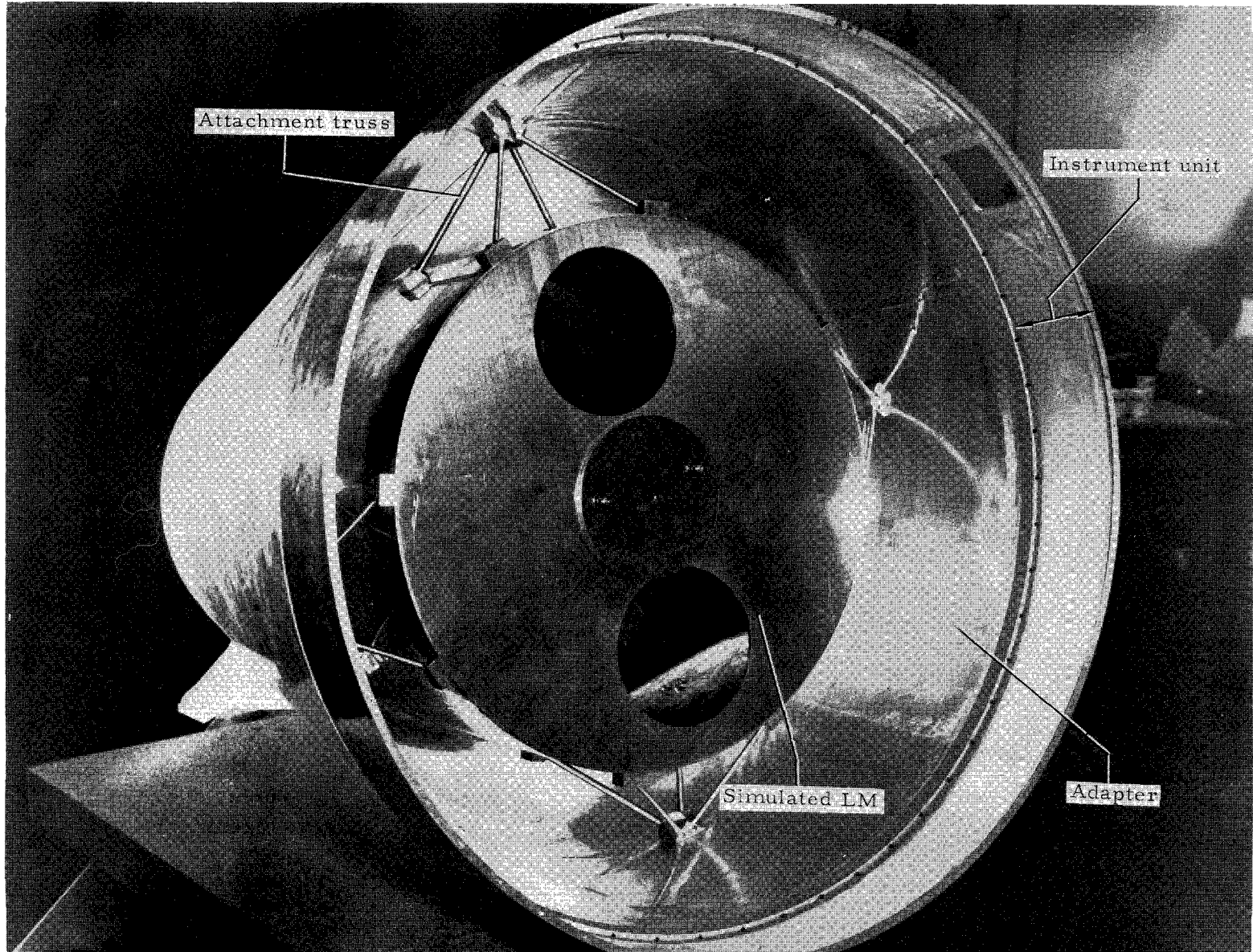


Figure 43.- Simulated lunar module mounted in adapter structure. 1/10-scale model.

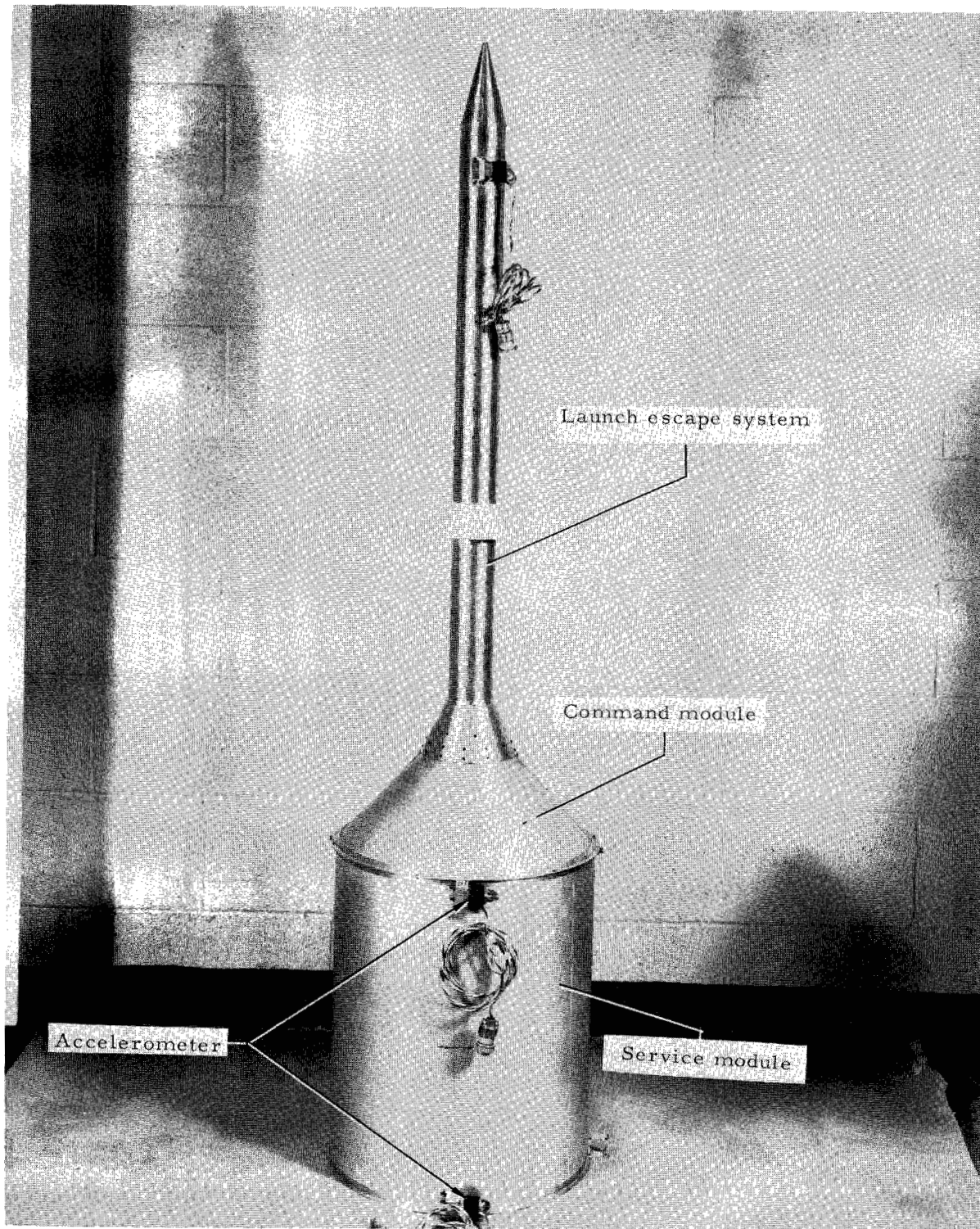
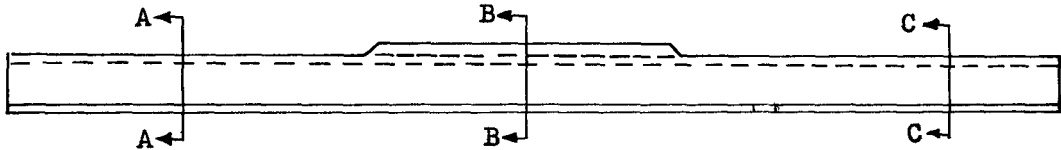
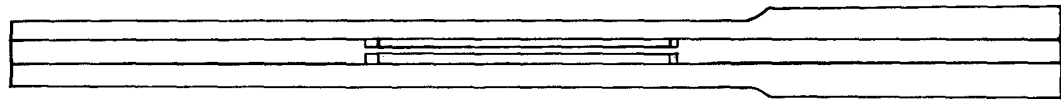
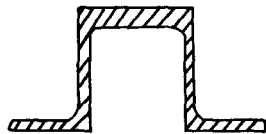


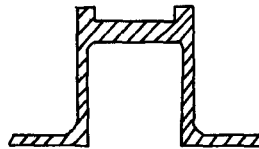
Figure 44.- Simulated command and service module assembly with launch escape system. 1/10-scale model. L-65-4229.1



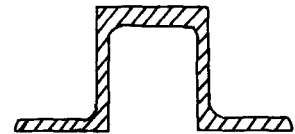
Direct scaling



View A-A

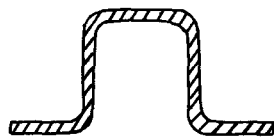


View B-B

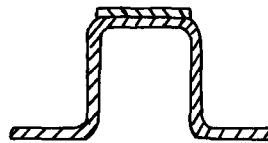


View C-C

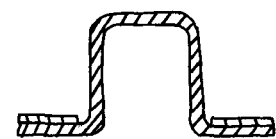
Model version



View A-A

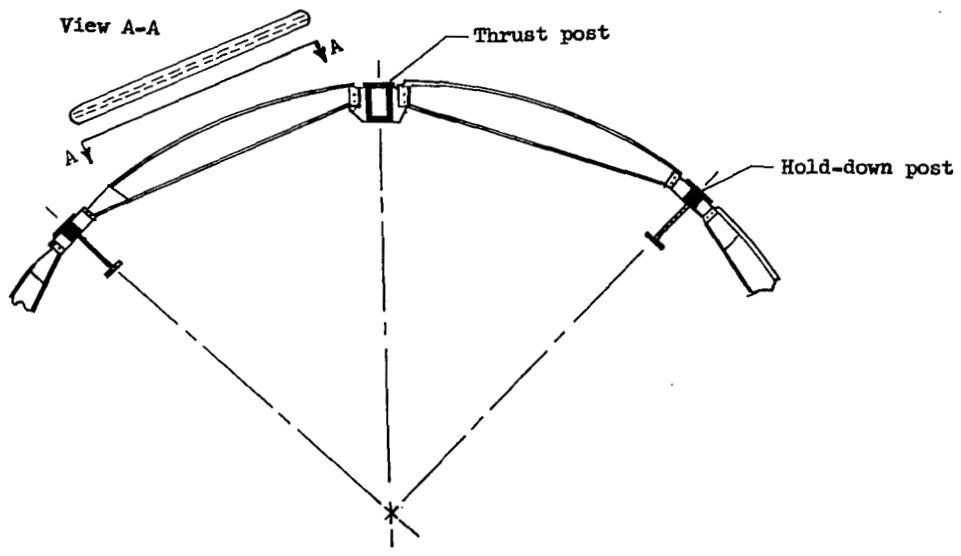


View B-B

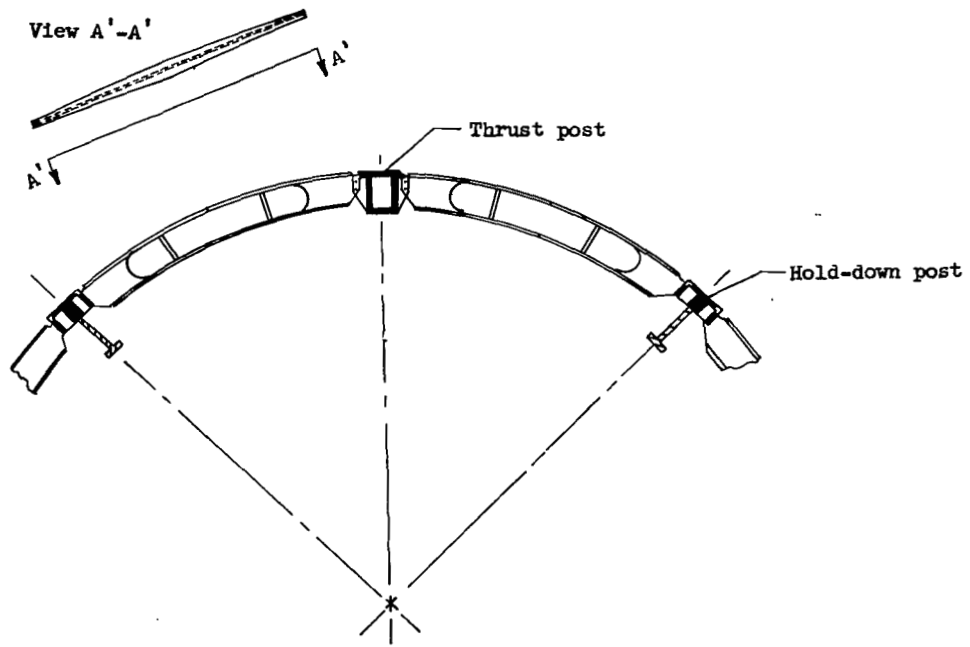


View C-C

Figure 45.- Typical model stringer design compared with the geometric scaling of a prototype stringer.

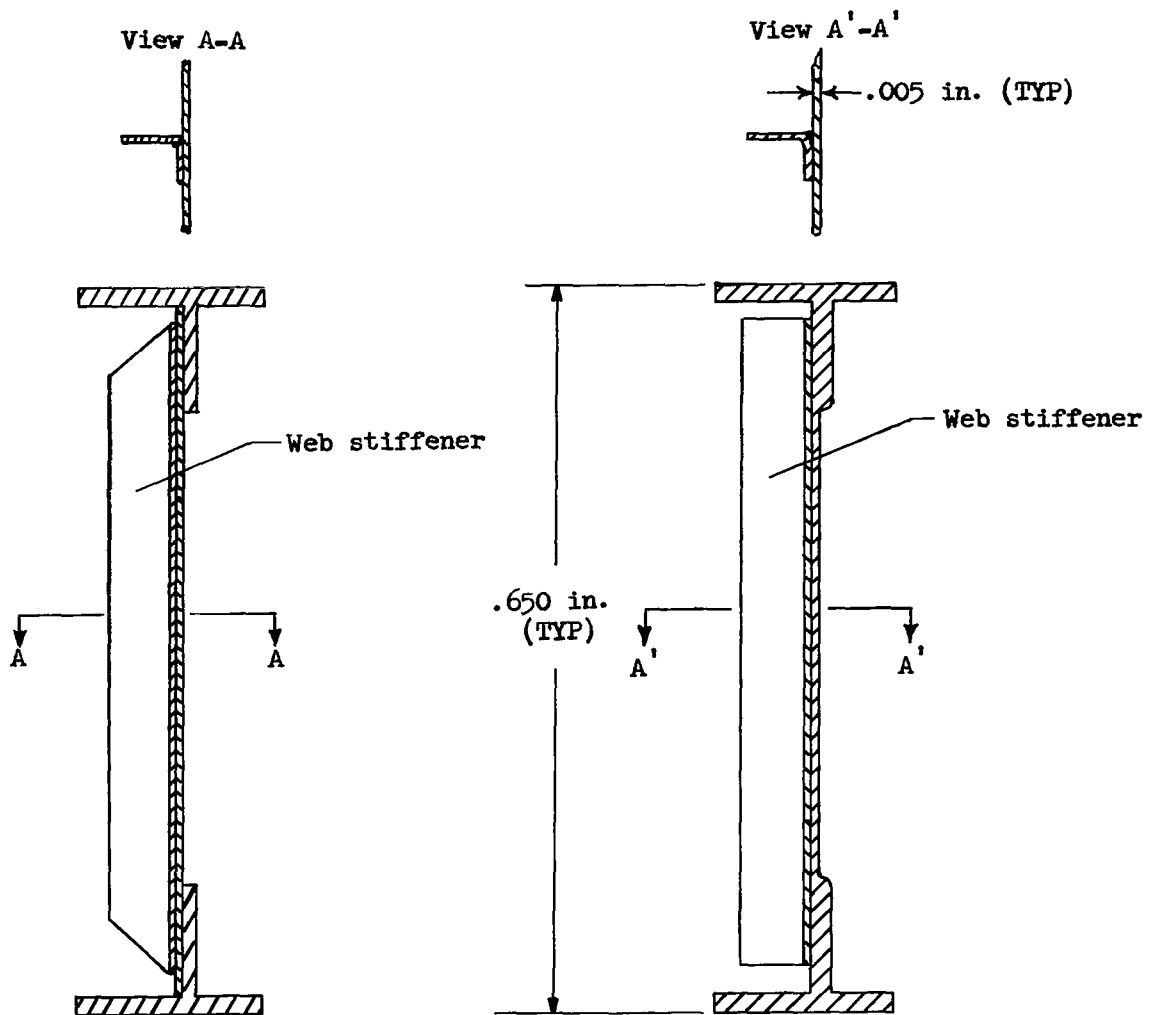


(a) Direct geometric scaling (variable width, constant thickness).



(b) Model design (constant width, variable thickness).

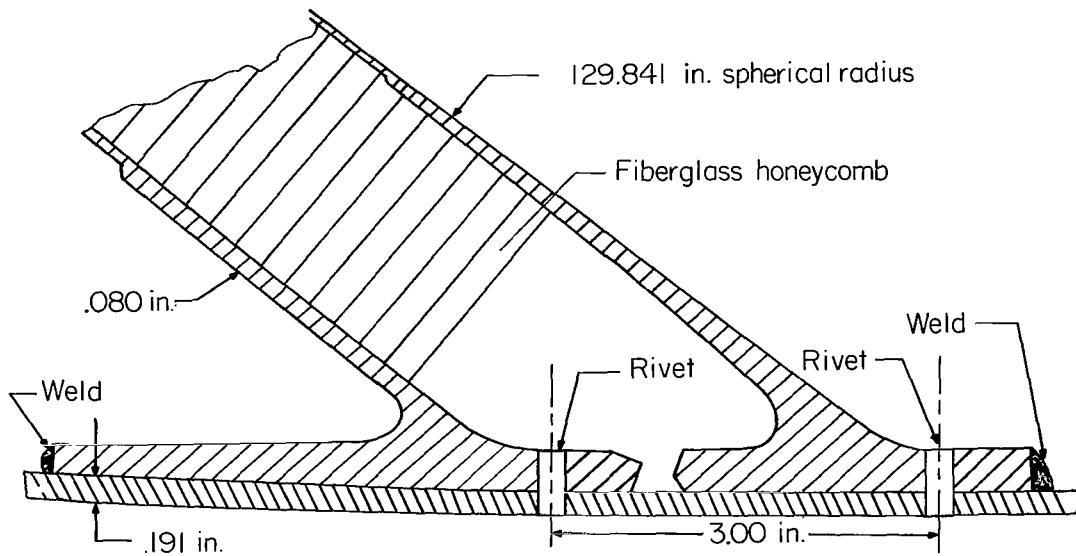
Figure 46.- Deviation from prototype geometric scaling of complex ring-frame structure.



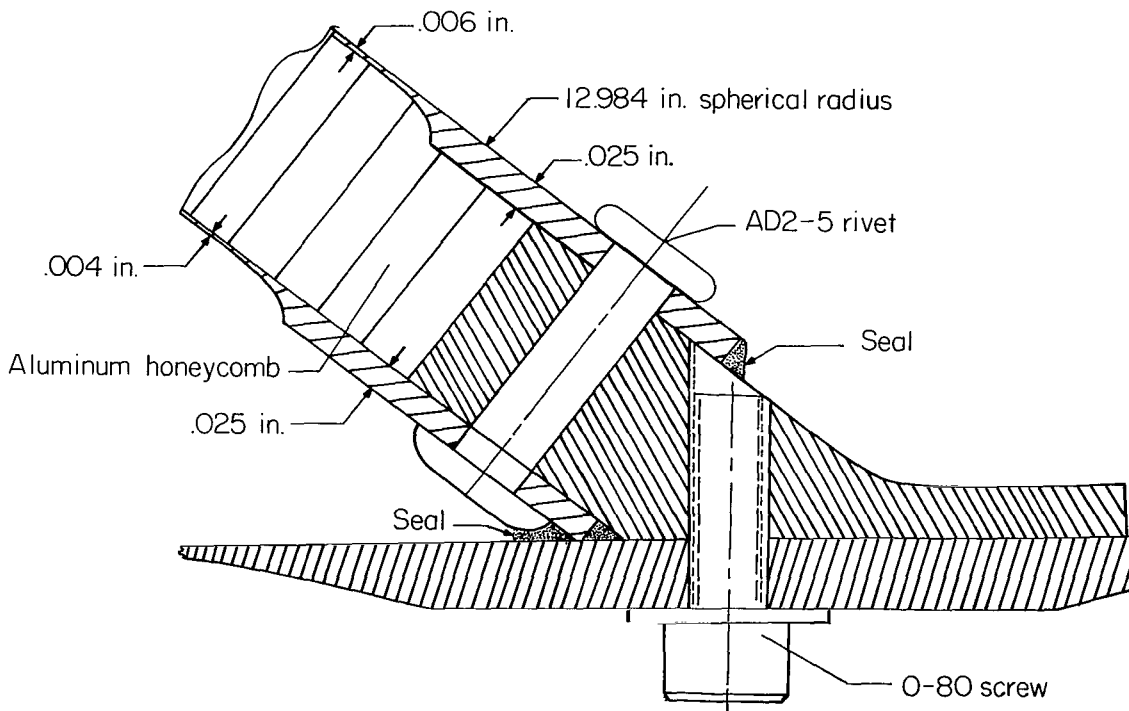
(a) Direct geometric scaling.

(b) Model design.

Figure 47.- Typical constant-cross-section model ring frame compared with direct geometrical scaling.

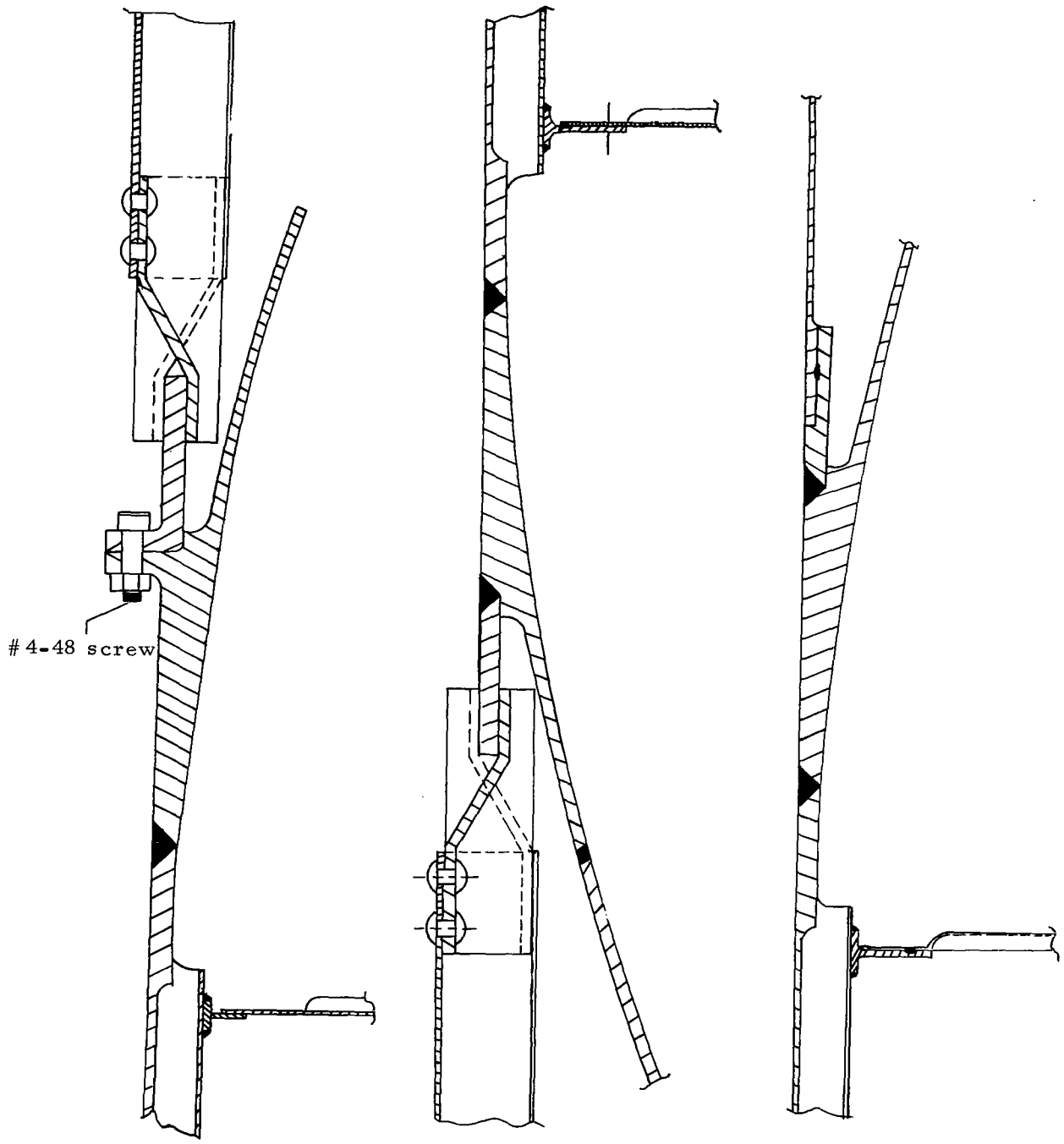


(a) Full scale.



(b) 1/10-scale model.

Figure 48.- Full scale and 1/10-scale model S-IVB common bulkhead.

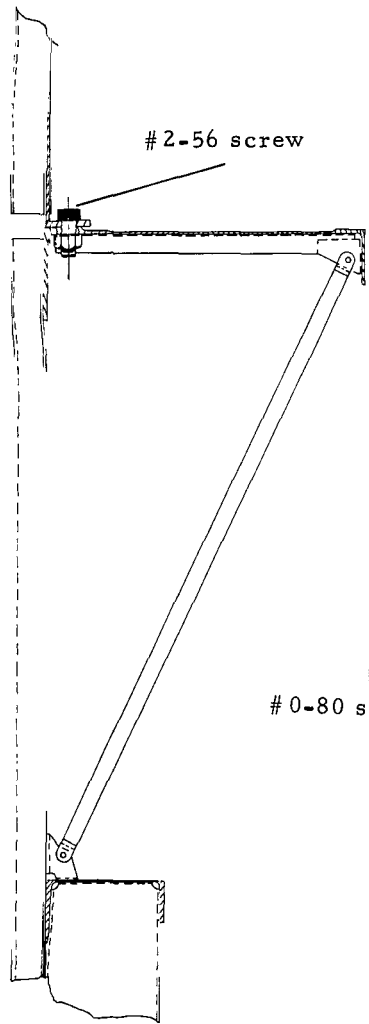


(a) Joint A from figure 6.

(b) Joint B from figure 6.

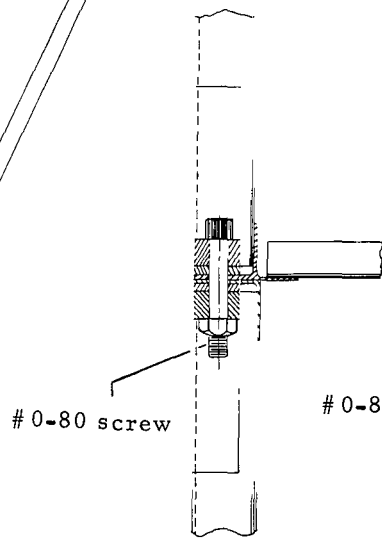
(c) Joint C from figure 6.

Figure 49.- Details of 1/10-scale model joints with identification letters referred to figure 6.



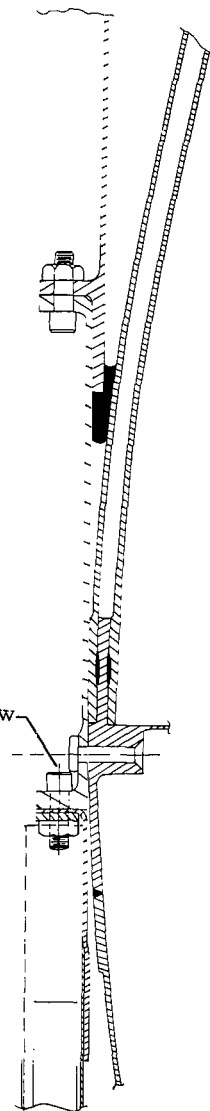
#2-56 screw

(d) Joint D from figure 6.



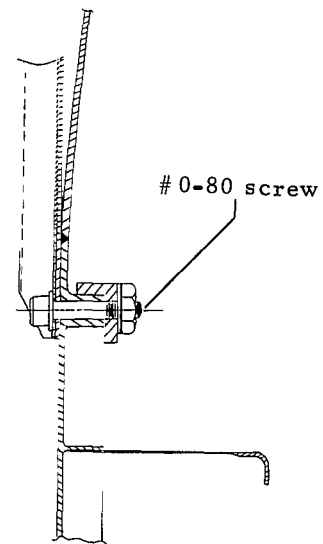
#0-80 screw

(e) Joint E from figure 6.



#0-80 screw

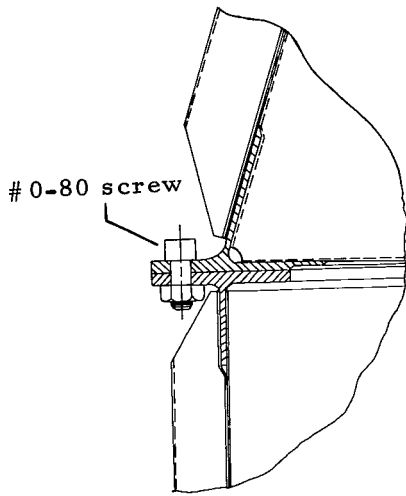
(f) Joint F from figure 6.



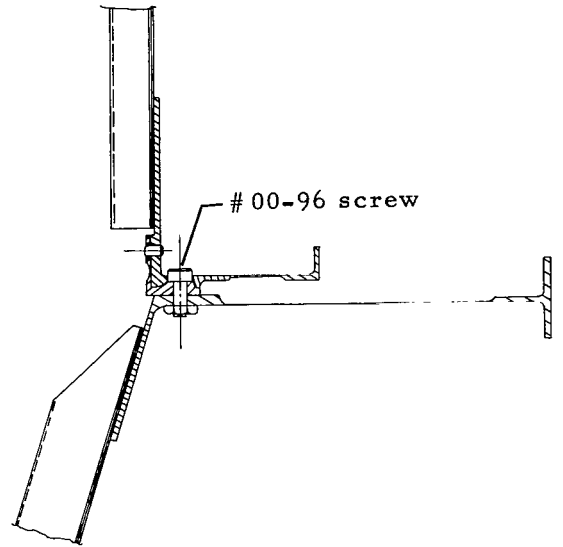
#0-80 screw

(g) Joint G from figure 6.

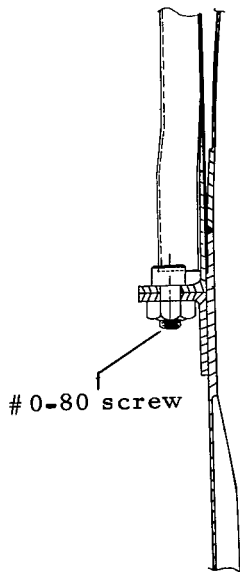
Figure 49.- Continued.



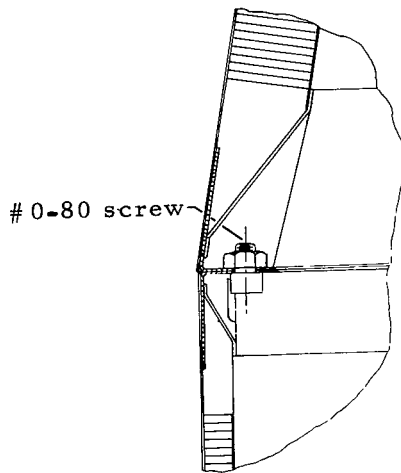
(h) Joint H from figure 6.



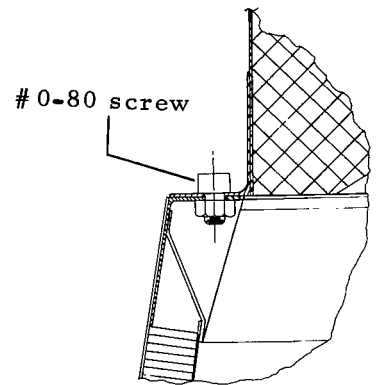
(i) Joint I from figure 6.



(j) Joint J from figure 6.



(k) Joint K from figure 6.



(l) Joint L from figure 6.

Figure 49.- Concluded.

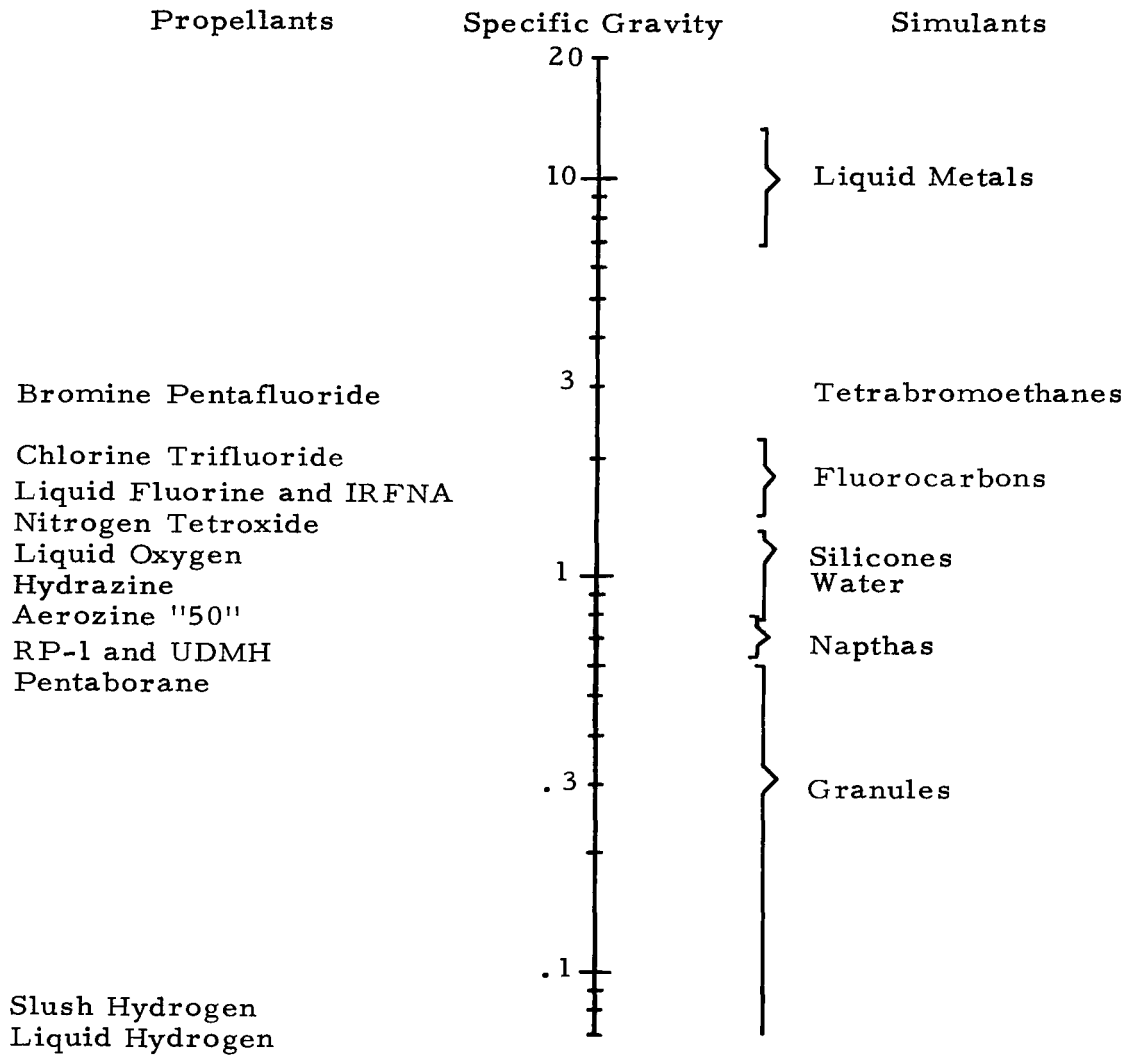


Figure 50.- Values of specific gravity for various propellants and simulants.

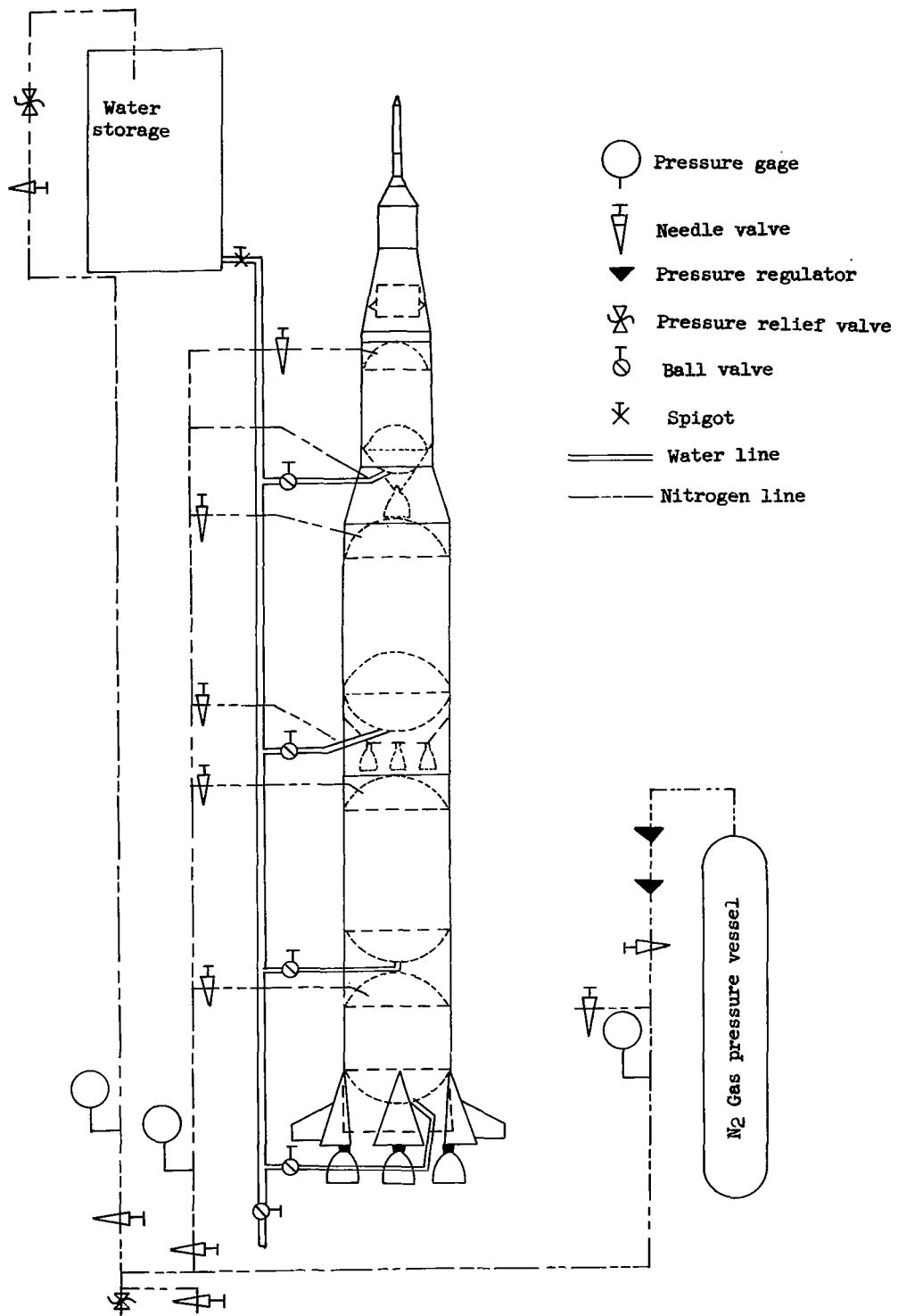
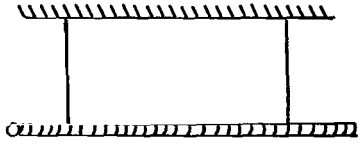
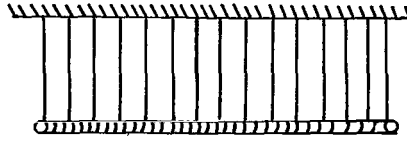


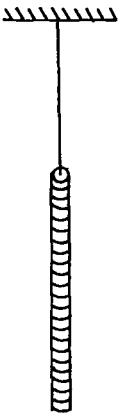
Figure 51.- Schematic of 1/10-scale model plumbing.



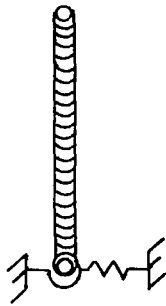
(a) Two-cable horizontal suspension.



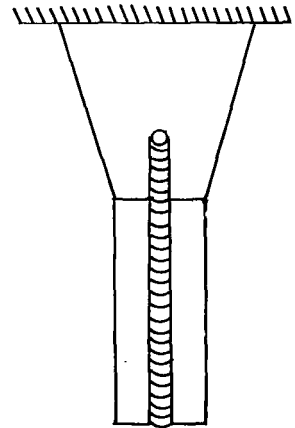
(b) Multi-cable horizontal suspension.



(c) One-cable vertical suspension.



(d) Base restraint vertical orientation.



(e) Harness vertical suspension.

Figure 52.- Types of model suspension systems.

*"The aeronautical and space activities of the United States shall be conducted so as to contribute . . . to the expansion of human knowledge of phenomena in the atmosphere and space. The Administration shall provide for the widest practicable and appropriate dissemination of information concerning its activities and the results thereof."*

—NATIONAL AERONAUTICS AND SPACE ACT OF 1958

## NASA SCIENTIFIC AND TECHNICAL PUBLICATIONS

**TECHNICAL REPORTS:** Scientific and technical information considered important, complete, and a lasting contribution to existing knowledge.

**TECHNICAL NOTES:** Information less broad in scope but nevertheless of importance as a contribution to existing knowledge.

**TECHNICAL MEMORANDUMS:** Information receiving limited distribution because of preliminary data, security classification, or other reasons.

**CONTRACTOR REPORTS:** Scientific and technical information generated under a NASA contract or grant and considered an important contribution to existing knowledge.

**TECHNICAL TRANSLATIONS:** Information published in a foreign language considered to merit NASA distribution in English.

**SPECIAL PUBLICATIONS:** Information derived from or of value to NASA activities. Publications include conference proceedings, monographs, data compilations, handbooks, sourcebooks, and special bibliographies.

**TECHNOLOGY UTILIZATION PUBLICATIONS:** Information on technology used by NASA that may be of particular interest in commercial and other non-aerospace applications. Publications include Tech Briefs, Technology Utilization Reports and Notes, and Technology Surveys.

*Details on the availability of these publications may be obtained from:*

SCIENTIFIC AND TECHNICAL INFORMATION DIVISION  
NATIONAL AERONAUTICS AND SPACE ADMINISTRATION  
Washington, D.C. 20546